DOKUZ EYLÜL UNIVERSITY
GRADUATE SCHOOL OF NATURAL AND APPLIED SCIENCES

OPTIMIZING THE DESIGN PARAMETERS OF OVEN DOOR

by
İlyas KILIÇ

February, 2014
İZMİR

OPTIMIZING THE DESIGN PARAMETERS OF OVEN DOOR

A Thesis Submitted to the
Graduate School of Natural and Applied Sciences of Dokuz Eylül University
In Partial Fulfillment of the Requirements for the Master of Science in
Mechanical Engineering, Energy Program

by
İlyas KILIÇ

February, 2014
İZMİR

M.Sc THESIS EXAMINATION RESULT FORM

We have read the thesis entitled **"OPTIMIZING THE DESIGN PARAMETERS OF OVEN DOOR"** completed by **İLYAS KILIÇ** under supervision of **PROF. DR. DİLEK KUMLUTAŞ** and we certify that in our opinion it is fully adequate, in scope and in quality, as a thesis for the degree of Master of Science.

Prof. Dr. Dilek KUMLUTAŞ

Supervisor

Prof. Dr. İsmail H. TAVMAN

(Jury Member)

Prof. Dr. Necdet ÖZBALTA

(Jury Member)

Prof. Dr. Ayşe OKUR
Director
Graduate School of Natural and Applied Science

ACKNOWLEDGEMENTS

First of all, I would like to express my very great appreciation to my supervisor, Prof. Dr. Dilek KUMLUTAŞ, for her immense knowledge and motivation, valuable advises and guidance throughout this thesis study.

This study is supported by the Scientific and Technological Research Council of Turkey, with the 3130615 encoded TEYDEB project.

Also, I would like to express special thanks to İhsan Doruk ÜNSALAN, Özgün ÖZER, Funda KURU, Hasan AVCI and Z. Haktan KARADENİZ for their motivation, support and sharing their valuable experiences with me.

Finally, I would like to gratefully thank to my family for their thrust, motivation, patience and encouragement throughout my entire life. Without them this thesis could not be completed.

İlyas KILIÇ

OPTIMIZING THE DESIGN PARAMETERS OF OVEN DOOR

ABSTRACT

The aim of this study is to investigate the heat transfer and fluid flow mechanics of domestic ovens that affect the average outer surface temperature of oven door glass which is critical for both safety of the user and the performance of the device, by using numerical and experimental methods.

Door of a domestic oven and its upper fan that provides active air suction from door unit were modeled using the Computational Fluid Dynamic and Heat Transfer (CFDHT) method. The numerical results were validated by comparing with the results obtained from experimental study. For optimization design parameters such as glass thickness, air thickness between the door glass, glass heights, active suction air velocity and the situation of using low-emissivity coating or not using were investigated. Effects of these parameters on the average outer surface temperature of oven door glass were determined. Active suction system provides the air circulation between the oven door glasses to cool down the oven door cavity. While oven door was modeled as two dimensional, active suction system was modeled as three dimensional. Both models were steady state. After modeling active suction system, modified numerical models were created to increase the average air velocity at inlet of inflow channel.

The success of this study is to investigate the design parameters of oven door that affect the average outer surface temperature of oven door glass at the same time and to increase the active suction average air velocity at inlet of inflow channel.

Keywords: Domestic ovens, computational fluid dynamics and heat transfer.

FIRIN KAPAKLARININ TASARIM PARAMETRELERİNİN OPTİMİZE EDİLMESİ

ÖZ

Bu çalışmanın amacı, ev tipi fırınlarda kullanıcı güvenliğine ve cihaz performansına etki eden ısı transferi ve akış karakteristiğini sayısal ve deneysel yöntemlerle incelenmesidir.

Ev tipi fırının kapısı ve kapıdan aktif hava çekişini sağlayan üst fan, Hesaplamalı Akışkanlar Dinamiği ve Isı Transferi (HADIT) kullanılarak modellenmiştir. Sayısal çalışma sonuçları deneysel çalışmadan elde edilen sonuçlarla karşılaştırılarak doğrulanmıştır. Optimizasyon için cam kalınlıkları, camlar arasındaki hava kalınlıkları, cam yükseklikleri, aktif çekiş hava hızı ve düşük yayma katsayılı kaplamanın olup olmaması durumu gibi tasarım parametreleri araştırılmıştır. Bu parametrelerin her birinin fırının dış camının ortalama yüzey sıcaklığı üzerindeki etkisi belirlenmiştir. Aktif çekiş sistemi kapı camları arasında kapı hacminin soğumasını sağlayan hava dolaşımını sağlar. Fırın kapısı iki boyutlu olarak modellenirken aktif çekiş sistemi üç boyutlu olarak modellenmiştir. Her iki model de kararlı rejimdedir. Aktif emiş sistemi modellendikten sonra emiş kanalının girişindeki ortalama hava hızını artırmak için modifiye edilmiş sayısal modeller oluşturulmuştur.

Bu çalışmanın başarısı, kapının dış cam yüzey sıcaklığına etki eden birçok parametrenin aynı anda incelenerek emiş kanalının girişindeki aktif çekiş ortalama hava hızının artırılmasıdır.

Anahtar kelimeler: Ev tipi fırın, hesaplamalı akışkanlar dinamiği ve ısı transferi.

CONTENTS

Page

THESIS EXAMINATION RESULT FORM ii
ACKNOWLEDGEMENTS iii
ABSTRACT iv
ÖZ v
LIST OF FIGURES ix
LIST OF TABLES xiv

CHAPTER ONE – INTRODUCTION 1

1.1 Literature Survey 1

CHAPTER TWO – NUMERICAL STUDY 7

2.1 Introduction of Numerical Study 7
2.2 Preparing Cad Model for Numerical Study 7
2.3 Meshing of the Oven Door Cavity 8
2.4 Boundary Conditions 11
2.5 Solver 14

CHAPTER THREE – EXPERIMENTAL STUDY AND VALIDATION 17

3.1 Experimental Study of the Oven Door 17
3.2 Validation of the Numerical Study 18

CHAPTER FOUR – OPTIMIZATION OF DESIGN PARAMETERS 19

4.1 Effect of the Glass Thickness 19
4.2 Effect of the Air Gaps between the Panes 20
4.2.1 Effect of the Gap between Glass Number 1 and 2 20
4.2.2 Effect of the Gap between Glass Number 2 and 3 21

4.2.3 Effect of the Gap between Glass Number 3 and 4..... 22
4.3 Effect of the Glass Heights..... 23
4.3.1 Effect of the Second Glass Height..... 24
4.3.2 Effect of the Third Glass Height..... 24
4.4 Effect of the Low Emissivity Coating..... 25
4.4.1 Effect of the Low Emissivity Coating on the Outer Side of First Glass.. 30
4.4.2 Effect of the Low Emissivity Coating on the Inner Side of Second Glass…. 31
4.4.3 Effect of the Low Emissivity Coating on the Outer Side of Second Glass…….. ……..33
4.4.4 Effect of the Low Emissivity Coating on the Inner Side of Third Glass…….. ……..35
4.4.5 Effect of the Low Emissivity Coating on the Outer Side of Third Glass…….. ……..37
4.4.6 Effect of the Low Emissivity Coating on the Inner Side of Fourth Glass…… ……..39
4.4.7 Effect of the Low Emissivity Coating on the Outer Side of Fourth Glass…… ... ……..40
4.4.8 Effect of the Low Emissivity Coating on the Inner Sides of Second and Third Glass..... 42
4.4.9 Effect of the Low Emissivity Coating on the Inner Side of Second Glass and Outer Side of Third Glass 44
4.4.10 Effect of the Low Emissivity Coating on the Outer Side of Second Glass and Inner Side of Third Glass..... 46
4.4.11 Effect of the Low Emissivity Coating on the Outer Side of Second Glass and Outer Side of Third Glass 48
4.4.12 Effect of the Low Emissivity Coating on the Outer Side of First Glass, Outer Side of Second Glass and Inner Side of Third Glass..... 50
4.4.13 Effect of the Low Emissivity Coating on the Outer Side of First Glass, Outer Side of Second Glass and Outer Side of Third Glass 52
4.4.14 Effect of the Low Emissivity Coating on the Outer Side of First Glass, Inner Side of Second Glass and Outer Side of Third Glass..... 54

4.4.15 Effect of the Low Emissivity Coating on the Outer Side of First Glass, Inner Side of Second Glass and Inner Side of Third Glass 56
4.4.15.1 Effect of the Gap between Glass Number 1 and 2 59
4.4.15.2 Effect of the Gap between Glass Number 2 and 3 60
4.4.15.3 Effect of the Gap between Glass Number 3 and 4 61
4.5 Effect of the Inlet Area at Inflow Channel 62
4.6 Effect of the Blocking Air Flow between the Glass Panes 63
4.6.1 Blocking the Air Flow between Glass Number 2 and Number 4 from Bottom 63
4.6.2 Blocking the Air Flow between Glass Number 2 and Number 4 from Bottom and Top 68
4.6.3 Blocking the Air Flow between Glass Number 1 and Number 2 from Top 72
4.7 Effect of Active Suction Air Velocity 76

CHAPTER FIVE – MODELING ACTIVE SUCTION SYSTEM 79

5.1 Preparing Cad Model for Numerical Study 79
5.2 Meshing of the Active Suction System 80
5.3 Defining the Boundary Conditions 81
5.4 Solver 82
5.5 Validation of Numerical Study 83
5.6 The Original and Modified Models of Active Suction Unit 84
5.7 The Results of Original and Modified Models 86

CHAPTER SIX – CONCLUSIONS 87

REFERENCES 90

LIST OF FIGURES

Page

Figure 2.1 Oven door glass (a) and air circulation of the oven (b). 8
Figure 2.2 Mesh structure of the uncoated original model 10
Figure 2.3 Definitions of the model. 13
Figure 2.4 Heat transfer residuals. 14
Figure 2.5 Turbulence residuals. 15
Figure 2.6 Momentum and mass residuals 15
Figure 2.7 Average temperatures at the outer surface of the fourth glass. 16
Figure 3.1 Locations of the thermocouples on the glass. 17
Figure 3.2 Results of the numerical and experimental studies. 18
Figure 4.1 Effect of the glass thickness. 19
Figure 4.2 Effect of the air thickness between first and second glass. 21
Figure 4.3 Effect of the air thickness between second and third glass. 22
Figure 4.4 Effect of the air thickness between third and outer glass. 23
Figure 4.5 Effect of the second glass height. 24
Figure 4.6 Effect of the third glass height. 25
Figure 4.7 Temperature contour of the uncoated original model. 27
Figure 4.8 Velocity vectors of the uncoated original model. 28
Figure 4.9 Velocity vectors of the flow between the glass panes and in the inlet of suction channel. 29
Figure 4.10 Velocity vectors of the air entering between the glass. 30
Figure 4.11 The temperature contour of the first model which has low emissivity coating on the outer side of first glass. 31
Figure 4.12 The temperature contour of the second model which has low emissivity coating on the inner side of second glass. 32
Figure 4.13 Upper side (a) and down side (b) temperature contours of the second model which has low emissivity coating on the inner side of second glass. 33
Figure 4.14 The temperature contour of the third model which has low emissivity coating on the outer side of second glass 34
Figure 4.15 Upper side (a) and down side (b) temperature contours of the third model which has low emissivity coating on the outer side of second glass. 35

Figure 4.16 The temperature contour of the fourth model which has low emissivity coating on the inner side of third glass..... 36
Figure 4.17 Upper side (a) and down side (b) temperature contours of the fourth model which has low emissivity coating on the inner side of third glass. 37
Figure 4.18 The temperature contour of the fifth model which has low emissivity coating on the outer side of third glass..... 38
Figure 4.19 Upper side (a) and down side (b) temperature contours of the fifth model which has low emissivity coating on the outer side of third glass. 38
Figure 4.20 The temperature contour of the sixth model which has low emissivity coating on the inner side of fourth glass. 39
Figure 4.21 Upper side (a) and down side (b) temperature contours of the sixth model which has low emissivity coating on the inner side of fourth glass..... 40
Figure 4.22 The temperature contour of the seventh model which has low emissivity coating on the outer side of fourth glass 41
Figure 4.23 Upper sides (a) and down side (b) temperature contours of the seventh model which has low emissivity coating on the outer side of fourth glass. 42
Figure 4.24 The temperature contour of the eighth model which has low emissivity coating on the inner side of second and glass 43
Figure 4.25 Upper sides (a) and down side (b) temperature contours of the eighth model which has low emissivity coating on the inner side of second and glass..... 44
Figure 4.26 The temperature contour of the ninth model which has low emissivity coating on the inner side of second glass and outer side of third glass..... 45
Figure 4.27 Upper sides (a) and down side (b) temperature contours of the ninth model which has low emissivity coating on the inner side of second glass and outer side of third glass. 46
Figure 4.28 The temperature contour of the tenth model which has low emissivity coating on the outer side of second glass and inner side of third glass..... 47
Figure 4.29 Upper sides (a) and down side (b) temperature contours of the tenth model which has low emissivity coating on the outer side of second glass and inner side of third glass. 48
Figure 4.30 The temperature contour of the eleventh model which has low emissivity coating on the outer sides of and third glass 49

Figure 4.31 Upper sides (a) and down side (b) temperature contours of the eleventh model which has low emissivity coating on the outer sides of second and third glass. …. 50
Figure 4.32 The temperature contour of the twelfth model which has low emissivity coating on the outer side of first glass, outer side of second glass and inner side of third glass…. 51
Figure 4.33 Upper sides (a) and down side (b) temperature contours of the twelfth model which has low emissivity coating on the outer side of first glass, outer side of second glass and inner side of third glass. 52
Figure 4.34 The temperature contour of the thirteenth model which has low emissivity coating on the outer side of first glass, outer side of second glass and outer side of third glass.. 53
Figure 4.35 Upper sides (a) and down side (b) temperature contours of the thirteenth model which has low emissivity coating on the outer side of first glass, outer side of second glass and outer side of third glass. 54
Figure 4.36 The temperature contour of the fourteenth model which has low emissivity coating on the outer side of first glass, inner side of second glass and outer side of third glass 55
Figure 4.37 Upper side (a) and down side (b) temperature contours of the fourteenth model which has low emissivity coating on the outer side of first glass, inner side of second glass and outer side of third glass. 56
Figure 4.38 The temperature contour of the fifteenth model which has low emissivity coating on the outer side of first glass, inner side of second glass and inner side of third glass… 57
Figure 4.39 Upper side (a) and down side (b) temperature contours of the fifteenth model which has low emissivity coating on the outer side of first glass, inner side of second glass and inner side of third glass. 58
Figure 4.40 Results of the numerical and experimental studies of the model which has low emissivity coating on the outer side of first glass, inner side of second glass and inner side of third glass. 59
Figure 4.41 Effect of the air thickness between first and second glass..... 60
Figure 4.42 Effect of the air thickness between second and third glass. 61

Figure 4.43 Effect of the air thickness between third and fourth glass. 62
Figure 4.44 The effect of the inflow channel area on the outer average temperature of fourth glass. 63
Figure 4.45 The prepared model (a) and detailed view (b) of the air blockage between second and fourth glass from top and bottom. 64
Figure 4.46 Velocity vectors of the model which airflow was blocked between glass number two and number four from bottom. 65
Figure 4.47 Upper side (a) and down blockage side (b) velocity vectors of the model which airflow was blocked between glass number two and number four from bottom.. 66
Figure 4.48 Temperature contour of the model which airflow was blocked between glass number two and number four from bottom. 67
Figure 4.49 Upper side (a) and down blockage side (b) temperature contours of the model which airflow was blocked between glass number two and number four from bottom. 68
Figure 4.50 The prepared model which has air blockage between second and fourth glass from top and bottom 69
Figure 4.51 The top (a) and bottom (b) air blockage between second and fourth glass.. 69
Figure 4.52 Velocity vectors of the model which airflow was blocked between glass number two and number four from top and bottom. 70
Figure 4.53 Upper (a) and down (b) blockage side velocity vectors of the model which airflow was blocked between glass number two and number four from top and bottom.. 70
Figure 4.54 Temperature contour of the model which airflow was blocked between glass number two and number four from top and bottom. 71
Figure 4.55 Upper blockage side (a) and down blockage side (b) temperature contours of the model which airflow was blocked between glass number two and number four from top and bottom. 72
Figure 4.56 The prepared model which has air blockage between first and second glass from top 74

Figure 4.57 Velocity vectors of the model which airflow was blocked between glass number one and number two from top. 74
Figure 4.58 Upper blockage side (a) and down side (b) velocity vectors of the model which airflow was blocked between glass number one and number two from top. .. 74
Figure 4.59 Temperature contour of the model which airflow was blocked between glass number one and number two from top. 75
Figure 4.60 Upper blockage side (a) and down side (b) temperature contours of the model which airflow was blocked between glass number one and number two from top..... 75
Figure 4.61 The effect of active suction air velocity on the uncoated model. 77
Figure 4.62 The effect of active suction air velocity on model which has low emissivity coating on the outer side of first glass, inner side of second and third glass.. 77
Figure 5.1 The prepared model geometry of the active suction system..... 79
Figure 5.2 Mesh structure of the active suction system. 81
Figure 5.3 Momentum and mass residuals..... 82
Figure 5.4 Turbulence residuals. 83
Figure 5.5 The modified geometry for the case one. 85
Figure 5.6 The modified geometry for the case two. 85

LIST OF TABLES

Page

Table 2.1 The study of determining optimum mesh model. 9
Table 2.2 The study of determining optimum number of iterations for model..... 11
Table 2.3 Thermophysical properties of the glass plate..... 12
Table 4.1 Thermophysical properties of the Low-e glass. 26
Table 4.2 Low emissivity coating application sides of the models prepared..... 26
Table 5.1 Results of the numerical and experimental studies. 84
Table 5.2 The average inlet air velocity of inflow channel. 86

CHAPTER ONE
INTRODUCTION

1.1 Literature Survey

Energy efficiency of a house is related to domestic goods that are energy efficient or not. Energy consumption of a domestic machine affects energy efficiency of a house. As we know, ovens have one of the great rates of energy consumption rate of a house. Manufacturing more efficient domestic ovens means less energy consumption. To manufacture more efficient ovens can be achieved by trying new methods.

Developing technology and science bring new methods and products to humanity. Computational Fluid Dynamics (CFD) is a method that has proved its reliability. It is used to understand and aid the better products. By using CFD both time and money can be saved. Instead of making new prototypes new models can be prepared in less time and with less money. Because of these reasons CFD is commonly used designing of new products. Nowadays, people are looking for energy efficient, durable and cheap goods. So manufacturers have to produce a product that has more efficiency, cheap and can operate properly for long time of period.

This study is used a prototype which is pyrolytic type domestic oven. Pyrolytic type oven has an automatic cleaning function which happens by heating inside of the oven that reaches over 500° C. So at that temperature any food residue and grime stuck to the walls is simply burned off. While high temperatures wanted at the oven inner cavity due to standards and user health outer glass has to be at low temperatures. High temperatures don’t only affect the outer glass temperature it affects the electronic components that are inside the oven. At high degrees they get harmed. The cooling circuit was necessary to carry away excess heat and prevent critical areas such as the door and the electronics from overheating. Because of these,

pyrolytic oven has active suction system that provides air through the door between panes, thereby reducing the door's external surface temperature.

Shaughnessy & Newborough (2000) studied on a low-emissivity oven (LEO) which provides energy-efficient alternative to a conventional domestic electric oven. A prototype domestic LEO was described. Its energy performance is assessed and compared with a current generation domestic electric oven. The prototype achieved energy-savings of 36±57% when compared with the commercially-available oven. Then they recommended that manufacturers implement low-emissivity oven designs for domestic users as a means of speeding thermal performance, reducing energy consumption, and thereby reducing the emissions and peak electrical demands associated with domestic cooking.

Abraham & Sparrow (2004) developed algebraic method for the prediction of the timewise temperature variation of a thermal load situated in an electrically heated oven. The method takes into account both natural convection within the oven cavity and radiation between the thermal load and the oven walls. Their model provides a complete description of heat transfer external to the thermal load. The model was able to accommodate loads of various shapes, sizes, materials, and radiation surface finishes. They performed experiments to validate the predictive method. Measurements were transient response of the thermal load. And they collected temperature data from the oven walls. Among the walls, the temperatures on the oven door were the lowest, whereas the highest temperatures were encountered on the oven floor and on the top wall.

Alvarez et al (2005) applied ZnS (40nm)-CuS (150nm) and ZnS (40nm) - Bi_2S_3 (75nm)-Cus (150nm) chemical baths to 3 mm thick glass. The solar heat gain coefficient was evaluated for these glazing at exterior temperatures of 15° C and 32° C for an exterior convective heat transfer coefficient of 6–100 W/m^2K using a mathematical model. The model predicted the extent of reduction in solar heat gain coefficient as a function of exterior convective heat transfer coefficient and hence helps to decide on the relative benefit, which may be derived through their use in

different locations. They detected the most suitable coating type for windows at different climates. Coatings have different characteristics at different conditions.

Mistry, Ganapathi-subbu, Dey, Bishnoi & Castillo (2006) studied transient natural convection heat transfer in ovens. The CFD modeling of electric oven involves three-dimensional, unsteady, natural convective flow-thermal field coupled with radiative heat transfer. The front doors have a double glazed window, which helps the operator to monitor the cooking without opening the door. They had a Tin oxide coated inner glass walls to ensure low transmissivity for reduced radiation losses. For radiation models, they studied on the discrete ordinate (DO) and surface-to-surface (S2S) radiation models. The DO model takes into account media participation in addition to the surface-to-surface radiation effects. But surface-to-surface radiation model considers only surface-to-surface radiation effects. But they found the difference of temperature prediction at the center of the oven and oven walls by the DO and S2S models for a simplified but similar geometry were of the order of 0.2%. Although the comparison of the thermal field was similar, the computational time for S2S model was almost half of the DO model for an identical grid.

Xamán, Arce, Álvarez & Cháveza (2008) studied a two-dimensional numerical combined heat transfer (laminar and turbulent natural convection, surface thermal radiation and conduction) in a square cavity with a glass wall. They modeled cavity as one vertical isothermal wall, two horizontal adiabatic walls and one vertical glass wall. Numerical results in the cavity are obtained by means of a control volume approach where the conditions are set as: 21° C uniform temperature in the isothermal wall, 35 ° C outside ambient temperature and 750W/m^2 constant direct normal solar irradiation over the glass wall. The Rayleigh number was varied between the range $10^3 \leq Ra \leq 10^{12}$. At results the flow pattern was not symmetric due to the combined effect of non-isothermal glass wall and radiative exchange inside the cavity. They obtained a correlation for the total Nusselt number for both laminar and turbulent flow considering conjugate heat transfer. They revealed the results of different Rayleigh numbers so that we can see the results of laminar and turbulent natural convection

Fahey, Wakes & Shaw (2008) studied cooling on circuit of the door of a pyrolytic oven. They used CFD and experimental techniques to understand the flow behavior of the oven. The CFD results were validated with experimental hot-wire velocity measurements. They tried to understand oven door's cooling circuit but they did not determine the effect of it or determine the design parameters and didn't do any changes on the model.

Fang, Hyde, Hewitt, Eames & Norton (2009) predicted thermal performance of vacuum glazing by using two-dimensional finite element and three-dimensional finite volume models. In this study the in 2-D model, the vacuum space, including the pillar arrays, was represented by a material whose effective thermal conductivity was determined from the specified vacuum space width, the heat conduction through the pillar array and the calculated radiation heat transfer between the two interior glass surfaces within the vacuum gap. In the 3-D model, the support pillar array was incorporated and modeled within the glazing unit directly. A guarded hot box calorimeter was used to determine the experimental thermal performance of vacuum glazing. In this study the importance of low-emission coating was observed.

Chhanwal, Anishaparvin, Indrani, Raghavarao & Anandharamakrishnan (2010) studied on an electric heating baking oven for bread baking process. They emphasized the importance of radiation and developed three radiation model discrete transfer radiation model (DTRM), surface to surface (S2S) and discrete ordinates (DO). They found almost similar results from different models. They modeled the oven as a transient model. DO radiation model was selected for bread baking simulation and validated with the experimental measurement of bread temperature.

Rek, Rudolf & Zun (2012) modeled new generation oven. Oven was multifunctional, radiation, conduction; natural and forced convection mechanisms of heat transfer were used. They used discrete ordinate model used for radiation and described the density of air by incompressible ideal gas equation in a natural convection model. They aim was to create the best possible baking conditions for

different heating systems. Several discrete models were created to achieve best possible baking conditions for different heating systems. The influence of geometry change and boundary conditions variations to the velocity and temperature field distribution in the oven cavity was analyzed. The results of numerical simulations were validated with measurements taken from an oven prototype. They studied five different radiation models and found the Discrete Ordinate model only appropriate. There are many factors that have influence on the conditions inside the oven, such as: the shape and power of heaters, fan rotor rotational speed, thickness and quality of insulation, the design of oven doors, etc. Optimum conditions can be approached through the variation of these factors. They changed the oven cavity geometry and boundary conditions to approach optimum conditions. The conditions were all about the inside cavity of the oven.

The aim of this study is to investigate design parameters of oven door which are used commonly at households, by using numerical and experimental methods. Door of a domestic oven and its upper fan that provides active air suction from door unit were modeled using the Computational Fluid Dynamic and Heat Transfer (CFDHT) method. The numerical results were validated by comparing with the results obtained from experimental study. For optimization design parameters such as air thickness between the door glass, thickness of glass, glass heights, active suction air velocity and the situation of using low-emissivity coating or not using were investigated. Oven door was modeled as two dimensional and steady state. Two dimensional models provided that more analysis were done in less time.

As it is seen from literature there are many studies on the oven. Studies were temperature and velocity distribution inside the oven cavity. Some studies were on industrial ovens. Only a few ones are about oven door and heat transfer mechanism in the door. But none of them are about the parameter that affects the oven door heat transfer mechanism. The success of this study is optimize design parameters such as air thickness between the door glass, thickness of glass, glass heights, active suction air velocity and the situation of using low-emissivity coating or not using. In this study the design parameters of oven door that affect the outer surface temperature of

oven door glass were investigated at the same time and to increase the active suction average air velocity at inlet of inflow channel.

To see the effect of a design parameter, that design parameter must be given different values. With the results of different values effect of that parameter can be obtained. Because of this parametric study is a good way to understand the effect of a variable.

For optimum values, effects of the parameters were investigated. The design parameters of oven door that affect the outer surface temperature of oven door glass were investigated at the same time. Optimum values and alternative choices were defined for the model. The active suction average air velocity at inlet of inflow channel was increased.

CHAPTER TWO
NUMERICAL STUDY

2.1 Introduction of Numerical Study

To optimize the design parameters of oven door a two dimensional mathematical model was prepared for the domestic oven. Optimization includes many different parameters such glass thickness, air thickness between the door glass, glass heights, active suction air velocity and the situation of using low-emissivity coating or not using were investigated. As the number of parameters increase number of analysis increases too. Because of this a two dimensional model that validates with the experimental results was studied. After the results that show the importance of active suction air velocity, active suction fan unit was modeled. In numerical study a commercial computational fluid dynamic package program was used for modeling.

2.2 Preparing Cad Model for Numerical Study

The cad model of the oven door has been taken from a white goods company for the numerical study. A door model which consists quadruple glass was prepared For this study. Modeling process is first step of Computational Fluid Dynamics (CFD). If prepared model is most likely the real prototype the results gets better convergence to the experimental results. On the other hand more complicated models needs much more time to get solved by the solver manager. Because of that a necessary and sufficient details must be specified during the modeling process.

Active suction system gets air between the panes of door glass and from the chimney of the oven. Cad model was a pyrolytic type oven that has quadruple glass door with active suction system. Oven has a chimney that is opening to the active suction system. Inflow channel gets air from the chimney and door. As it is shown in Figure 2.1 mathematical model has been established according to measurements taken from prototype. The “A” side shown in Figure 2.1 is the oven inner cavity direction and the “B” side is the outside of the oven. Glass number 1 (inner glass

pane) is the pane that contacts with the oven inner cavity and glass number 4 (outer glass pane) contacts with the ambient atmosphere of the oven.

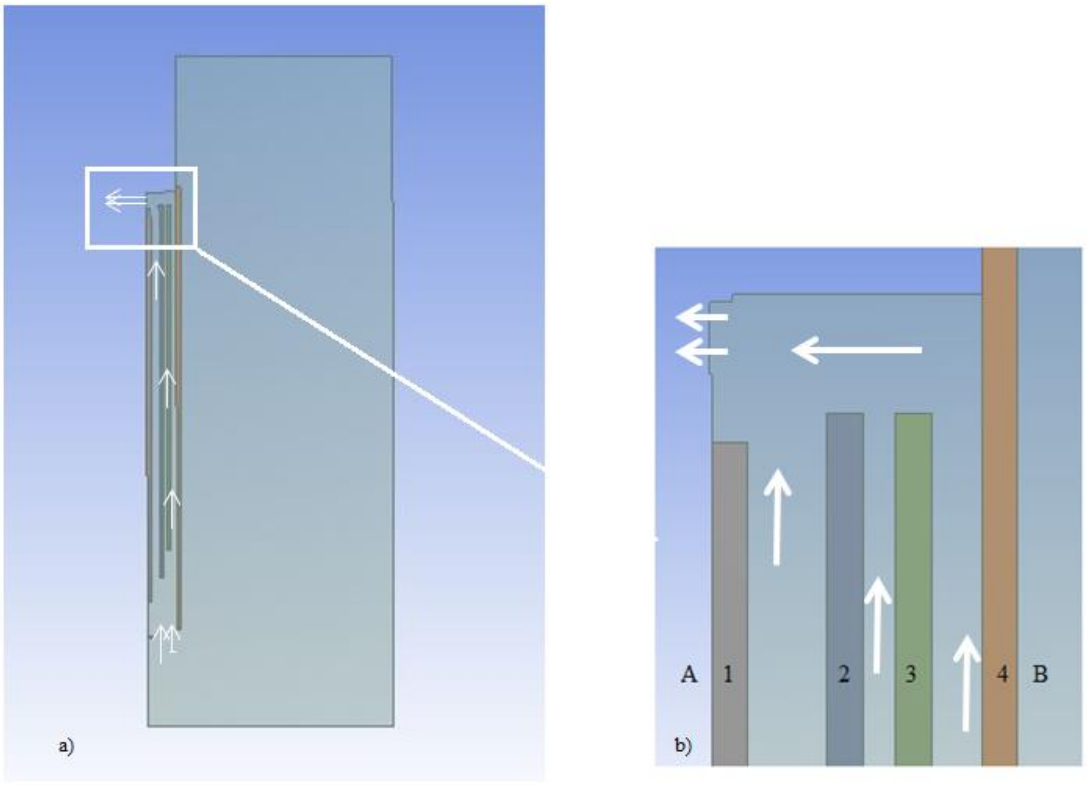


Figure 2.1 Oven door glass (a) and air circulation of the oven (b).

Package program needs a 3D model so 2D model extruded 10 mm. 10 mm is enough for the model because more extrusion depths can cause directional heat transfers that can manipulate the numerical model. For modeling the ambient air and seeing the ambient air movements 250 mm thickness of air was created. For determining this value different thickness were studied and selected the optimal thickness of ambient air.

2.3 Meshing of the Oven Door Cavity

After preparing prepared computer aided design (CAD) model process is finished meshing process starts. Meshing quality is one of the parameter that affects the results of the CFD study. Because of this meshing process must be done properly to

reach the closest results. After CAD model imported to the mesh module and meshing was started.

Oven door consists of very small and very large entities. Air gaps between the glass panes, glass thicknesses are very small entities comparing to ambient air cavity. Because of these reasons meshing process need detailed attention to get best results.

Glass, small air thickness and other critical areas were meshed with small element size that is necessary for the accurate results. Different sizes of mesh elements was applied to the model and tried to find optimal number of elements for the final model. As it seen from Table 2.1 different number of mesh was applied to the CAD model. For comparing the cases average temperature of the outer surface of fourth glass pane were noted. This is the "B" side of fourth glass. Five models were prepared to see the effect of the number of elements and nodes. Even the model, which has the minimum number of elements and nodes (Case 1) having 1 degree accuracy.

Table 2.1 The study of determining optimum mesh model.

Case	Number of Nodes	Number of Elements	Temperature at Outer Surface [K]
Case 1	223996	182450	339.654 [K]
Case 2	246307	201640	340.262 [K]
Case 3	307552	260760	339.632 [K]
Case 4	330432	282150	339.62 [K]
Case 5	7073827	6654606	340.575 [K]

If the number of elements increases solver needs more time to get results but if number of elements is not enough model cannot validate the experimental results. If the other parameters that affect the CFD results are done properly, to get best converging results meshing process needs more time to spend on. Case 3 was chosen for this study as a final model. Small air gaps, glass and the entities that are critical, meshed with fine elements sizes. Figure 2.2 shows detailed information of the

numerical model. This model is uncoated original model. Mesh quality was checked and surfaces, bodies were named for the ease of definitions.

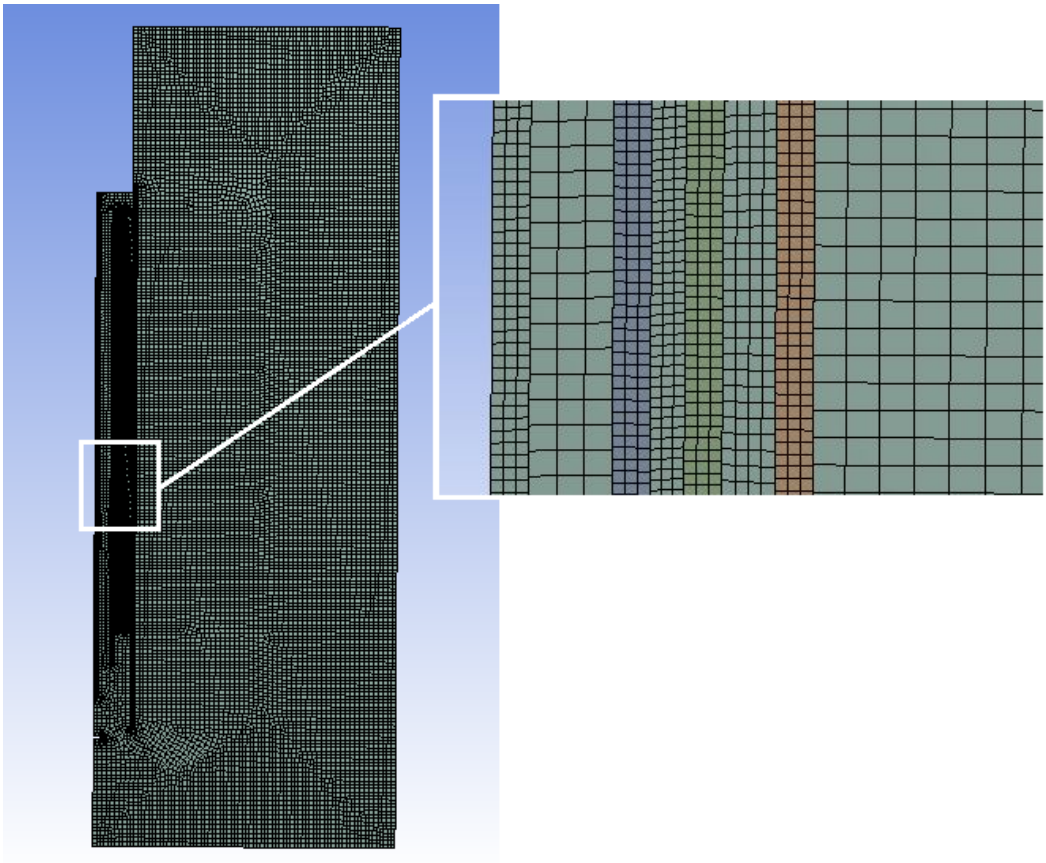


Figure 2.2 Mesh structure of the uncoated original model.

After determining the optimum mesh structure, models were prepared to define optimum number of iterations. Number of iterations is another parameter that affects convergence. For this study four different numbers of iterations were studied. As the number of iterations increase the solving time the model increases.

To understand if the number of iterations is enough or not residuals for the analysis must be monitored. As it is seen from Table 2.2 number of iterations range is quite large but the temperature at outer surface has small range that is about 1 degree accuracy. It takes 3 more times program to solve the case four.

Table 2.2 The study of determining optimum number of iterations for model.

Case	Number of Iterations	Temperature at Outer Surface [K]
Case 1	400	339.73 [K]
Case 2	500	339.806 [K]
Case 3	550	339.825 [K]
Case 4	600	339.867 [K]
Case 5	1500	339.963 [K]

2.4 Boundary Conditions

After meshing process is done, the prepared numerical model of the oven door has been transferred to the program's preprocessing module. In this module boundary conditions is set up. This process is the last section before the solving process. Boundary conditions, material properties, solver controls, expressions number of iterations and other options like monitors that are wanted to see during solution process are set up in this module.

Model has glass and air bodies. Thermophysical properties of the glass plate that are used in prototype shown in Table 2.3. These values were used to describe glass. Oven door has four solid and one fluid body (domain). Air is the fluid domain and glass is the solid domain.

Since the model is two dimensional the surfaces that are on the symmetry axis they were all set to symmetry boundary condition. Domains are connected by interface surfaces. Interface surfaces have big effect on heat transfer so each interface surface is defined properly. As a heat transfer option thermal energy was defined and analysis type defined as steady state.

To get the best converging results in least time number of iterations must be chosen properly. For this study 550 iterations was found enough for the further modeling. Residual target was set to $1x10^{-6}$.

Table 2.3 Thermophysical properties of the glass plate.

Properties	Value
Density	2500 kg/m^3
Poisson coefficient	0.2
Specific heat	0.72 x 10^3 J/(kg K)
Emissivity	0.837
Conductivity	1 W/(m K)

Active suction system gets air by inflow channel. Air goes in the inflow channel by passing through the glass panes of the door. To simulate this flow velocity outlet boundary condition was defined to the surface that contacts with the inflow channel. Air gets in the door from ambient atmosphere and goes out to the inflow channel of active suction system. The velocity value 2.18336 m/s was obtained as a result of the experiments.

Figure 2.3 shows boundary definitions of the model. Ambient atmosphere was defined as opening, symmetry surfaces were defined. Outer surfaces of the air model that is opening to ambient atmosphere was defined as opening boundary condition. Opening temperature was 25 º C. Buoyancy was defined. As it is seen from literature for turbulence model k-Epsilon turbulence model was defined.

Also for radiation model, from literature (Mistry, Ganapathi-subbu, Dey, Bishnoi et al. 2006) there were different radiation model options before defining it some studies were done. For radiation model different models were prepared and the results were close to each other for our model. Surface to surface radiation model was chosen for the study.

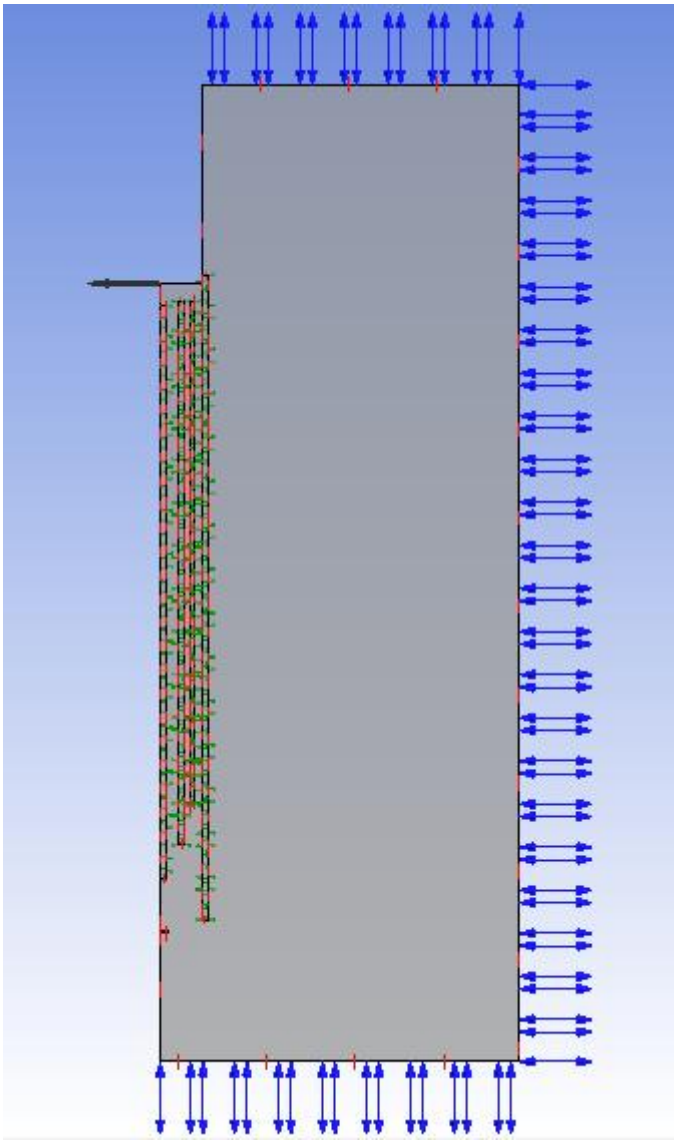


Figure 2.3 Definitions of the model.

Inner cavity of the oven was not modeled so temperature value which is obtained from the experiments defined to first glass inner surface that intersects with the oven inner cavity.

Emissivity coefficient of the all surfaces and interfaces was obtained. The surfaces that contact to the oven upper panel and the remaining surfaces were defined as wall.

2.5 Solver

After defining the initial conditions, number of iterations, analysis type and finishing the set up solver controls must be defined. In solver module residuals and solver process can be monitored. Figure 2.4 shows the heat transfer residuals. Heat transfer residuals are between 10^{-3} and 10^{-4} . Figure 2.5 shows the turbulence residuals that are below10^{-6}. Figure 2.6 shows the momentum and mass residuals that are below10^{-6}. To see the convergence of the solver and to see the average outer temperature of the fourth glass a monitor was created. This monitor results are shown in the Figure 2.7.

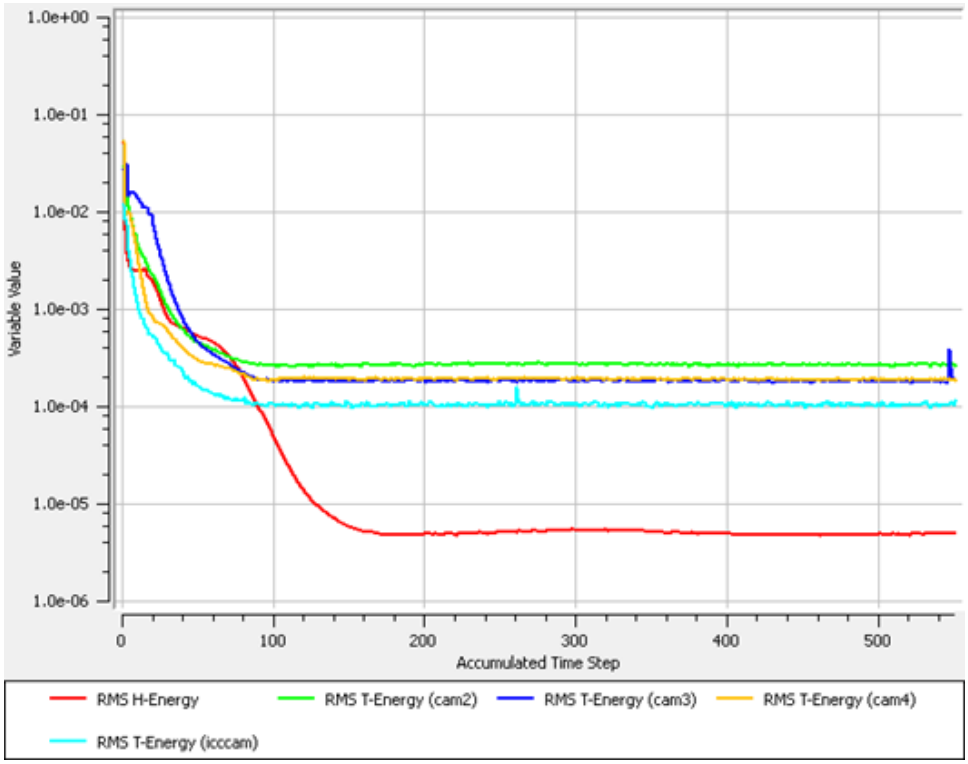


Figure 2.4 Heat transfer residuals.

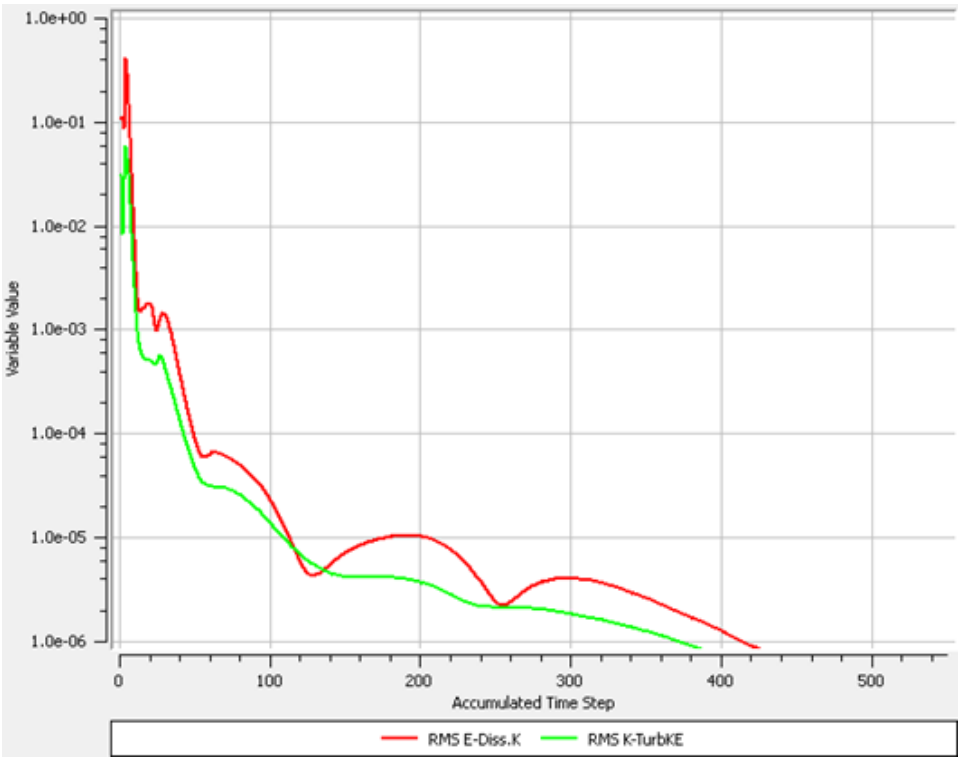


Figure 2.5 Turbulence residuals.

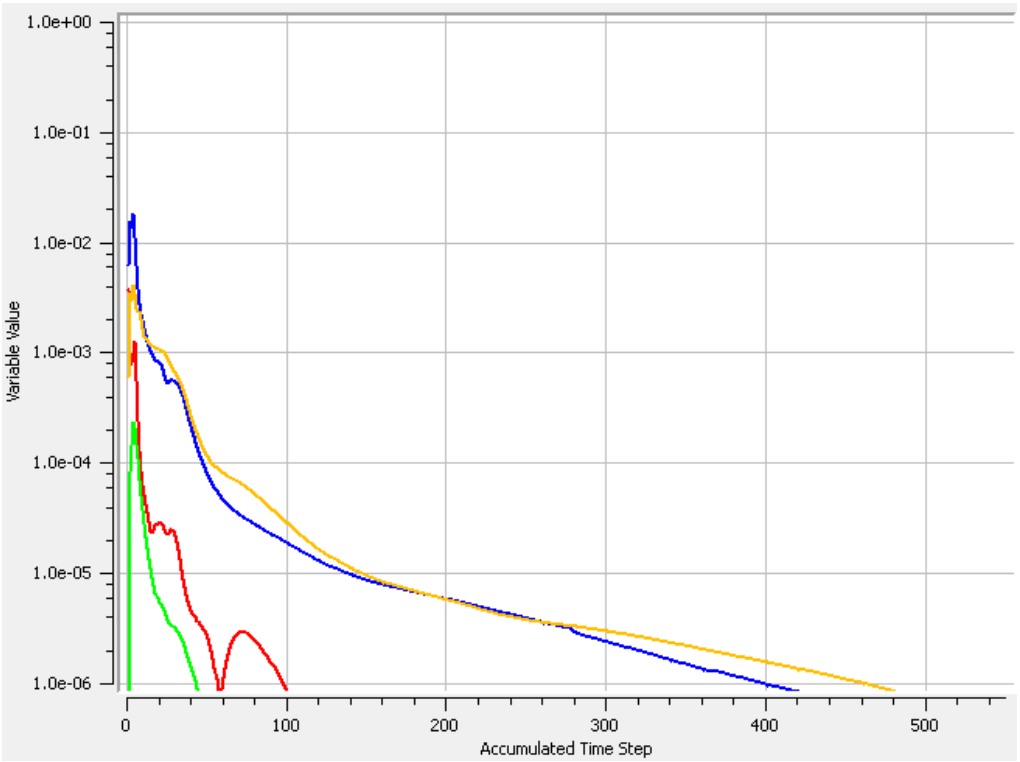


Figure 2.6 Momentum and mass residuals.

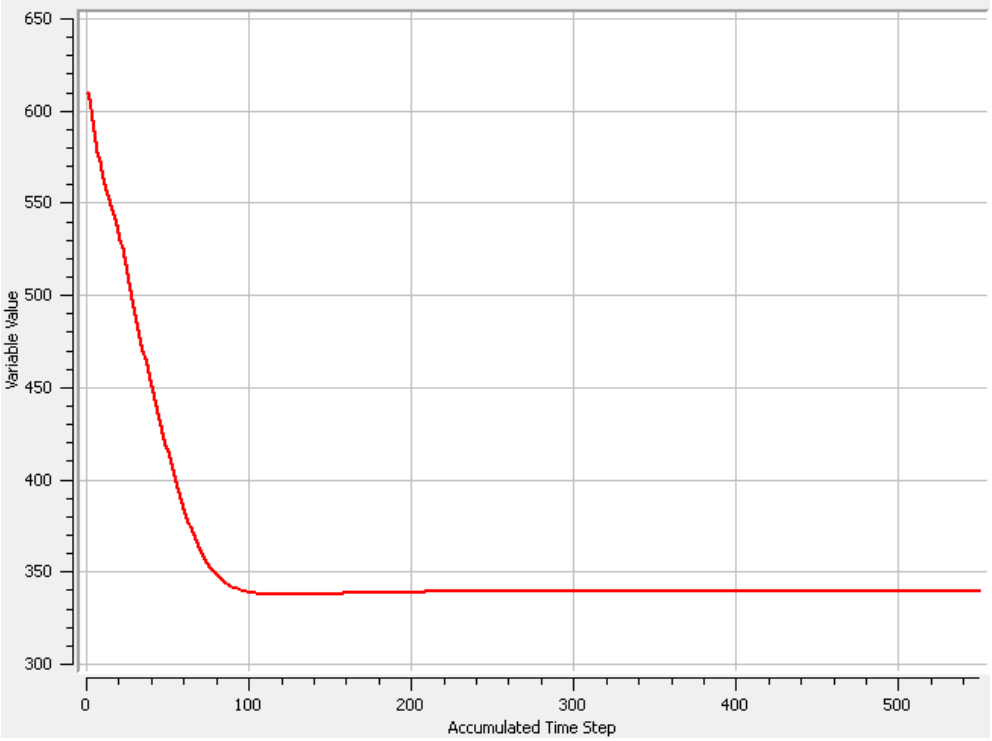


Figure 2.7 Average temperature at the outer surface of the fourth glass.

CHAPTER THREE
EXPERIMENTAL STUDY AND VALIDATION

3.1 Experimental Study of the Oven Door

To validate the CFD results experiments were carried out during the study. For validation and defining the boundary conditions temperature and velocity experiments were done. During the all experiments ambient temperature was 25˚C.

Temperature experiment was done during the pyrolytic cycle. In every five seconds data were saved to the computer by data logger. Nine thermocouples were placed properly to the first glass inner. Each pane had nine thermocouples. As it is shown in Figure 3.1 while thermocouples were being installed to the windows, the ones that are on the corners were 5 cm away from the both edges. Thermocouples were installed by 3 rows and 3 columns. The inner average temperature of the first glass was needed to define boundary condition for the model. For the prototype, pyrolytic mode lasts 90 minutes.

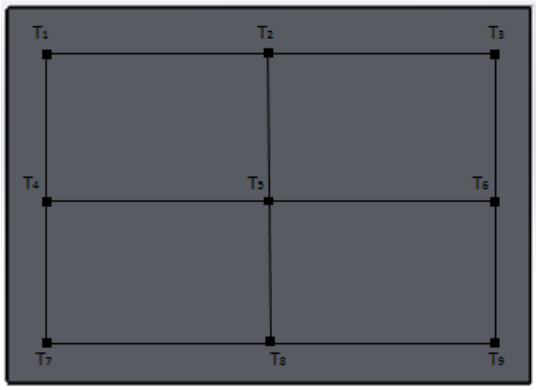


Figure 3.1 Locations of the thermocouples on the glass

In this study K type thermocouples which has continuous temperature range is 0 ˚C to 1100 ˚C, short term temperature range is b-180 °C to 1300 °C and tolerance is ±1.5 between −40 °C and 375 °C ±0.004×T between 375 °C and 1000 °C was used.

For velocity experiment velocity and temperature measurement probe were used. During this experiment data was saved in every 0.3 seconds. Six probes were placed to the inflow channel of the active suction unit where air goes in the channel. And four probes were placed to the outflow channel of the fan where air goes out to the ambient atmosphere.

3.2 Validation of the Numerical Study

Results of the numerical and experimental studies are shown in Figure 3.2 experimental results are the average of temperature values obtained from thermocouples. Experimental temperature values are from the average outer surface temperature of the each glass. The horizontal axis shows the number of glass since number one is the inner glass. Vertical axis is the temperature values in Kelvin.

The discrepancy is calculated by dividing the temperature difference of average surface temperature that are obtained from numerical and experimental result by the numerical result.

Average discrepancy of the model is 5.8 %. Since the first glass inner temperature is obtained from the experimental study, this temperature is not included to the average. This discrepancy is within acceptable limits, so that the numerical results of the model are reliable and can be studied on (Rek, Rudolf & Zun, 2012).

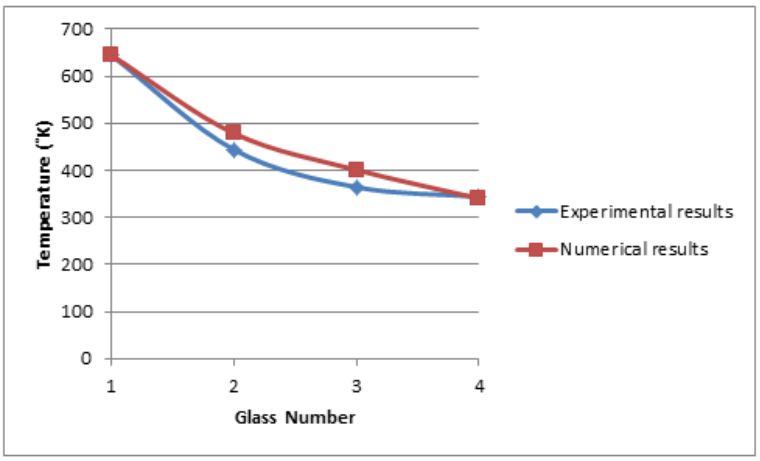


Figure 3.2 Results of the numerical and experimental studies.

CHAPTER FOUR
OPTIMIZATION OF DESIGN PARAMETERS

There are many variables that affect the heat transfer mechanism of the oven door. Heat transfer mechanism of the oven changes with even a small modification. Radiation, convection and conduction heat transfer quantities change by modifications. Modifications can be changing a door's height, air thickness between the doors, glass thickness, cooling air velocity, using low emissivity coating and etc. Parametric study provides to see the effect of the variables at different values.

4.1 Effect of the Glass Thickness

To see the effect of the glass thickness, thicknesses were changed from 3 mm to 4 mm. While these thicknesses were changing other parameters were fixed. Figure 4.1 shows the effect of the changing glass thicknesses. Vertical axis shows the average outer surface temperature of fourth glass in K.

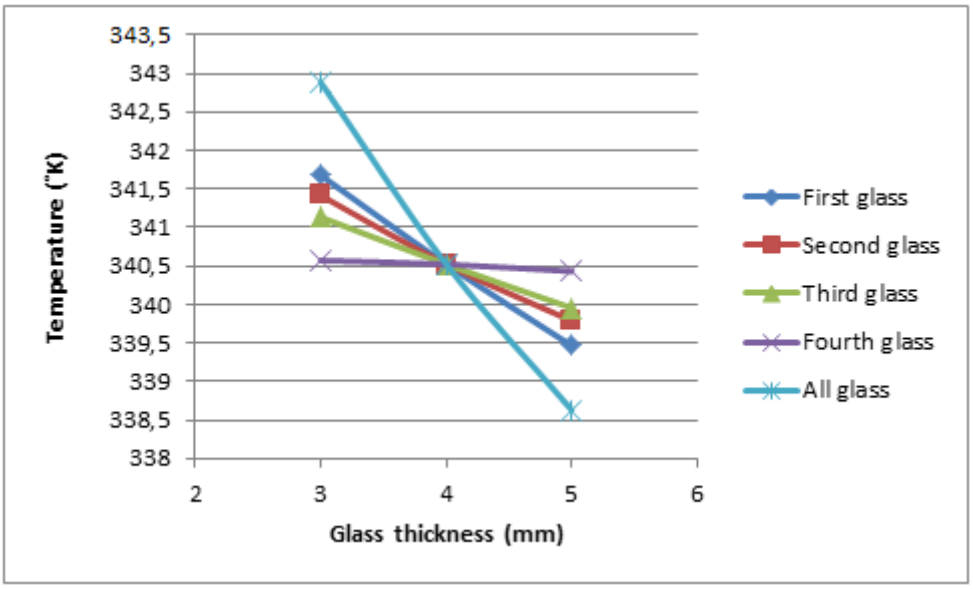


Figure 4.1 Effect of the glass thickness.

As it is seen from Figure 4.1 glass thicknesses don't have massive effect on the outer average temperature of fourth glass. But as it is seen change of thickness of the

first glass has greater effect than change of thickness of the second glass. Likewise change of thickness of the second glass has greater effect than change of thickness of the second glass. Effects of the glass thickness on the outer average temperature of fourth glass decreases as they get away from the oven cavity. As it is seen instead of changing each glass thickness, changing all glass thickness 2 mm, average temperature changes about 2 K.

4.2 Effect of the Air Gaps between the Panes

Air gaps between the glass panes affect the heat transfer mechanism. The air velocity of the active suction system was assumed fixed and analyses were done. While a parameter is changing other parameters were fixed to see the effect of chosen parameter.

4.2.1 Effect of the Gap between Glass Number 1 and 2

To see the effect of the air thickness between first and second glass on the average outer temperature of fourth glass of oven, thickness was changed from 1 mm to 16 mm. While this thickness was changing other gaps were fixed. This air gap is the closer to inner cavity of oven than second and third gap. Second gap is between second and third glass, third gap is between third and fourth glass. Effect of the air thickness between first and second glass is studied.

As it is seen from Figure 4.2 when the second glass closer to first glass outer average temperature of the fourth glass decreases. The air thickness between first and second glass has great effect on the average outer temperature of fourth glass. The temperature range is quite large, which is about 30 K.

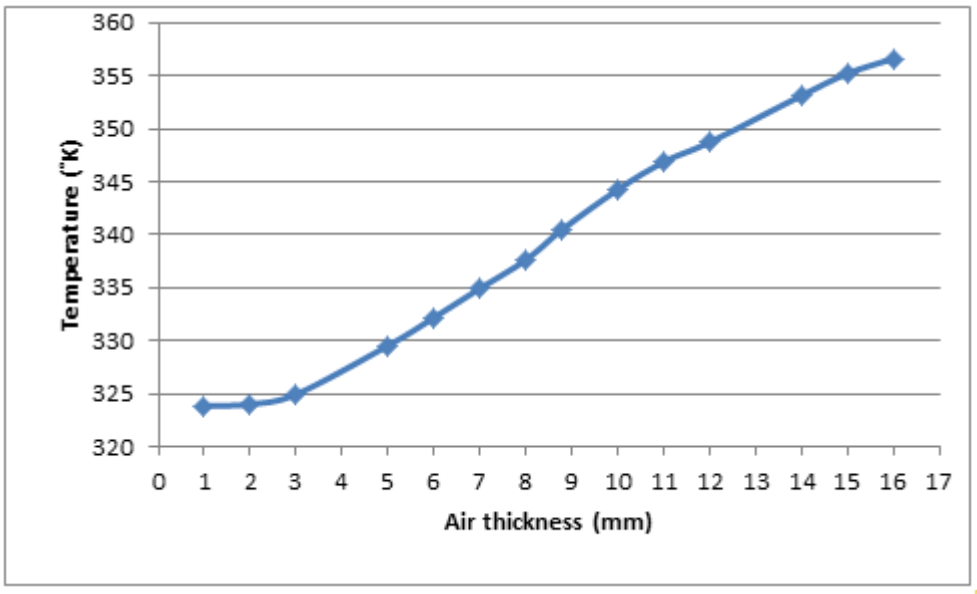


Figure 4.2 Effect of the air thickness between first and second glass.

4.2.2 Effect of the Gap between Glass Number 2 and 3

To see the effect of the air thickness between second and third glass, thickness was changed from 1 mm to 12 mm. While this thickness was changing other gaps were fixed.

As it is seen from Figure 4.3 when the third glass closer to second glass outer average temperature of the fourth glass decreases until a point then it starts to increases again. Where the air thickness is 5 mm the outer temperature goes to minimum. As it is seen between 3mm and 5 mm the temperature is quite close to each other. If the thickness of the door is wanted to be thinner other air thickness like 3 mm can be chosen instead of 5mm. Alternative design can be, if the outer temperature of fourth glass is not so critical or 2K can be ignored, 2mm of air thickness can be another choice.

As it is seen from Figure 4.2 and 4.3, effect of the air thickness between first and second glass is more than effect of the air thickness between second and third glass on the average outer temperature of fourth glass.

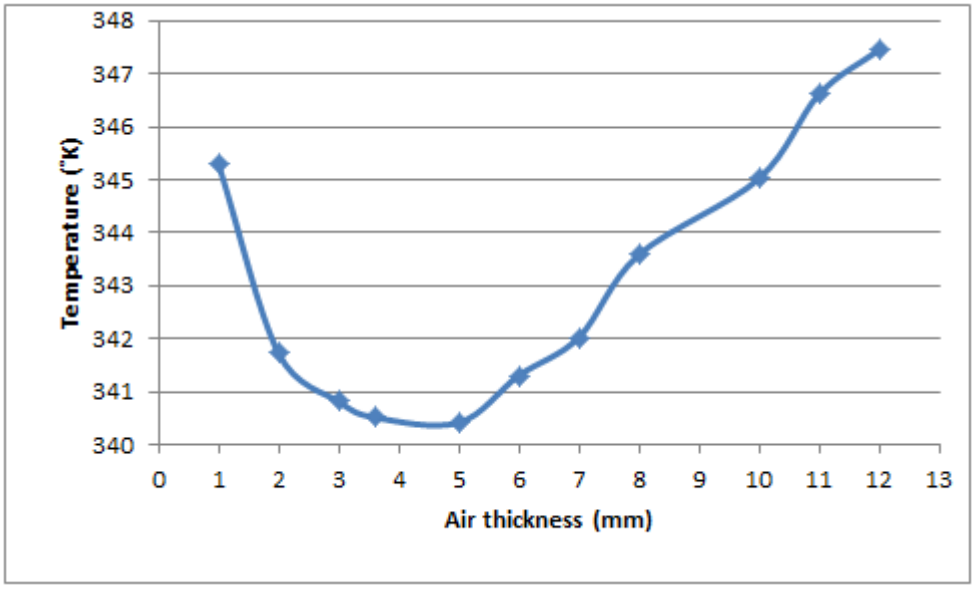


Figure 4.3 Effect of the air thickness between second and third glass.

4.2.3 Effect of the Gap between Glass Number 3 and 4

To investigate the effect of the air thickness between third and outer glass, thickness was changed from 1 mm to 12 mm. While this thickness was changing other gaps were fixed.

As it is seen from Figure 4.4 while the air thickness is increasing, the outer average temperature of the fourth glass decreases until 4 mm then it starts to increase with a low slope until 8 mm. After 8 mm the slope of the increasing temperature gets high. Optimum design point can be 3-4mm air gap between second and third glass.

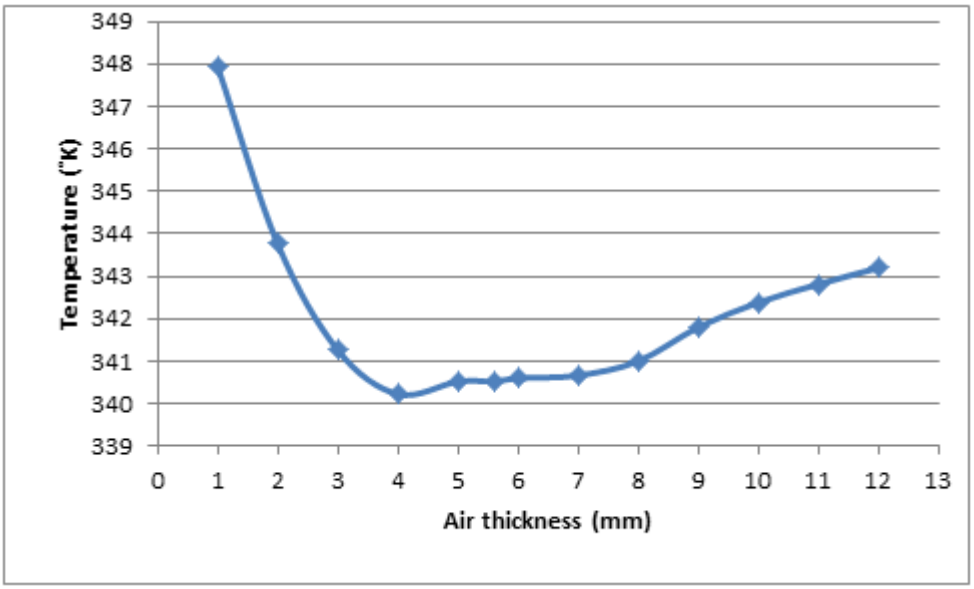


Figure 4.4 Effect of the air thickness between third and outer glass.

The effect of the air thickness between second and third glass is nearly equal to effect of the air thickness between third and fourth glass.

4.3 Effect of the Glass Heights

After investigating the effect of air thickness between the glass panes effect of glass height was studied. Since the all glass widths, lengths and depths are not changed only the vertical positions of the glass are changed. Other parameters except the glass height are fixed. The position of inner and outer glass is fixed due to structure and location of the oven door. So, second and third glass heights are the parameters for this study. The “0” position is the original position of the glass and “+X mm” indicates glass is moved up by X mm. “-X mm” indicates that glass is moved down by X mm. while glass was moving up they weren’t blocking the air flow between the panes they were resisting air flow.

4.3.1 Effect of the Second Glass Height

To see the effect of second glass height on the outer average temperature of the fourth glass, second glass was moved 9 mm downwards and 12 mm upwards. Door structure limits the movements of the glass.

As it is seen from Figure 4.5 when the second glass moves down until nearly - 4 mm temperature decreases but after 4 mm it starts to increase again. Optimum glass height can be 4 mm downwards of second glass.

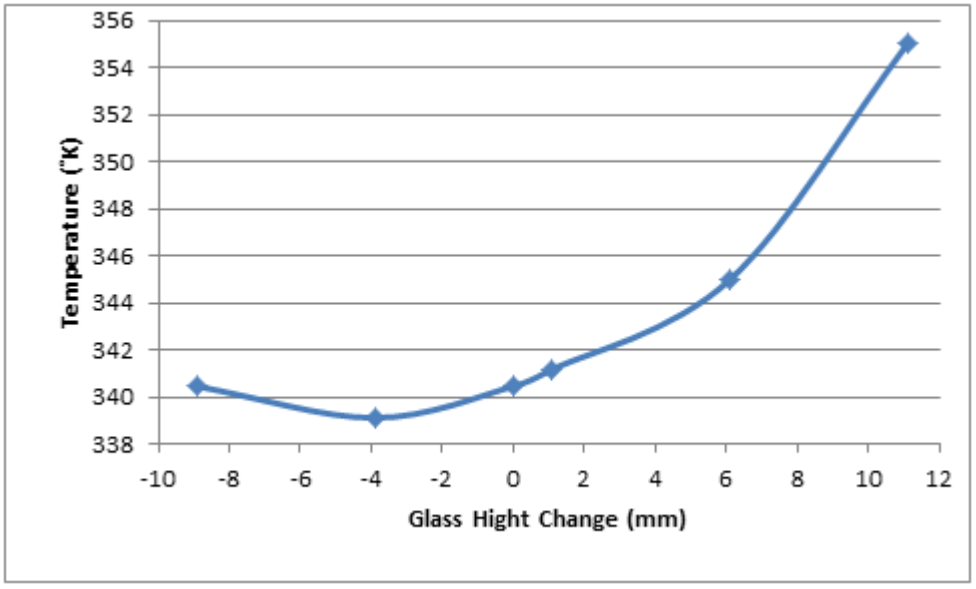


Figure 4.5 Effect of the second glass height.

4.3.2 Effect of the Third Glass Height

To see the effect of third glass height on the outer average temperature of the fourth glass, third glass was moved 16.5 mm downwards and 13.5 mm upwards. Effect of the third glass height is shown in Figure 4.6. As it is seen it appears to have less effect on the outer average temperature of the fourth glass than other glass effects. And the temperature change is nearly linear and horizontal.

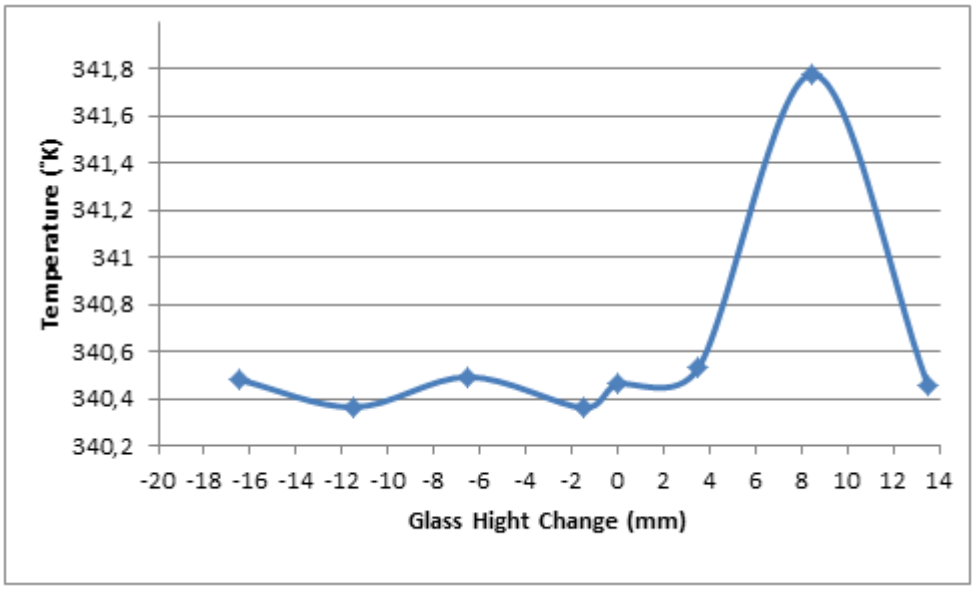


Figure 4.6 Effect of the third glass height.

4.4 Effect of the Low Emissivity Coating

Radiation is the most dominant heat transfer mode in a domestic oven. But, since pyrolytic type ovens inner temperatures much higher than conventional domestic oven radiation has massive effect on heat transfer mechanism.

Low emissivity coating was used to reduce the outer average temperature of the fourth glass. In the oven inner cavity thermal radiation that is emitted by the heating elements gets absorbed by the food, walls and oven door. Low emissivity improves the thermal efficiency by absorbing less thermal radiation and this also allows inside air temperature of the oven react more quickly (Shaughnessy & Newborough, 2000)

Thermophysical properties of the Low-e glass are shown in Table 4.1. Low emissivity coating can be applied to the all surfaces of the glass panes but because of economic reasons low-e glazing is not used on the fourth glass. As it can be seen from the results glazing effect at different surfaces are different. And glazing was not applied to the inner surface of the first glass because of the effect to the visibility in long-term usage.

To see the effect of low emissivity coating on the average outer temperature of fourth glass surface, fifteen models were prepared. Prepared models can be seen in Table 4.2. Model zero is the uncoated original model which is unmodified. Thermophysical properties of the Low-e coating are fixed and all glazing have same emissivity value.

Table 4.1 Thermophysical properties of the Low-e glass.

Property	Value
Surface resistance (Ω/sq)	20
Thickness of the coating (nm)	350-400
Emissivity	0.22
IR-waviness of 2500 nm (%)	≥60
Temperature resistance 10.000h (˚C)	280
Roughness rms in nm	13-18

Table 4.2 Low emissivity coating application sides of the models prepared.

	Low Emissivity Coating Application Side						
	Glass 1	Glass 2		Glass 3		Glass 4	
	Side	Side		Side		Side	
MODEL NO	Outer	Inner	Outer	Inner	Outer	Inner	Outer
0	-	-	-	-	-	-	-
1	Lowe	-	-	-	-	-	-
2	-	Lowe	-	-	-	-	-
3	-	-	Lowe	-	-	-	-
4	-	-	-	Lowe	-	-	-
5	-	-	-	-	Lowe	-	-
6	-	-	-	-	-	Lowe	-
7	-	-	-	-	-	-	Lowe
8	-	Lowe	-	Lowe	-	-	-
9	-	Lowe	-	-	Lowe	-	-
10	-	-	Lowe	Lowe	-	-	-
11	-	-	Lowe		Lowe	-	-
12	Lowe	-	Lowe	Lowe	-	-	-
13	Lowe	-	Lowe	-	Lowe	-	-
14	Lowe	Lowe	-	-	Lowe	-	-
15	Lowe	Lowe	-	Lowe	-	-	-

Temperature distribution of the first model which is uncoated is shown in Figure 4.7. Outer average temperature of the fourth glass is 340.477 K. The air thickness and all other dimensions are the same as its original. The velocity vectors of the uncoated model are shown in Figure 4.8.

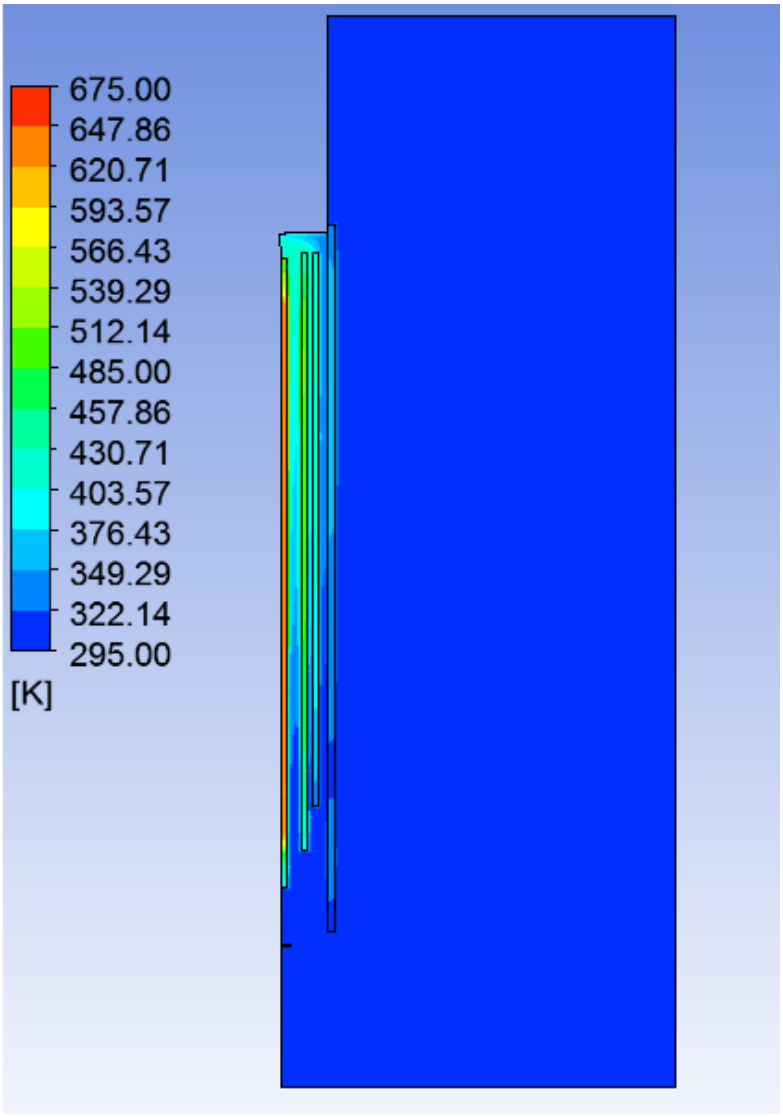


Figure 4.7 Temperature contour of the uncoated original model.

As it can see from Figure 4.8, 4.9 and 4.10 velocity of the air between first and second glass is higher than the other air gaps. The ambient air which contacts to the outer surface of the oven door moves by the effect of natural convection. This movement can be seen from Figure 4.9.

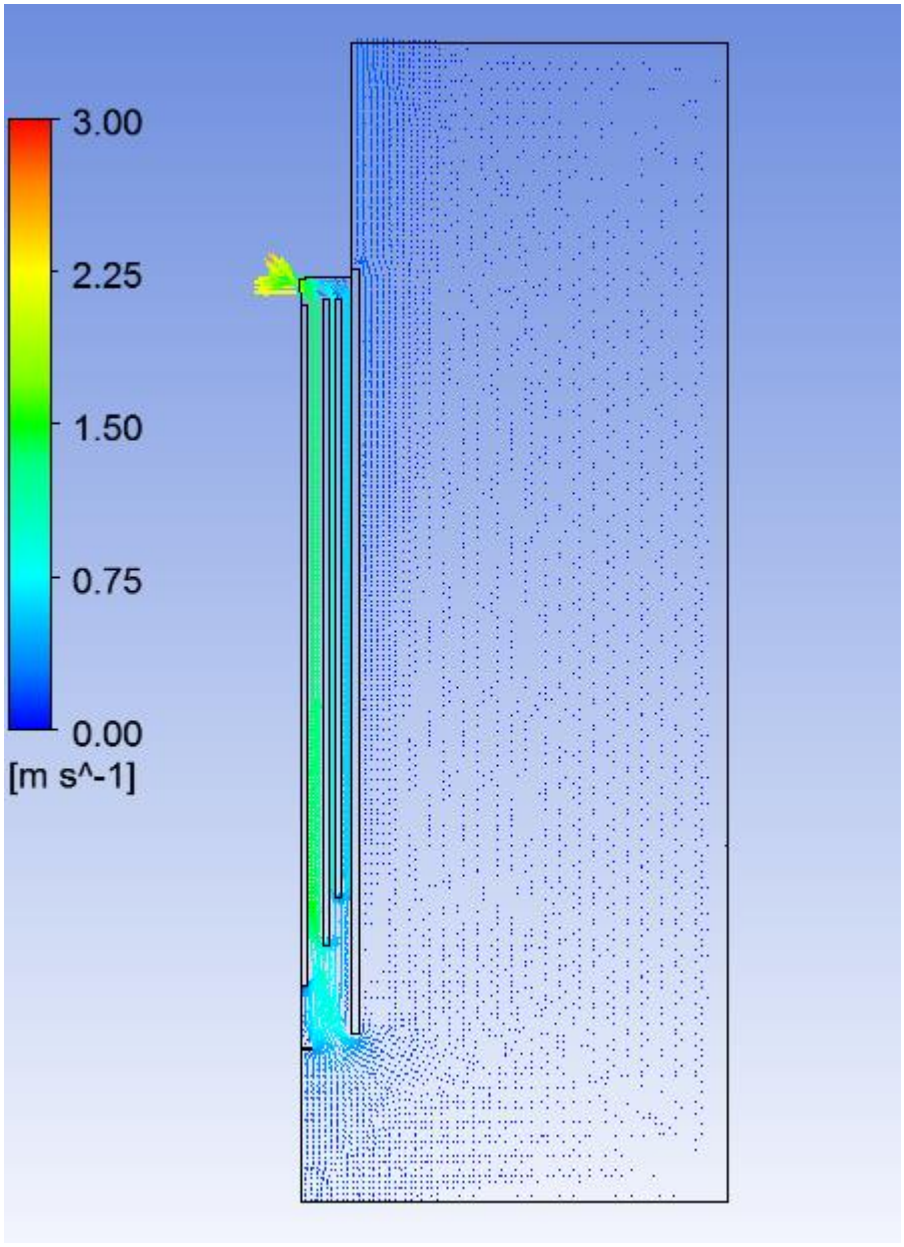


Figure 4.8 Velocity vectors of the uncoated original model.

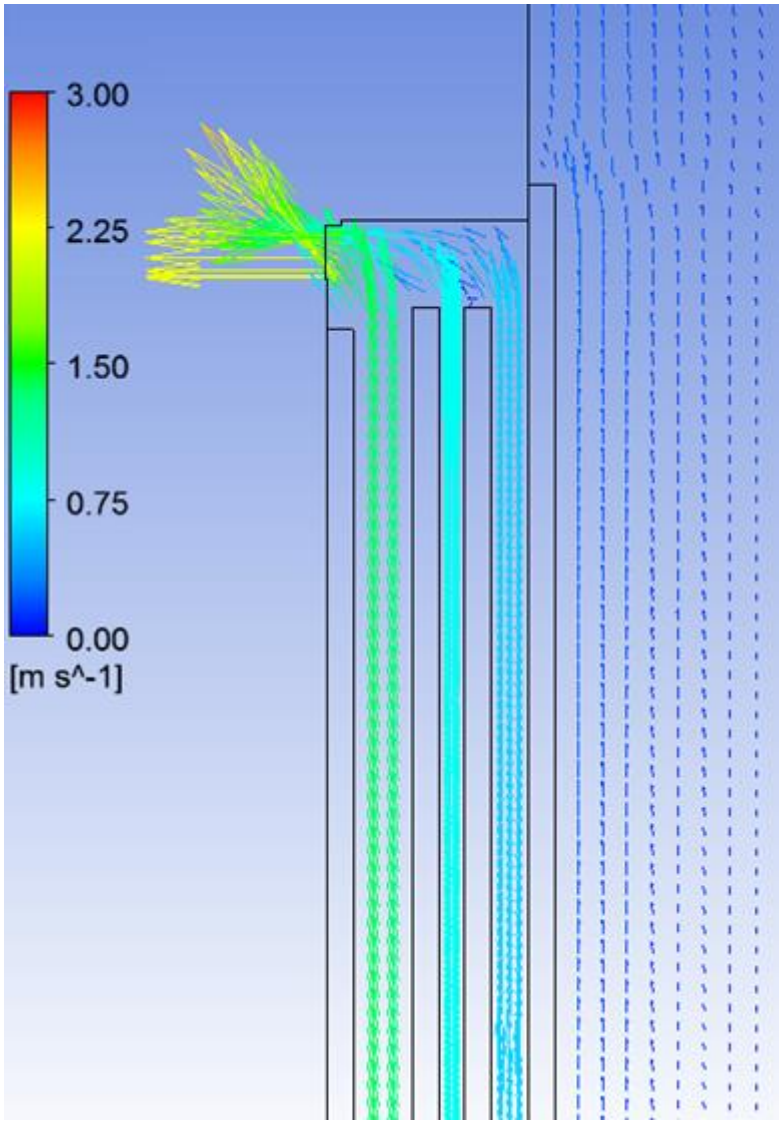


Figure 4.9 Velocity vectors of the flow between the glass panes and in the inlet of suction channel.

Figure 4.10 shows the suction of the air and distribution of air to the air gaps between panes.

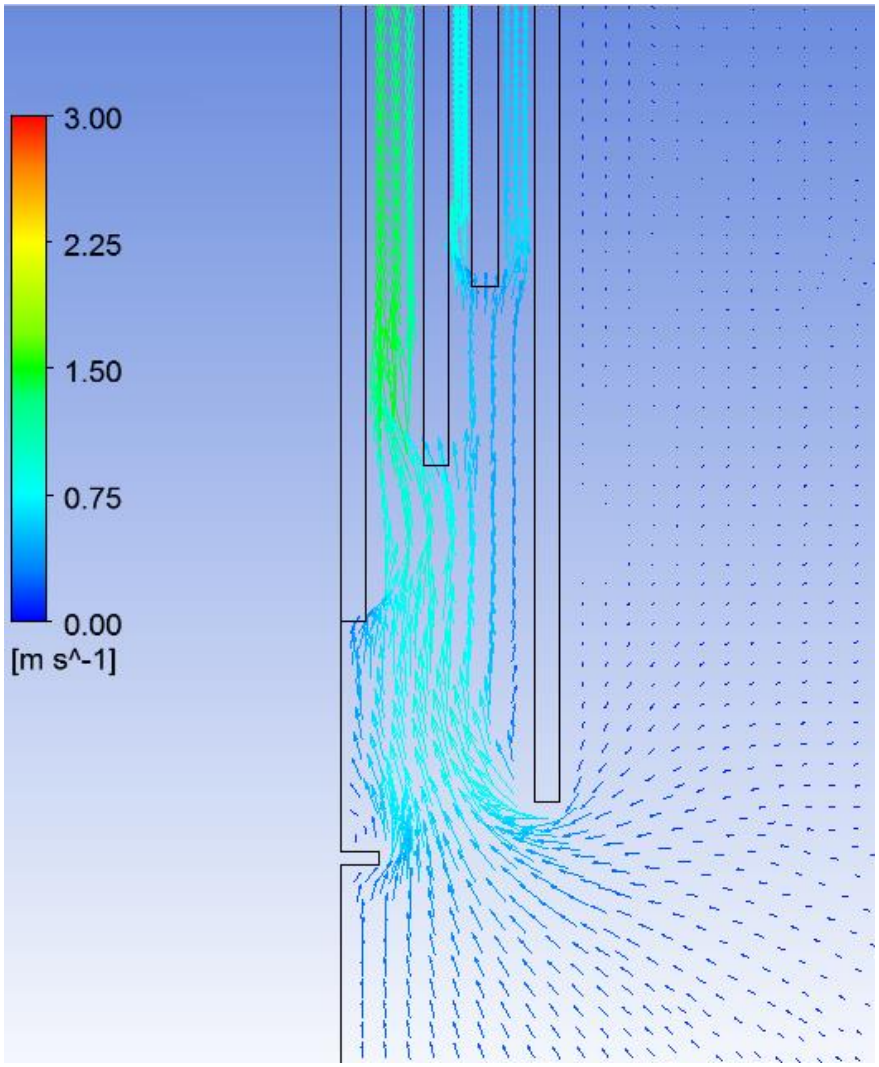


Figure 4.10 Velocity vectors of the air entering between the glass.

4.4.1 Effect of the Low Emissivity Coating on the Outer Side of First Glass

Low emissivity coating applied to the outer surface of first glass was modeled. Figure 4.11 shows the temperature contour of the model. In this study outer average temperature of the fourth glass is 314.551 K. This model is first model from the Table 4.2. As it is seen when the coating applied to the outer side of first glass second third glass temperatures are lower than uncoated model. Radiation that is emitted from the oven heaters causes heating glass.

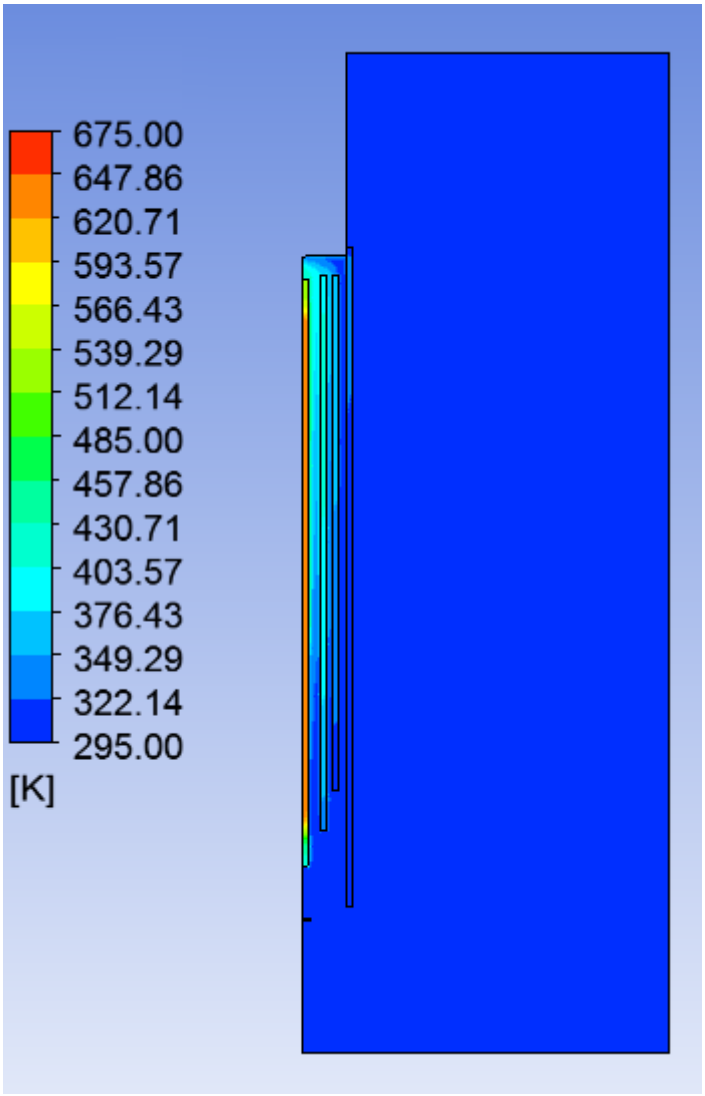


Figure 4.11 The temperature contour of the first model which has low emissivity coating on the outer side of first glass.

Velocity vectors of the models which have low emissivity coatings have same velocity vectors of the uncoated model.

4.4.2 Effect of the Low Emissivity Coating on the Inner Side of Second Glass

Low emissivity coating applied to the inner surface of second glass was modeled. Figure 4.12 shows the temperature contour of the model. In this study outer average temperature of the fourth glass is 318.456 K. This model is second model from the Table 4.2. The effect of the applying low emissivity coating to the inner side of second glass is less than applying the coating on the outer side of first glass.

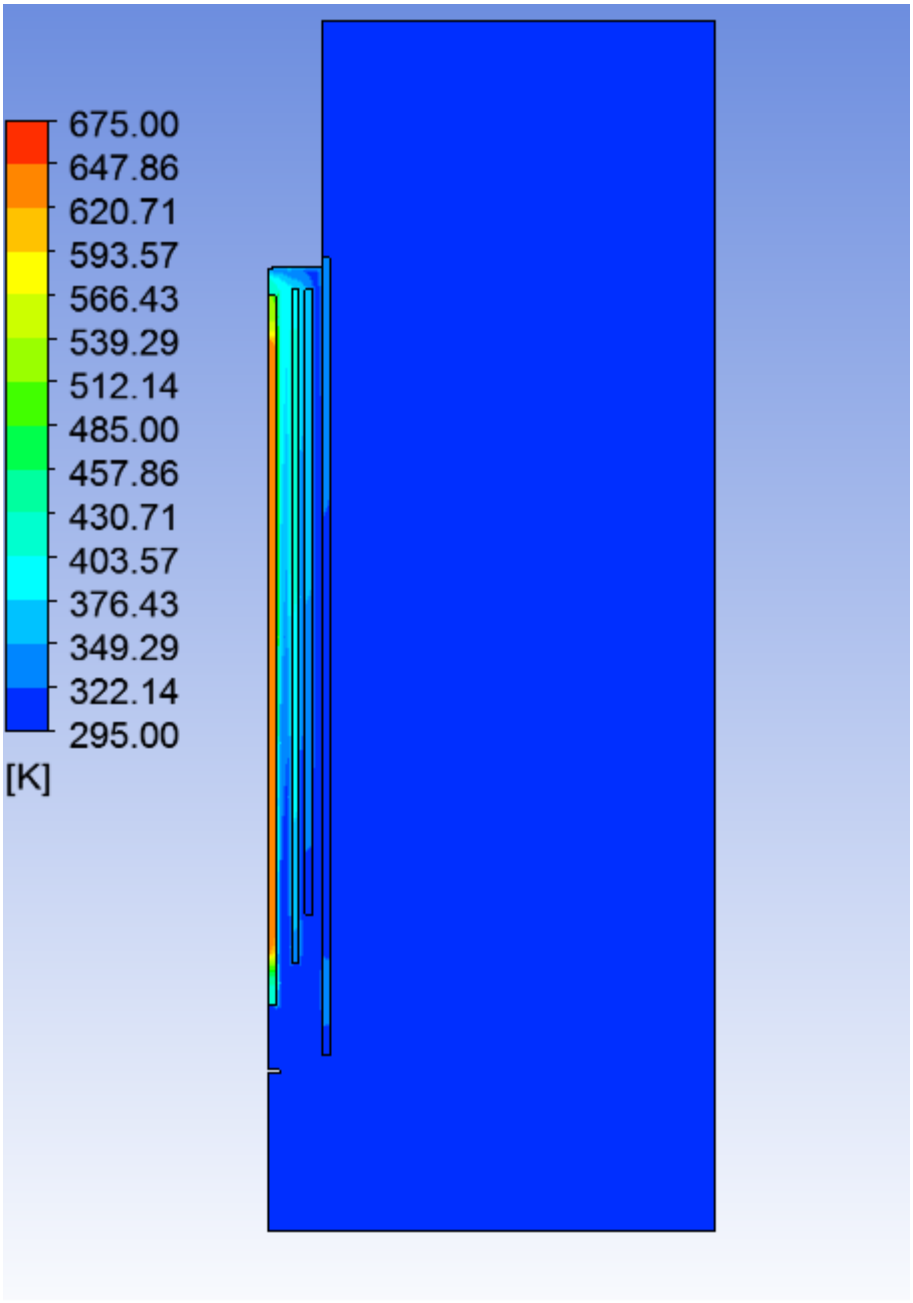


Figure 4.12 The temperature contour of the second model which has low emissivity coating on the inner side of second glass.

Outer glass height is more than the other glass due to covering the other glass and door inner structure. Since the coating was applied to the second glass, the areas on the fourth glass that second glass cannot cover by coating have higher temperatures comparing to lower region of the glass. This effect can be seen on Figure 4.13b.

As it is seen from Figure 4.13a, outer average temperature of the fourth glass is higher than the previous models.

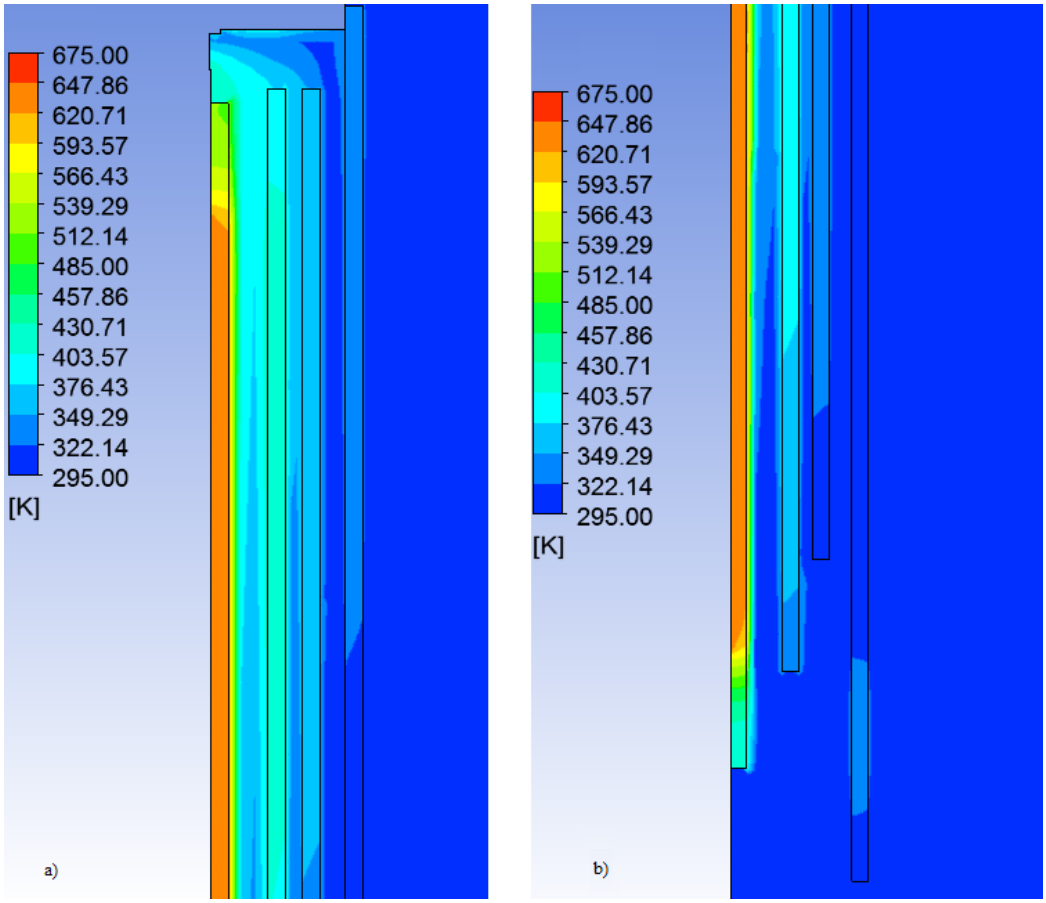


Figure 4.13 Upper side (a) and down side (b) temperature contours of the second model which has low emissivity coating on the inner side of second glass.

4.4.3 Effect of the Low Emissivity Coating on the Outer Side of Second Glass

After seeing the effect of applying the coating to the inner surface of second glass, low emissivity coating applied to the outer surface of second glass was modeled. This model is third model from the Table 4.2. In this study outer average temperature of the fourth glass is 325.459 K. The effect of the applying low emissivity coating to the outer side of second glass is less than applying the coating on the outer side of first glass and second glass inner side.

It can be said that from this results as the coating side gets away from the oven effect of it decreases. Figure 4.14 shows the temperature contour of the model.

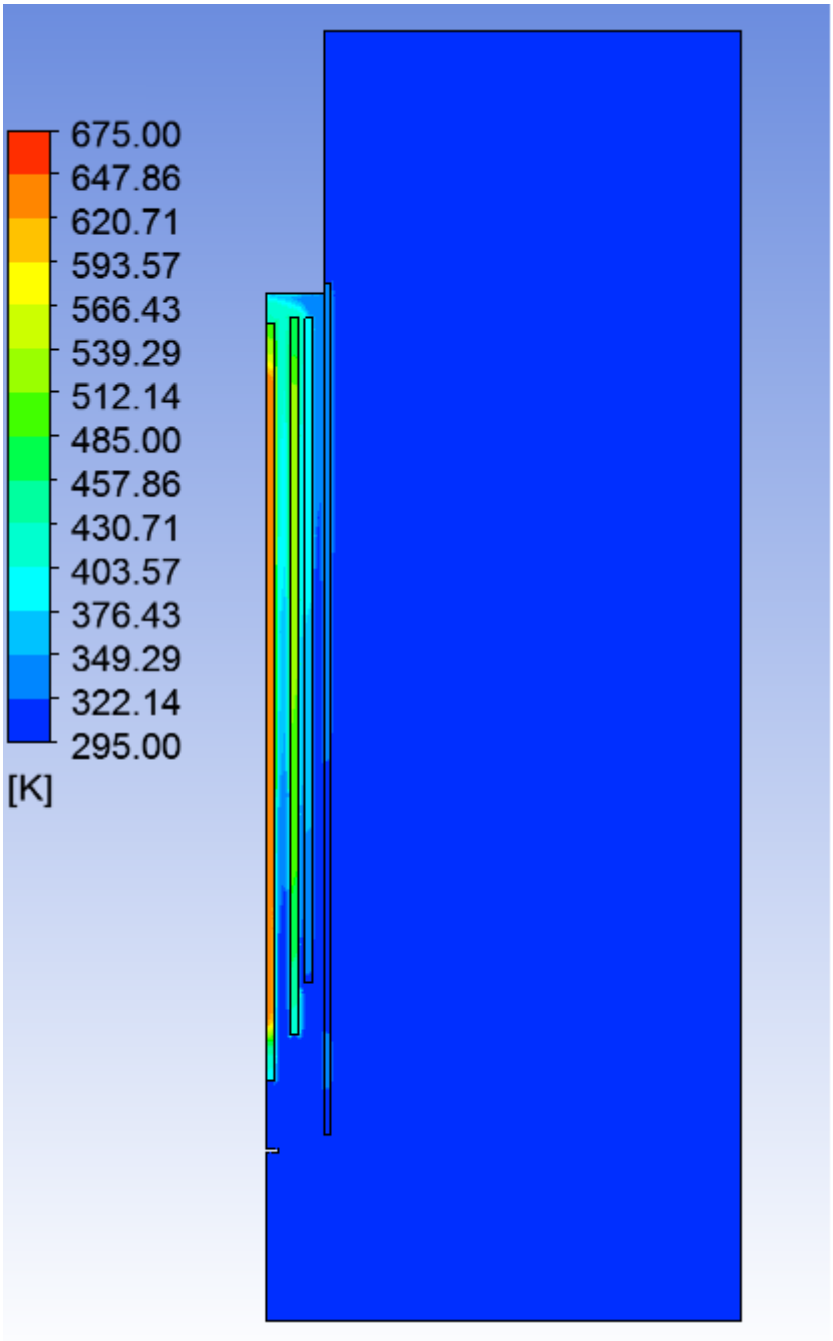


Figure 4.14 The temperature contour of the third model which has low emissivity coating on the outer side of second glass.

As it is seen from Figure 4.15, the outer average temperature of the fourth glass is higher than previous models. When we compare Figure 4.11a and 4.15a, we can see the temperature increasing.

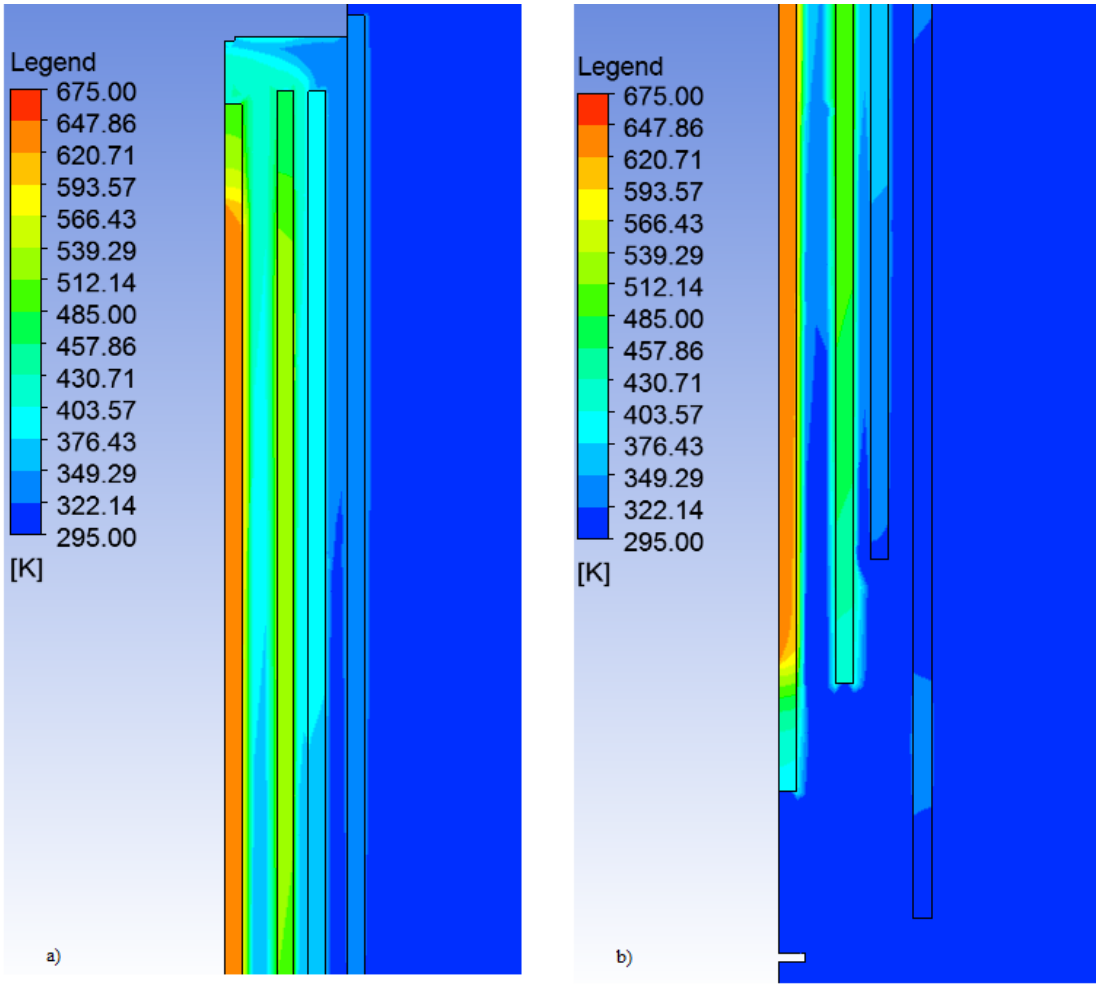


Figure 4.15 Upper side (a) and down side (b) temperature contours of the third model which has low emissivity coating on the outer side of second glass.

4.4.4 Effect of the Low Emissivity Coating on the Inner Side of Third Glass

Low emissivity coating applied to the inner surface of third glass was modeled. Figure 4.16 shows the temperature contour of the model. This model is fourth model from the Table 4.2. In this study outer average temperature of the fourth glass is 327.181 K. The effect of the applying low emissivity coating to the inner side of third glass is less than previous coating applications. Figure 4.17a and Figure 4.17b shows the detailed temperature distribution of the model. As it is seen comparing to

the previous coating applications high temperatures are present at the oven door cavity.

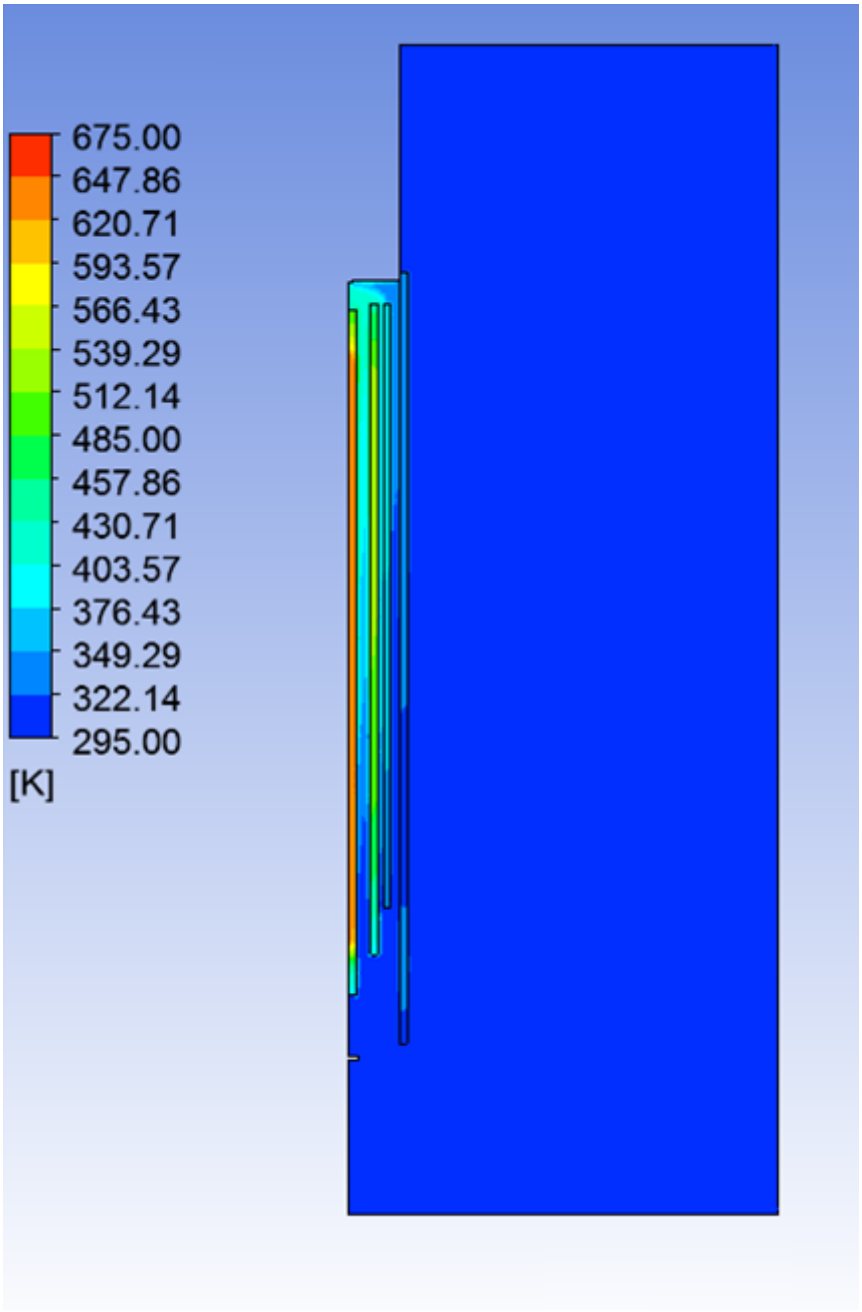


Figure 4.16 The temperature contour of the fourth model which has low emissivity coating on the inner side of third glass.

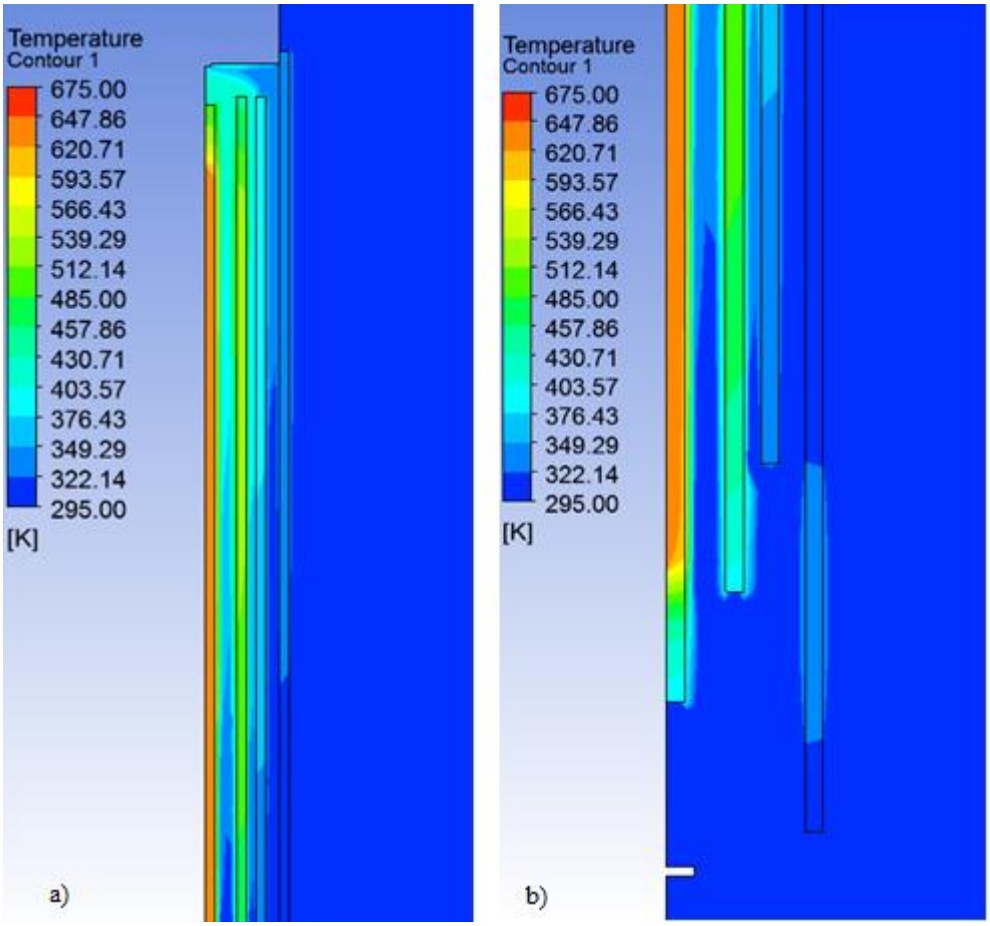


Figure 4.17 Upper side (a) and down side (b) temperature contours of the fourth model which has low emissivity coating on the inner side of third glass.

4.4.5 Effect of the Low Emissivity Coating on the Outer Side of Third Glass

After seeing the effect of low emissivity coating applied to the inner surface of third glass, a model which has low emissivity coating on the outer side was modeled. This model is fifth model from the Table 4.2. Figure 4.18 shows the temperature contour of the model. In this study outer average temperature of the fourth glass is 326.505 K. This Temperature is less than previous model outer average temperature of fourth glass which was 327.181 K Figure 4.19a and Figure 4.19b shows the detailed temperature distribution of the model. As it is seen comparing to the previous coating applications high temperatures are present.

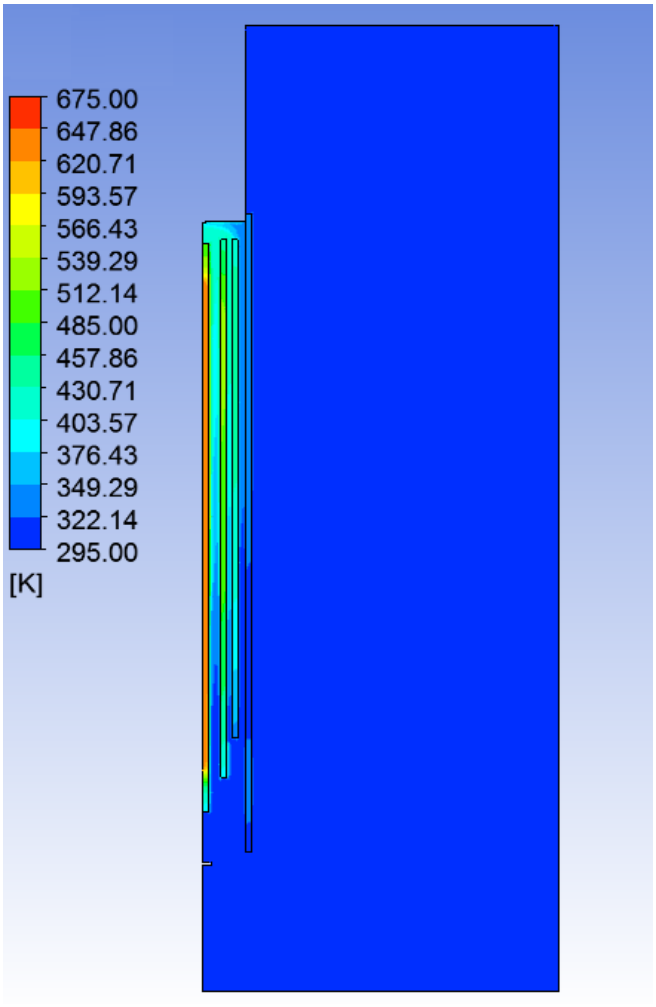


Figure 4.18 The temperature contour of the fifth model which has low emissivity coating on the outer side of third glass.

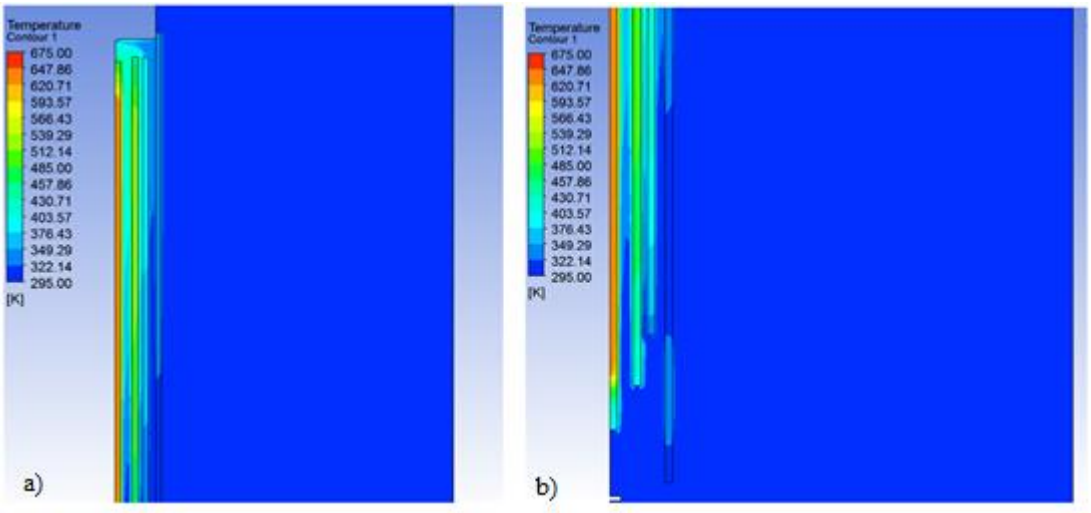


Figure 4.19 Upper side (a) and down side (b) temperature contours of the fifth model which has low emissivity coating on the outer side of third glass.

4.4.6 Effect of the Low Emissivity Coating on the Inner Side of Fourth Glass

Fourth glass is the outer glass of the oven door. A model that has low emissivity coating on the inner side of fourth glass was prepared. This model is sixth model from the Table 4.2. Outer temperature of the glass is 322.314 K this temperature is lower than applying the coating to the inner, outer side of third glass and outer surface of the second glass. Figure 4.20 shows the temperature contour of the model. Figure 4.20a and Figure 4.20b shows the detailed temperature distribution of the model.

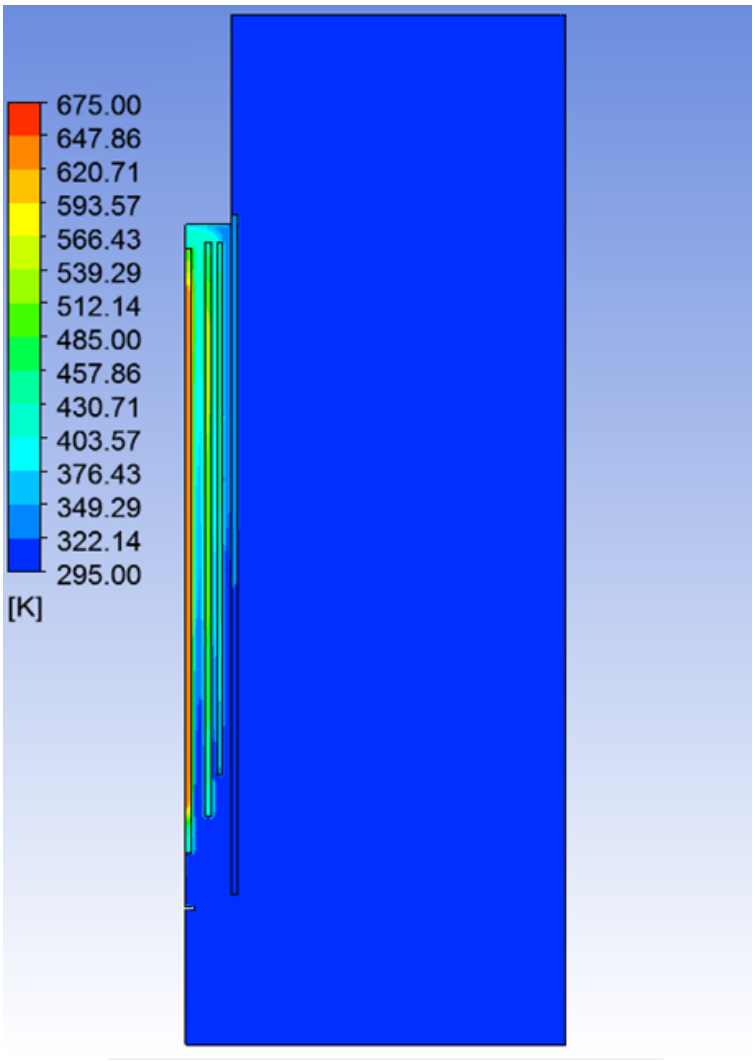


Figure 4.20 The temperature contour of the sixth model which has low emissivity coating on the inner side of fourth glass.

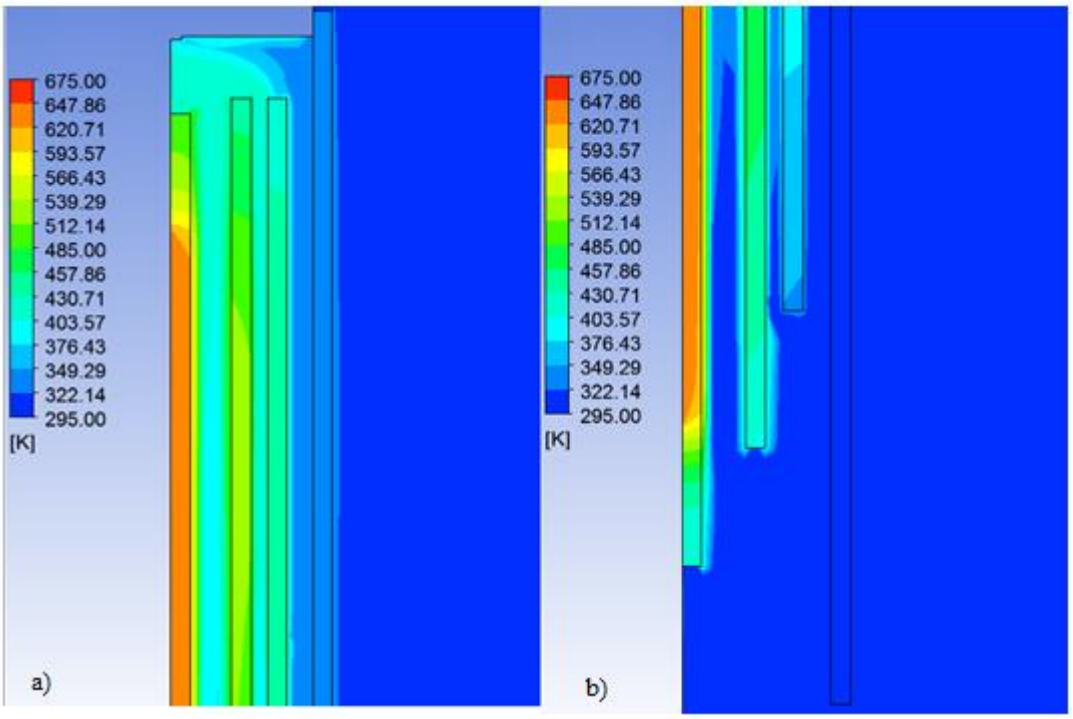


Figure 4.21 Upper side (a) and down side (b) temperature contours of the sixth model which has low emissivity coating on the inner side of fourth glass

As it can be seen from Figure 4.20 temperature of this model is lower than the previous model that has coating on the outer side of third glass. From Figure 4.21a and 4.21b the temperature rise of the fourth glass bottom which was present at previous model is not present at this model. This temperature rise was seen the models that the coating cannot cover this area, due to glass height that coating applied.

4.4.7 Effect of the Low Emissivity Coating on the Outer Side of Fourth Glass

A model that has low emissivity coating on outer side of the outer glass was prepared. Outer temperature of the glass is 355.112 K. This model is seventh model from the Table 4.2. This temperature is higher than previous models those are with coated ones and uncoated model. Figure 4.22 shows the temperature contour of the model. Figure 4.23a and Figure 4.23b shows the detailed temperature distribution of the model.

As it can be seen from Figure 4.22, temperature distribution of the model is higher than previous models. Since the coating is applied to the outer surface radiation effects can be seen first, second, third glass and inner sides of the outer glass.

Figure 4.23a shows upper side of the model, outer glass surface temperature is higher and from Figure 4.23b bottom sides of the glass shows the same result as the upper side.

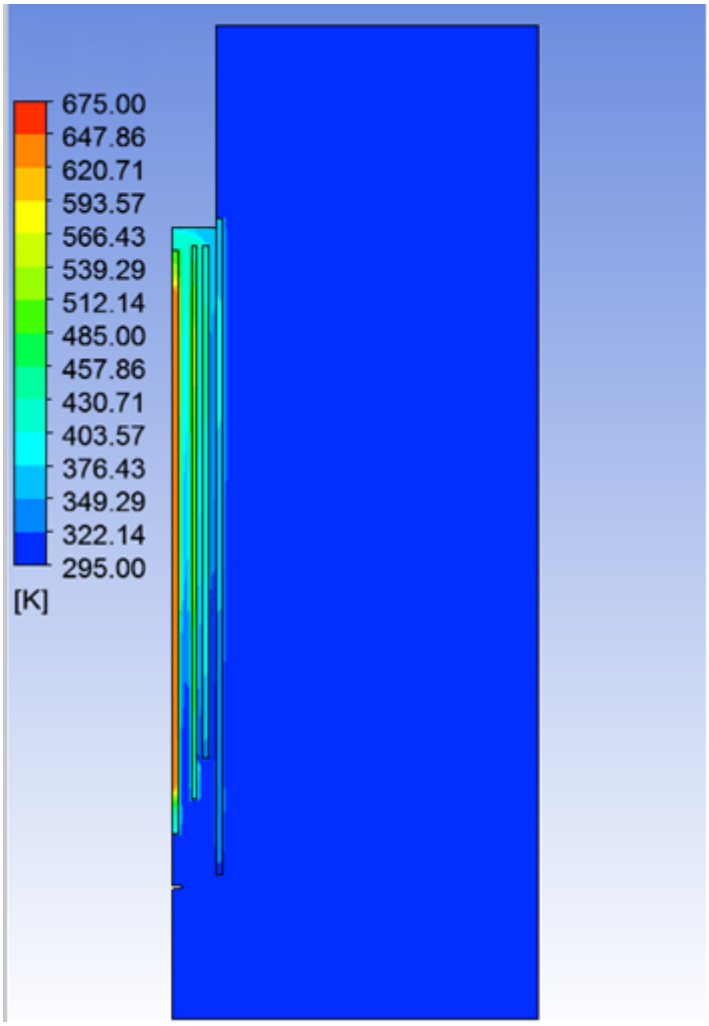


Figure 4.22 The temperature contour of the seventh model which has low emissivity coating on the outer side of fourth glass

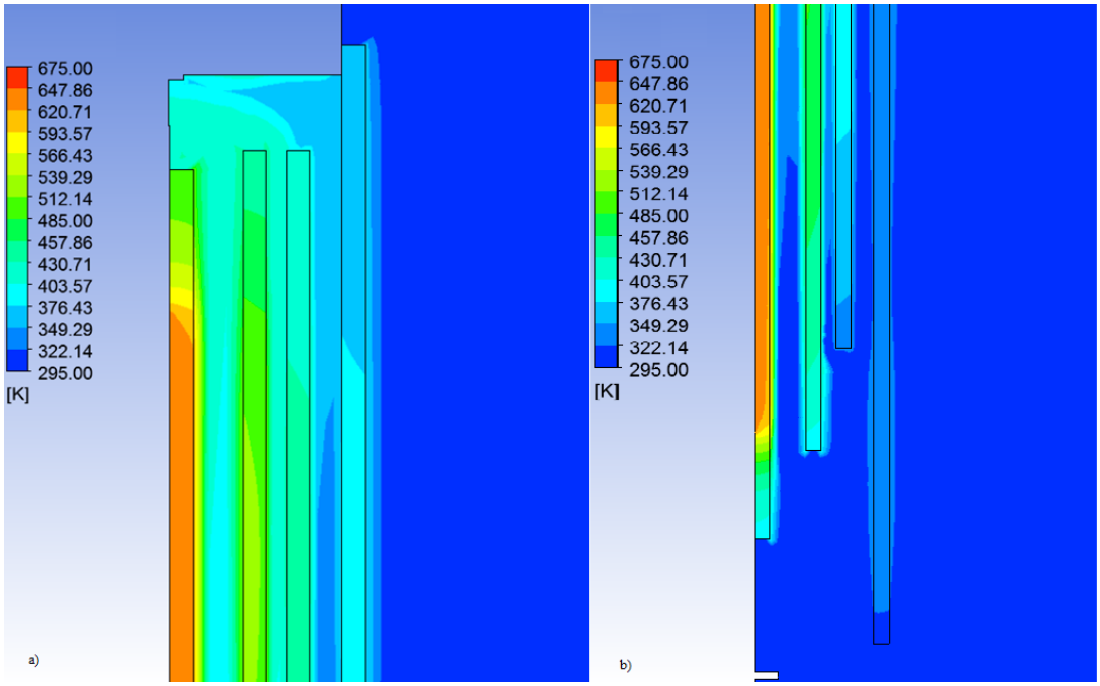


Figure 4.23 Upper sides (a) and down side (b) temperature contours of the seventh model which has low emissivity coating on the outer side of fourth glass.

4.4.8 Effect of the Low Emissivity Coating on the Inner Sides of Second and Third Glass

Low emissivity glazing can be applied to the all sides of the oven glass panes. Previous models had low emissivity coating on only one glass pane side. For this study a model was prepared that has coating on the inner side of second and third glass. This model is eighth model from the Table 4.2.

The outer average temperature of the fourth glass is 313.558 K. This temperature is lower than previous models. When low emissivity glazing was applied to outer side of first glass, the outer average temperature of the fourth glass surface was 314.551 K. The temperature difference between these two models is about 1 K. Instead of using two coated glass (Coating on the inner side of second and third glass.) using glazing outer side of first glass can be alternative choice. This is also economic an economic choice.

Figure 4.24 shows the temperature contour of the model that is prepared. As it is seen temperatures are relatively lower than other models.

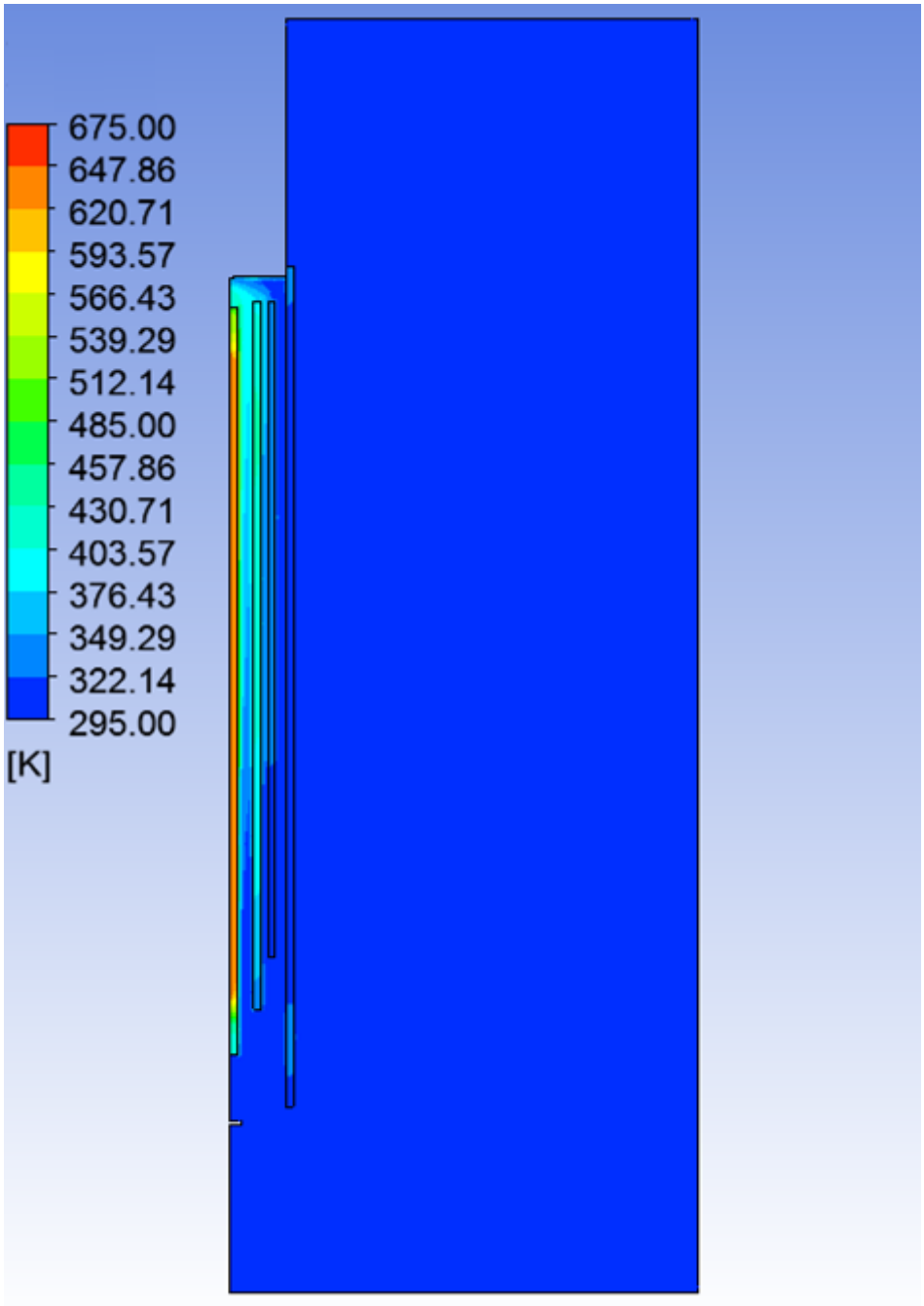


Figure 4.24 The temperature contour of the eighth model which has low emissivity coating on the inner side of second and glass.

Figure 4.25a shows upper side of the model, outer glass temperature is relatively lower than previous models. From Figure 4.25b bottom sides of the fourth glass

temperature is higher than middle side, radiation causes this because the coatings on the inner sides of second and third glass cannot cover fourth glass bottom and upper sides. This is because first, second and third glass length are lower than fourth glass and coating applied to first and second glass and also glass are not aligned from bottom sides.

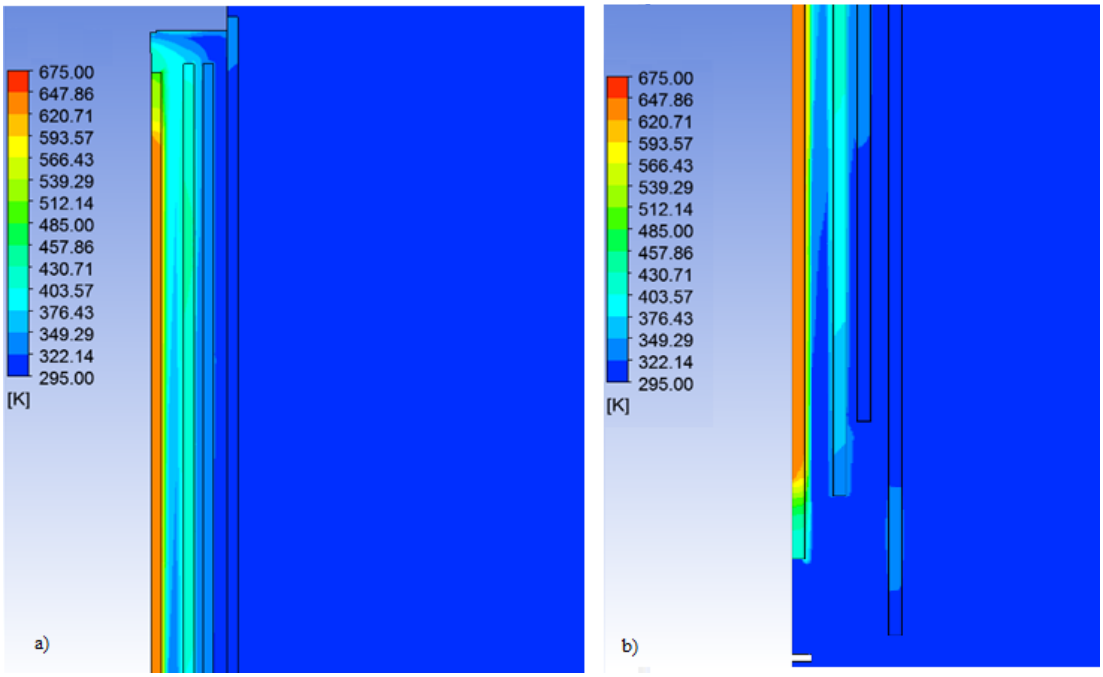


Figure 4.25 Upper sides (a) and down side (b) temperature contours of the eighth model which has low emissivity coating on the inner side of second and glass.

Figure 4.25a shows the shows upper side of the model, as it is seen upper side of the fourth glass temperature is higher than the middle side of the oven. This is because velocity vectors of the active suction air are low at this are. Because of low velocity vectors, heat transfer rate by convection decreases at this area.

4.4.9 Effect of the Low Emissivity Coating on the Inner Side of Second Glass and Outer Side of Third Glass

For this study a model was prepared that has coating on the inner side of second glass and outer side of third glass. This model is ninth model from the Table 4.2. The outer average temperature of the fourth glass surface is 312.619 K.

Figure 4.26 shows the temperature contour of the model that is prepared and Figure 4.27 shows upper side and down side temperature contour of the model.

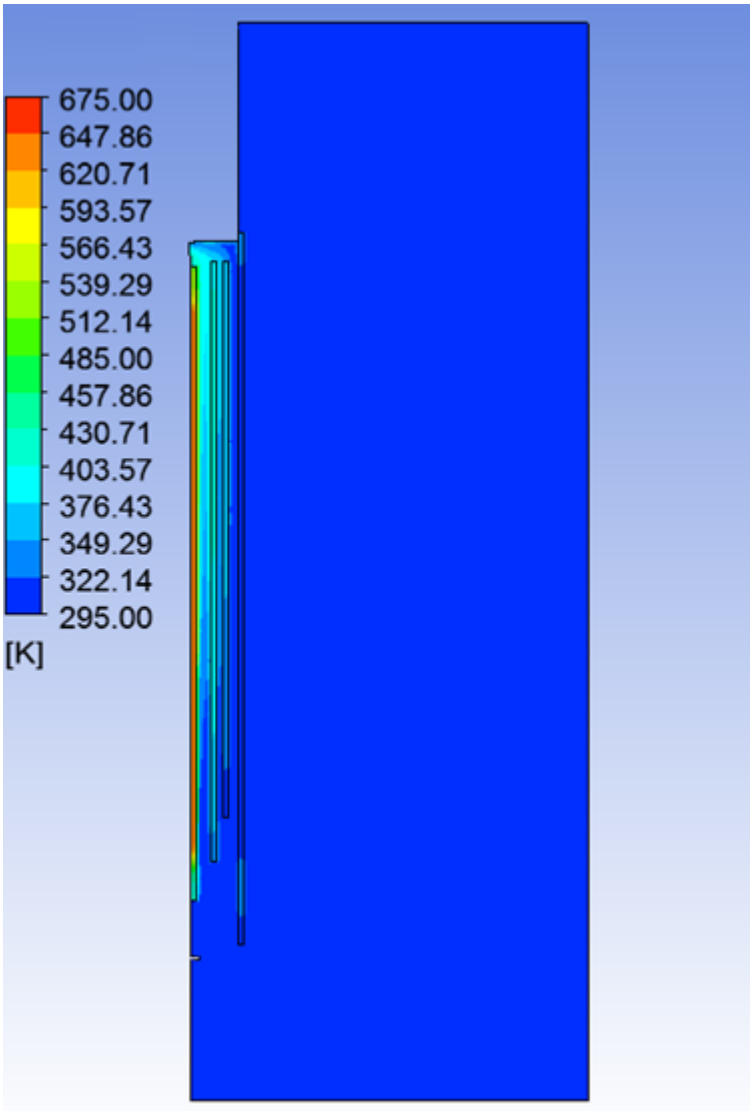


Figure 4.26 The temperature contour of the ninth model which has low emissivity coating on the inner side of second glass and outer side of third glass.

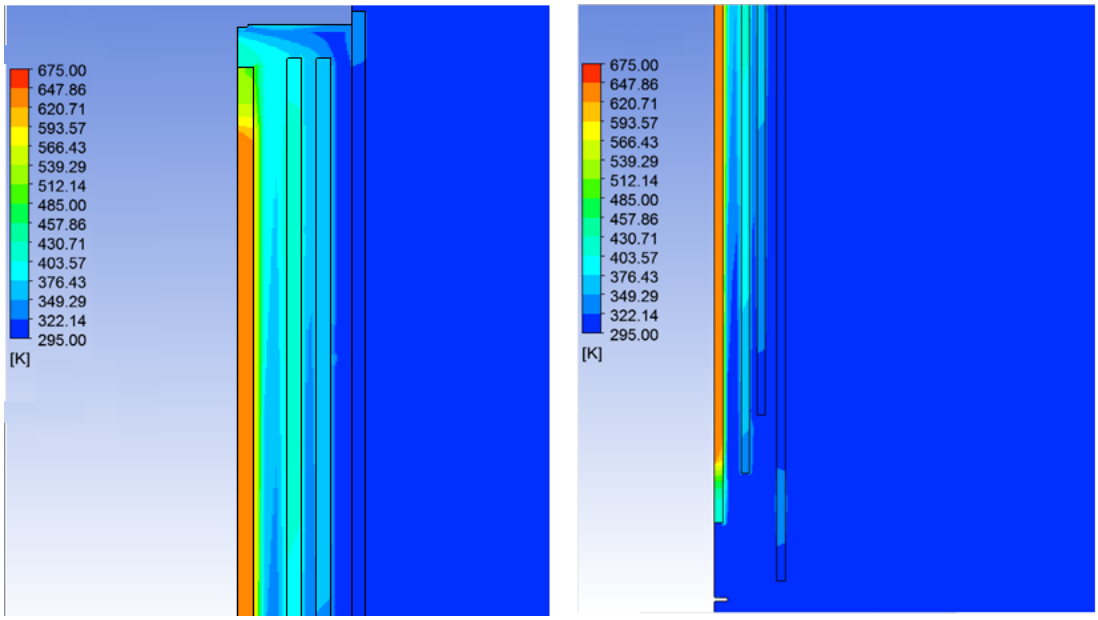


Figure 4.27 Upper sides (a) and down side (b) temperature contours of the ninth model which has low emissivity coating on the inner side of second glass and outer side of third glass.

4.4.10 Effect of the Low Emissivity Coating on the Outer Side of Second Glass and Inner Side of Third Glass

For this study a model that has coating on the outer side of second glass and inner side of third glass was prepared. This model is tenth model from the Table 4.2. The outer average temperature of the fourth glass is 321.325 K. This temperature is higher than the models that have coatings on two glass.

Figure 4.28 shows the temperature contour of the model that is prepared and Figure 4.29 shows upper side and down side temperature contour of the model. As it is seen from Figure 4.28 temperatures in the door cavity are higher than the previous model. When we compare Figure 4.26 and 4.28, high temperatures are present from top towards the center of fourth glass at Figure 4.28. Detailed temperature distribution is seen from Figure 4.28a and 4.28b. The temperature at the bottom of fourth glass has relatively high temperature to the center of fourth glass.

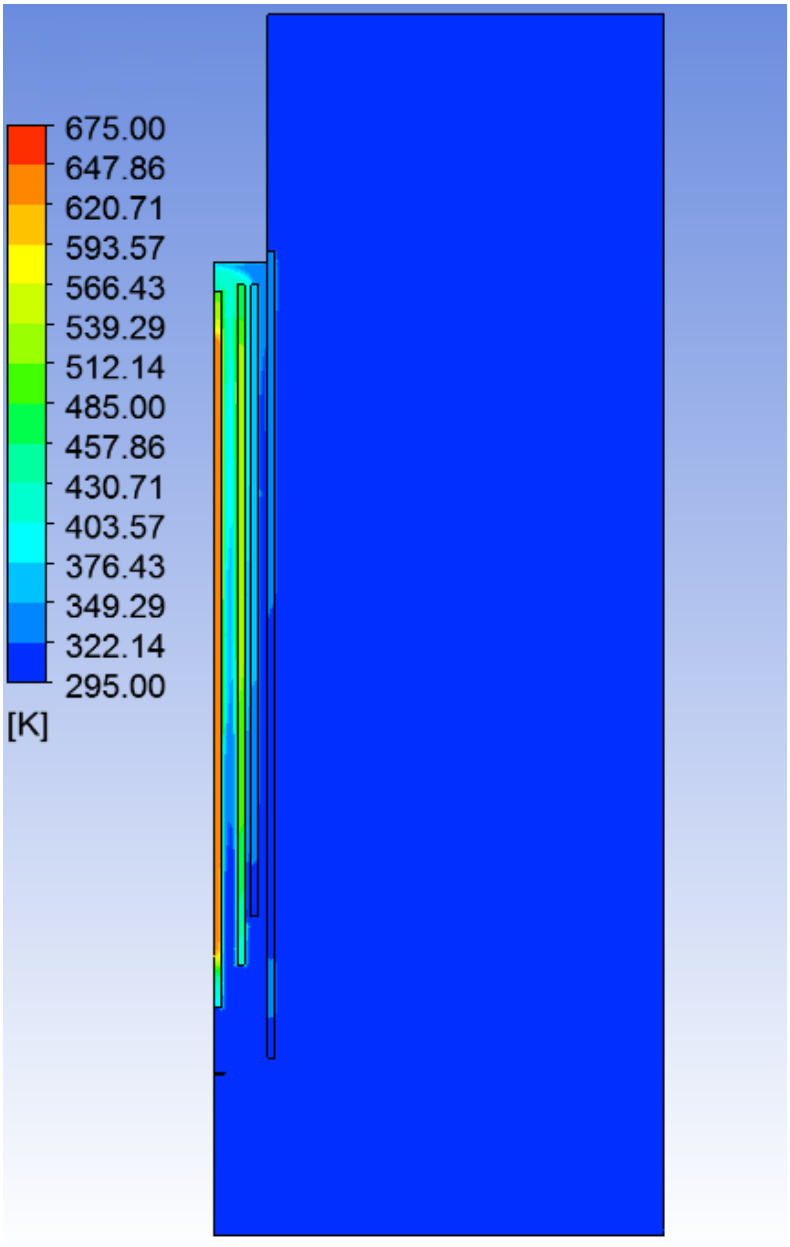


Figure 4.28 The temperature contour of the tenth model which has low emissivity coating on the outer side of second glass and inner side of third glass.

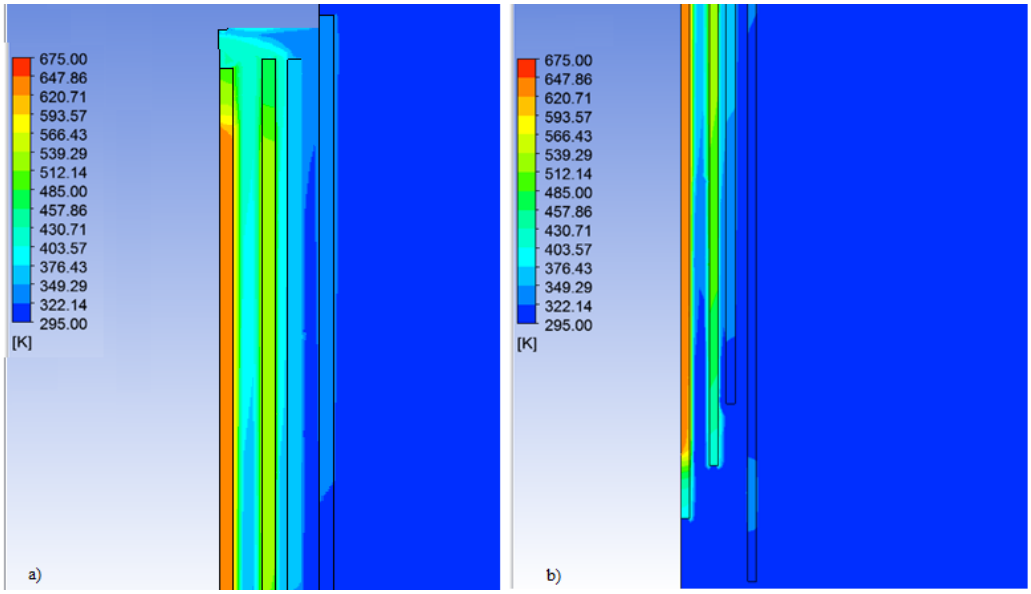


Figure 4.29 Upper sides (a) and down side (b) temperature contours of the tenth model which has low emissivity coating on the outer side of second glass and inner side of third glass.

4.4.11 Effect of the Low Emissivity Coating on the Outer Side of Second Glass and Outer Side of Third Glass

For this study a model that has coating on the outer sides of second and third glass was prepared. This model is eleventh model from the Table 4.2. The outer average temperature of the fourth glass is 317.006 K.

Figure 4.30 shows the temperature contour of the model that is prepared and Figure 4.31 shows upper side and down side temperature contour of the model. As it is seen from Figure 4.28 temperatures in the door cavity are lower than the previous model.

When we compare Figure 4.28 and 4.30 temperatures are lower than previous model. Detailed temperature distribution is seen from Figure 4.30a and 4.30b. The temperature at the bottom of fourth glass has relatively high temperature to the center of fourth glass.

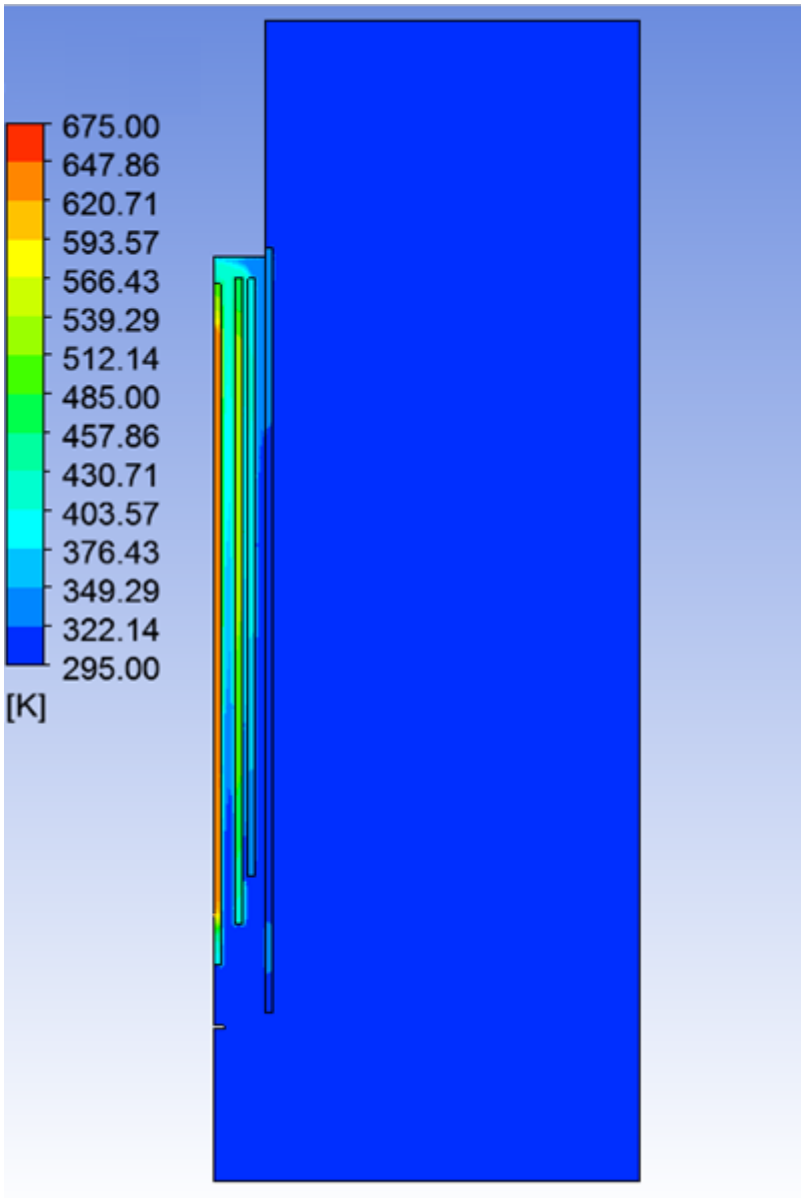


Figure 4.30 The temperature contour of the eleventh model which has low emissivity coating on the outer sides of and third glass.

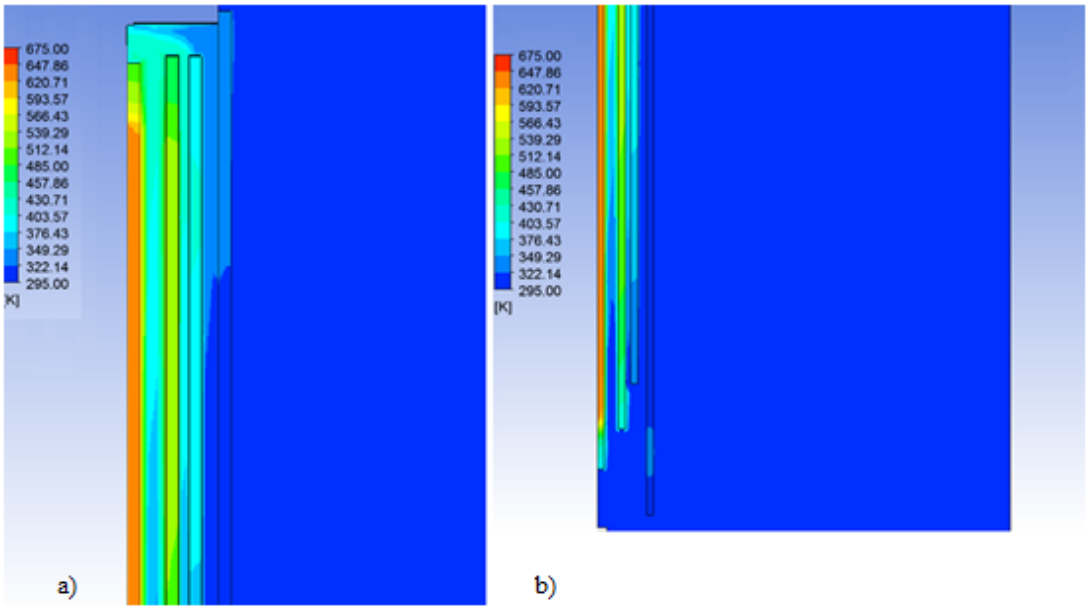


Figure 4.31 Upper sides (a) and down side (b) temperature contours of the eleventh model which has low emissivity coating on the outer sides of second and third glass.

4.4.12 Effect of the Low Emissivity Coating on the Outer Side of First Glass, Outer Side of Second Glass and Inner Side of Third Glass

Previous studies had low emissivity coating on two glass. This model has low emissivity glazing on three glass panes. This model is twelfth model from the Table 4.2. Low emissivity coating was applied on the outer side of first glass, outer side of second glass and inner side of third glass. Outer average temperature of the fourth glass is 307.512 K. This temperature is lower than previous model temperatures.

Figure 4.32 shows the temperature contour of the model that is prepared and Figure 4.32 shows upper side and down side temperature contour of the model. As it is seen from Figure 4.32 temperatures in the door cavity are lower than the previous models. As it is seen from Figure 33 temperatures of the fourth glass are quite low comparing to the previous models.

As it is seen from Figure 33a and 33b, third glass has low temperatures fat bottom of glass until the glass center.

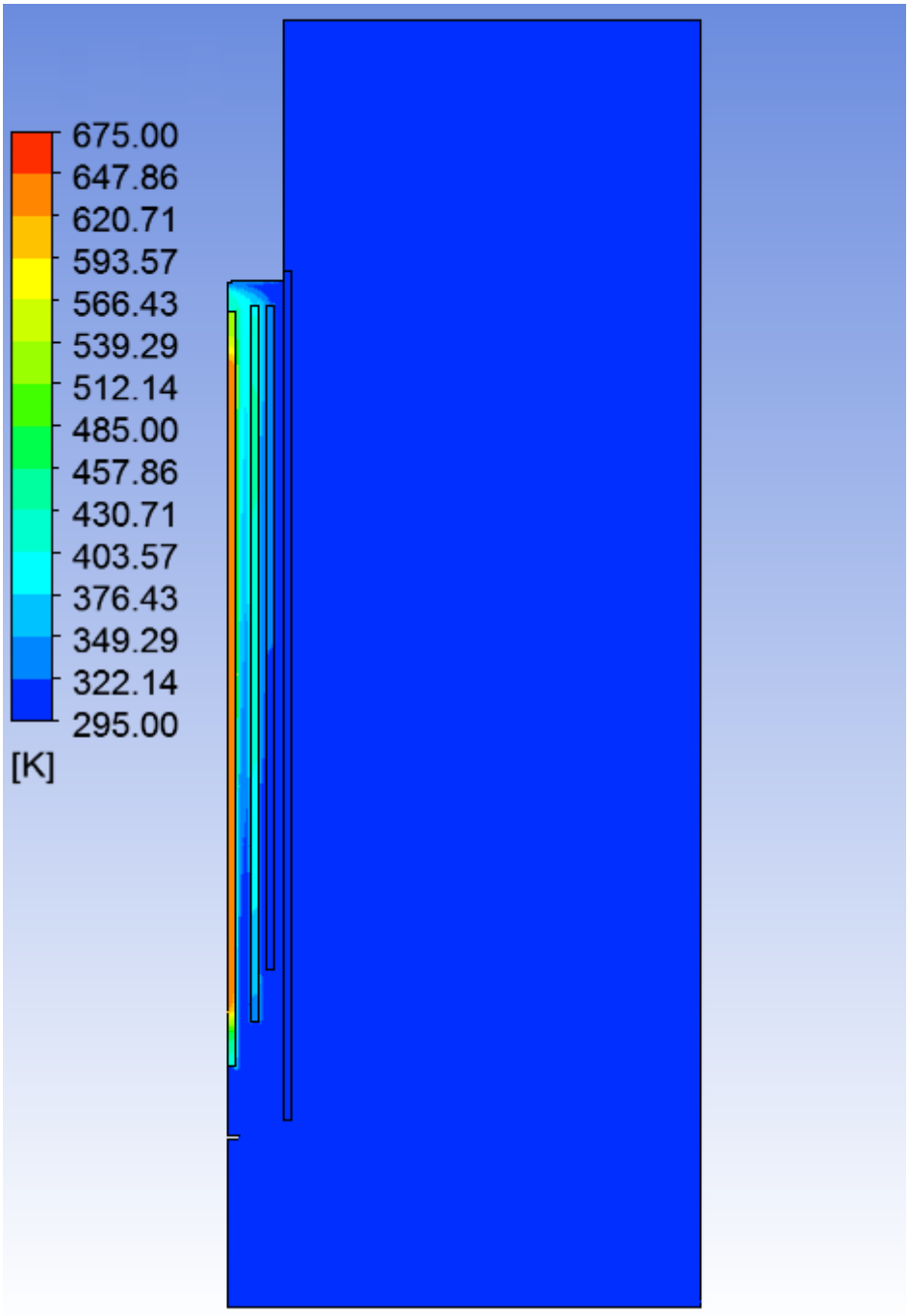


Figure 4.32 The temperature contour of the twelfth model which has low emissivity coating on the outer side of first glass, outer side of second glass and inner side of third glass.

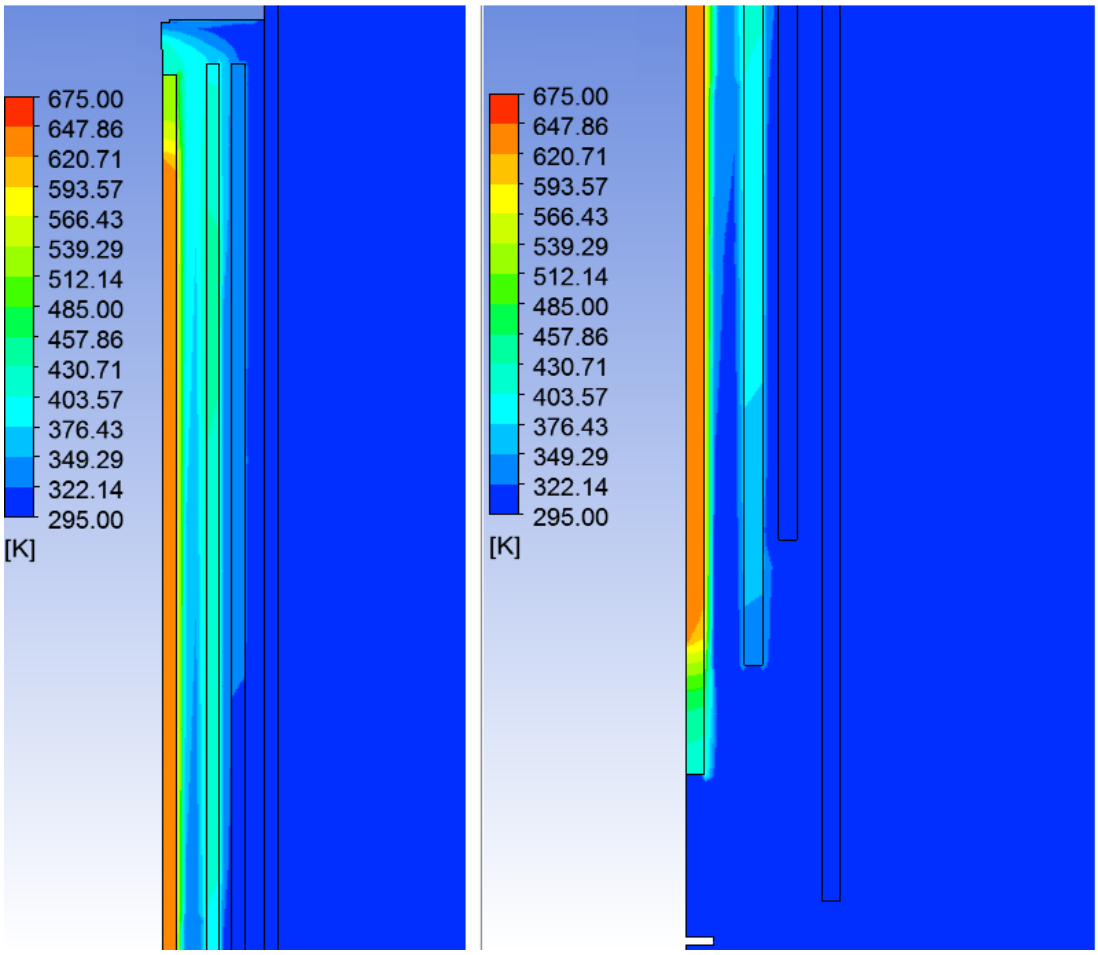


Figure 4.33 Upper sides (a) and down side (b) temperature contours of the twelfth model which has low emissivity coating on the outer side of first glass, outer side of second glass and inner side of third glass.

4.4.13 Effect of the Low Emissivity Coating on the Outer Side of First Glass, Outer Side of Second Glass and Outer Side of Third Glass

Low emissivity coating was applied on the outer side of first glass, outer side of second glass and outer side of third glass. This model is thirteenth model from the Table 4.2. For this study outer average temperature of the fourth glass is 305.739 K. This temperature is lower than previous model temperatures.

Figure 4.34 shows the temperature contour of the model that is prepared. As it is seen from Figure 4.34 temperatures in the door cavity are lower than the previous

models. As it is seen from Figure 4.35, temperatures of the fourth glass are quite low comparing to the previous models.

As it is seen from Figure 4.35a and 35b, third glass has low temperatures from bottom of glass towards to the glass center.

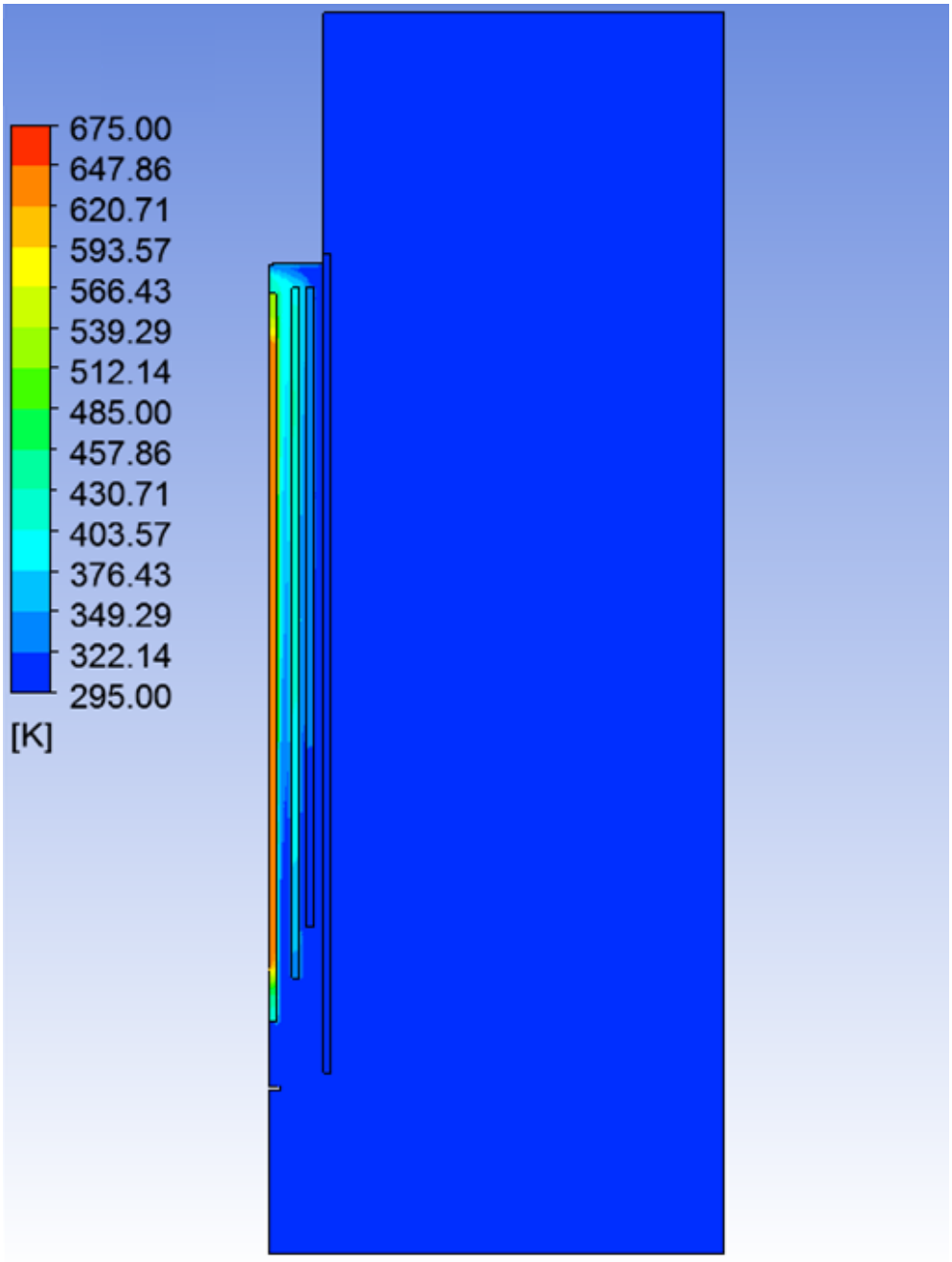


Figure 4.34 The temperature contour of the thirteenth model which has low emissivity coating on the outer side of first glass, outer side of second glass and outer side of third glass.

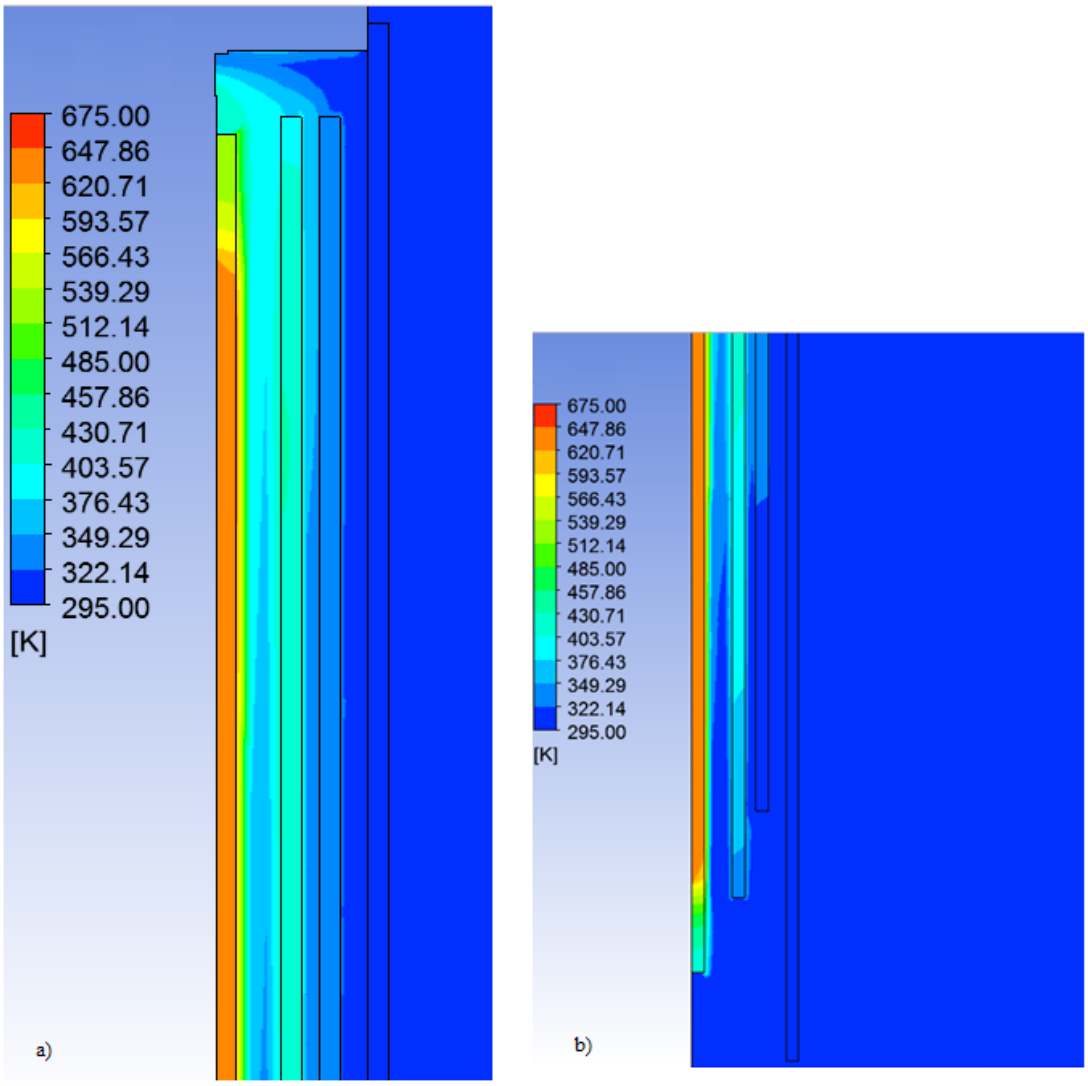


Figure 4.35 Upper sides (a) and down side (b) temperature contours of the thirteenth model which has low emissivity coating on the outer side of first glass, outer side of second glass and outer side of third glass.

4.4.14 Effect of the Low Emissivity Coating on the Outer Side of First Glass, Inner Side of Second Glass and Outer Side of Third Glass

A model which has low emissivity coating on the outer side of first glass, inner side of second glass and outer side of third glass was prepared for this study. This model is fourteenth model from the Table 4.2. The outer average temperature of the fourth glass is 307.683 K.

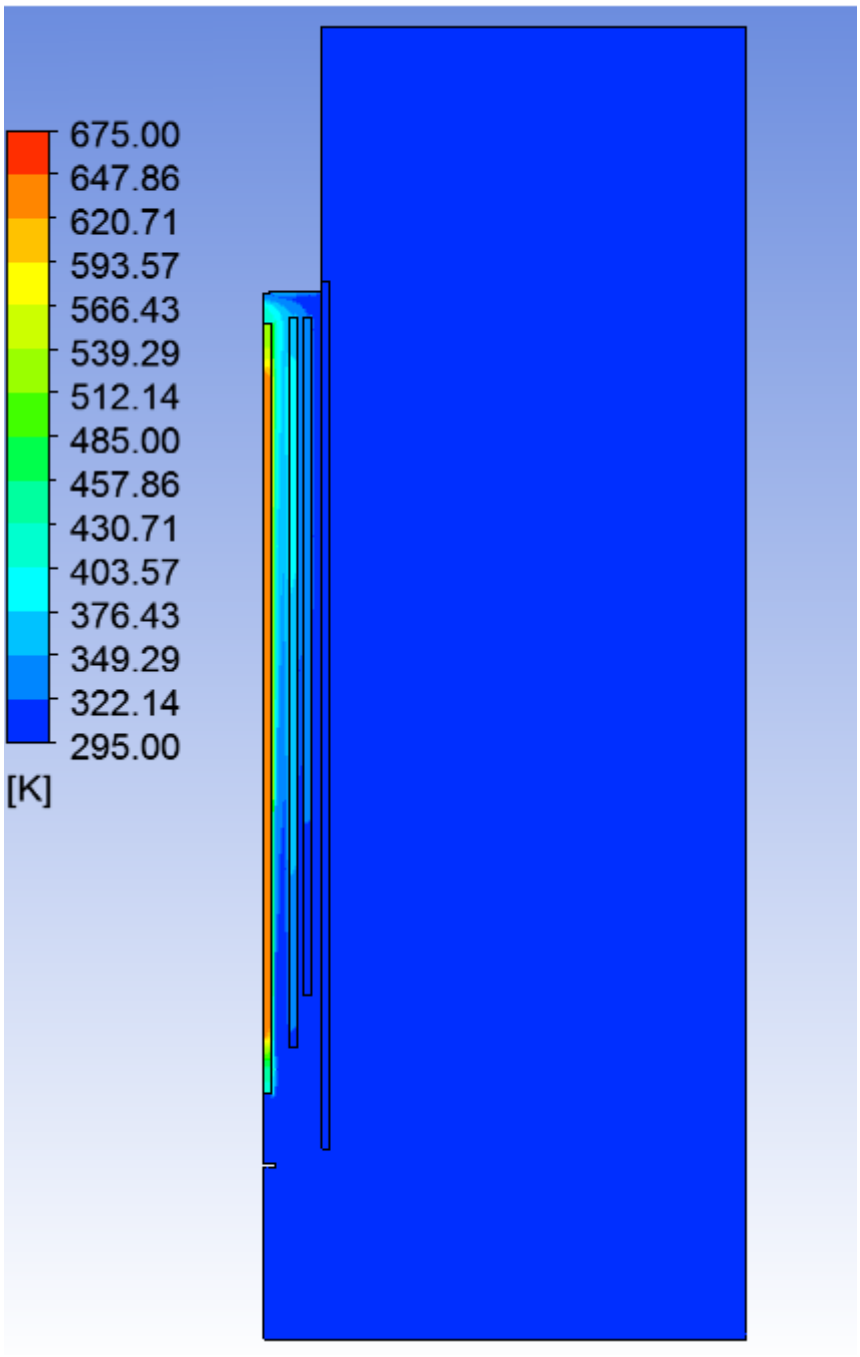


Figure 4.36 The temperature contour of the fourteenth model which has low emissivity coating on the outer side of first glass, inner side of second glass and outer side of third glass.

Figure 4.36 shows the temperature contour of the model that is prepared. Figure 4.37a and 37b show the detailed temperature distribution of the model. This model fourth glass has a bit higher outer average temperature than previous model. When we compare Figure 4.34 and Figure 4.36 differences are present at second and third glass.

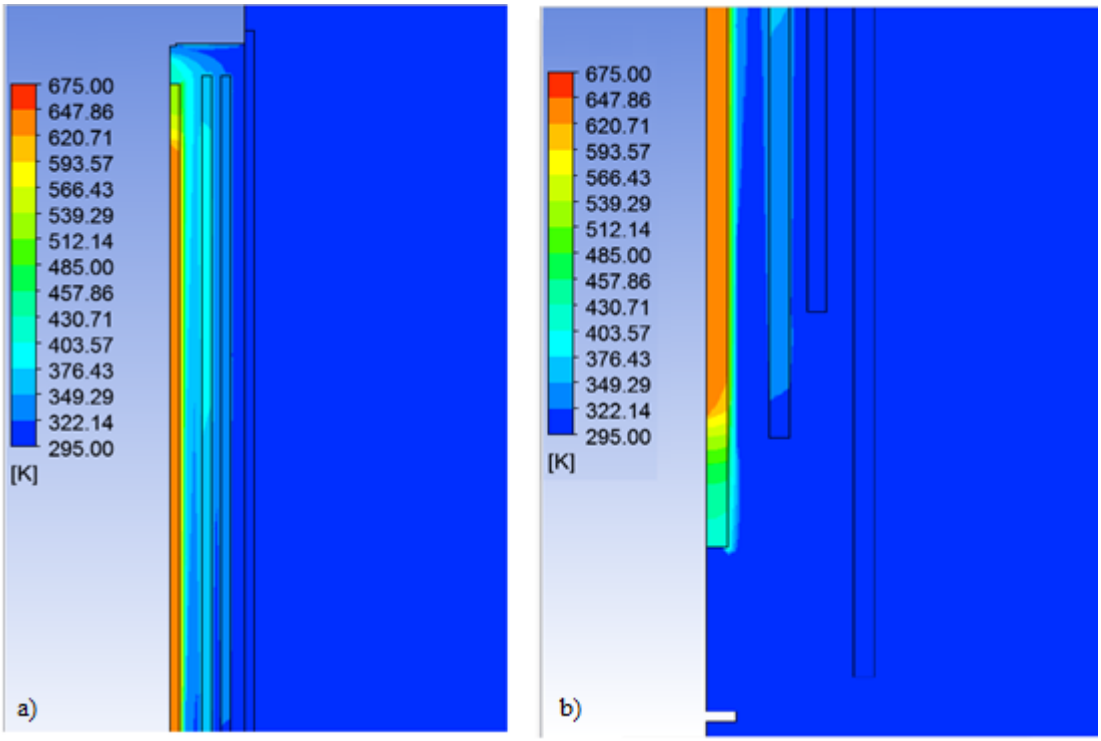


Figure 4.37 Upper side (a) and down side (b) temperature contours of the fourteenth model which has low emissivity coating on the outer side of first glass, inner side of second glass and outer side of third glass.

4.4.15 Effect of the Low Emissivity Coating on the Outer Side of First Glass, Inner Side of Second Glass and Inner Side of Third Glass

A model which has low emissivity coating on the outer side of first glass, inner side of second glass and inner side of third glass was prepared for this study. This model is fifteenth model from the Table 4.2. The outer average temperature of the fourth glass is 308.033 K.

Figure 4.38 shows the temperature contour of the model that is prepared. Figure 4.39a and 39b show the detailed temperature distribution of the model.

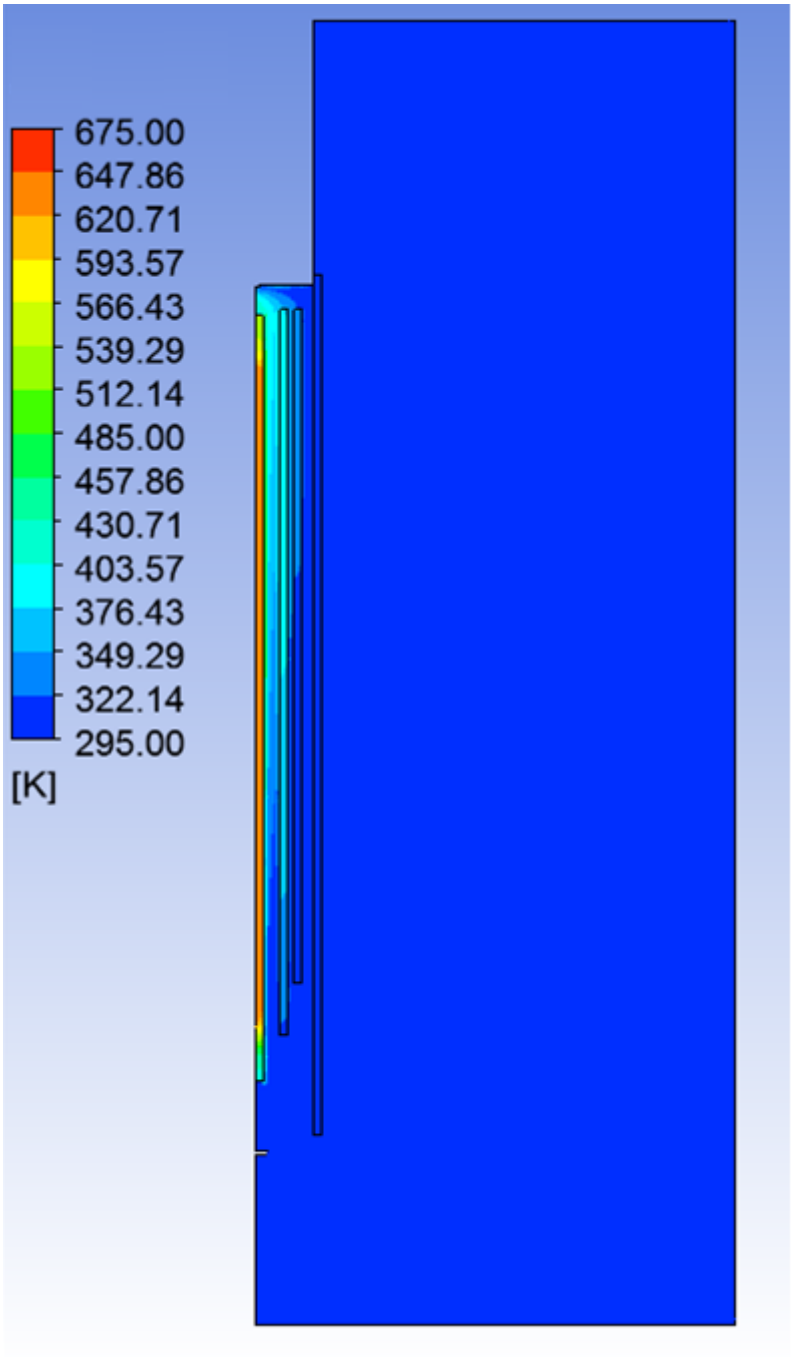


Figure 4.38 The temperature contour of the fifteenth model which has low emissivity coating on the outer side of first glass, inner side of second glass and inner side of third glass.

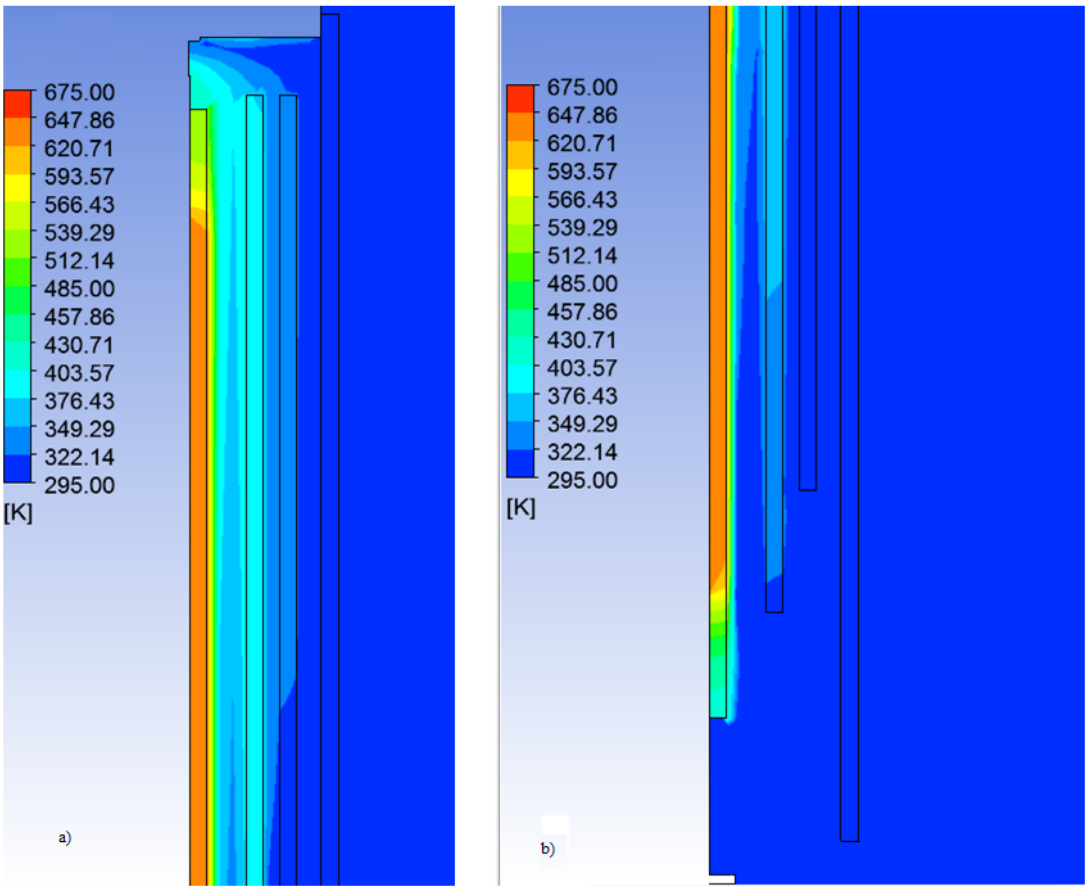


Figure 4.39 Upper side (a) and down side (b) temperature contours of the fifteenth model which has low emissivity coating on the outer side of first glass, inner side of second glass and inner side of third glass.

After this model was modeled and obtained results from the numerical study temperature experiment was done. Low emissivity coating was applied to the prototype. Low emissivity was applied on the outer side of first glass, inner side of second glass and inner side of third glass. Then temperature experiment was done. Figure 4.40 shows the results of experimental and numerical results. Vertical axis shows temperature value in K and horizontal axis shoes the glass number.

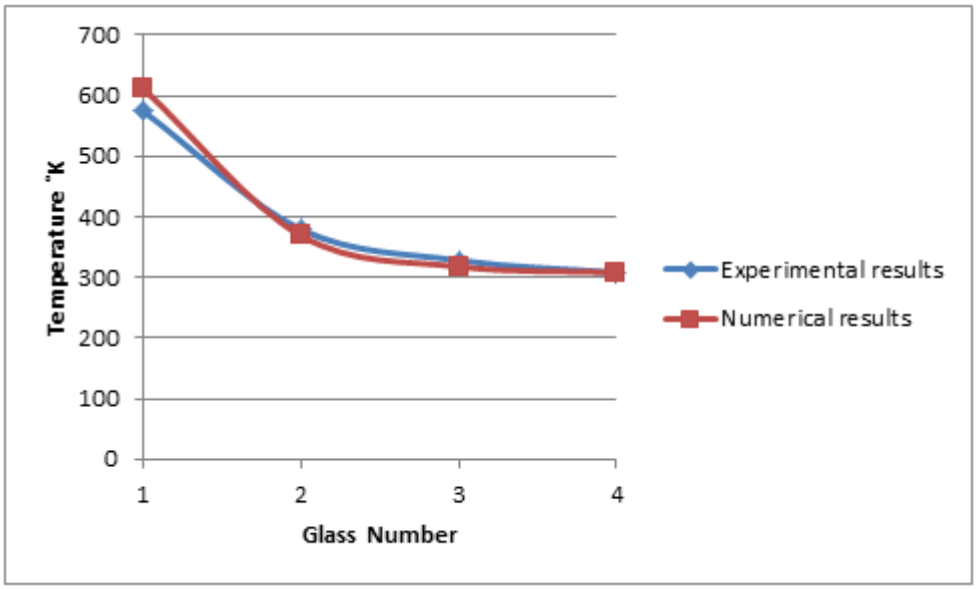


Figure 4.40 Results of the numerical and experimental studies of the model which has low emissivity coating on the outer side of first glass, inner side of second glass and inner side of third glass.

Average discrepancy between numerical and experimental results the model are 3.04 %. As it is seen from Figure 4.40 results are close.

Using low emissivity coating on the glass of oven door has big effect on the design of oven door. These experimental and numerical results prove the importance of low emissivity coating.

After modeling, the effect of the air gaps between the panes on the outer average temperature of the fourth glass is investigated. Using low emissivity coating on the panes of oven door changes the heat transfer rate of radiation.

4.4.15.1 Effect of the Gap between Glass Number 1 and 2

To see the effect of the air thickness between first and second glass thickness for the model which has low emissivity coating on the outer side of first glass, inner side of second and third glass. Air thickness was changed from 1 mm to 12 mm. While this thickness was changing other gaps were fixed.

Figure 4.41 shows the effect of the air thickness between first and second glass thickness for the model .Vertical axis shows the average outer temperature of fourth glass in K. And horizontal axis shows the air thickness change in mm.

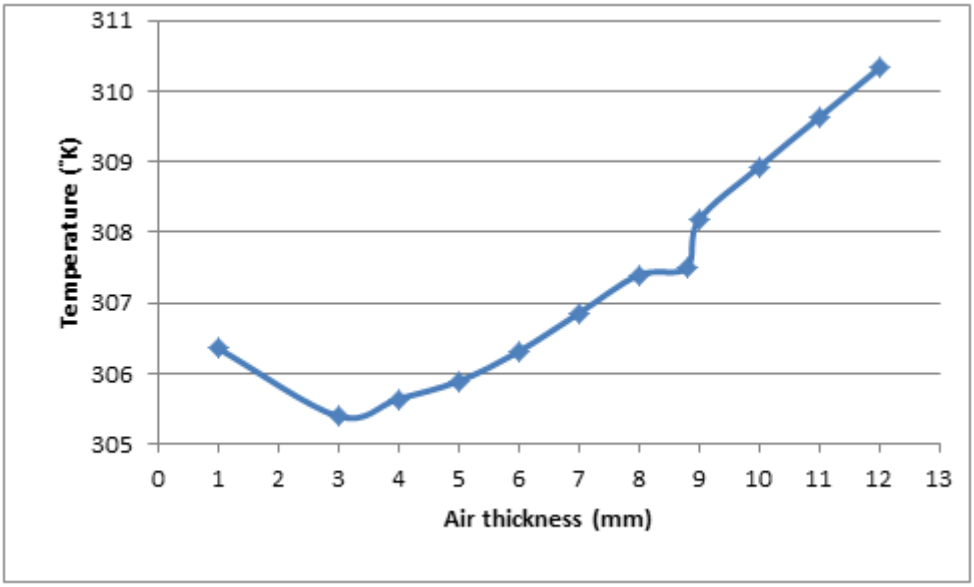


Figure 4.41 Effect of the air thickness between first and second glass.

As it is seen from Figure 4.41 while air thickness between first and second glass uncoated model had great effect on the outer average temperature of fourth glass, it has less effect on the model which has low emissivity coating on the outer side of first glass, inner side of second and third glass. As it is seen from figure 4.41 when the second glass gets closer to first glass outer average temperature of the fourth glass decreases until a point then it starts to increases again. But the temperature changes on the outer average temperature of fourth glass are not as big as uncoated model.

4.4.15.2 Effect of the Gap between Glass Number 2 and 3

To see the effect of the air thickness between second and third glass, thickness was changed from 1 mm to 9 mm. While this thickness was changing other gaps were fixed. Figure 4.42 shows effect of the air thickness on the outer average temperature of fourth glass.

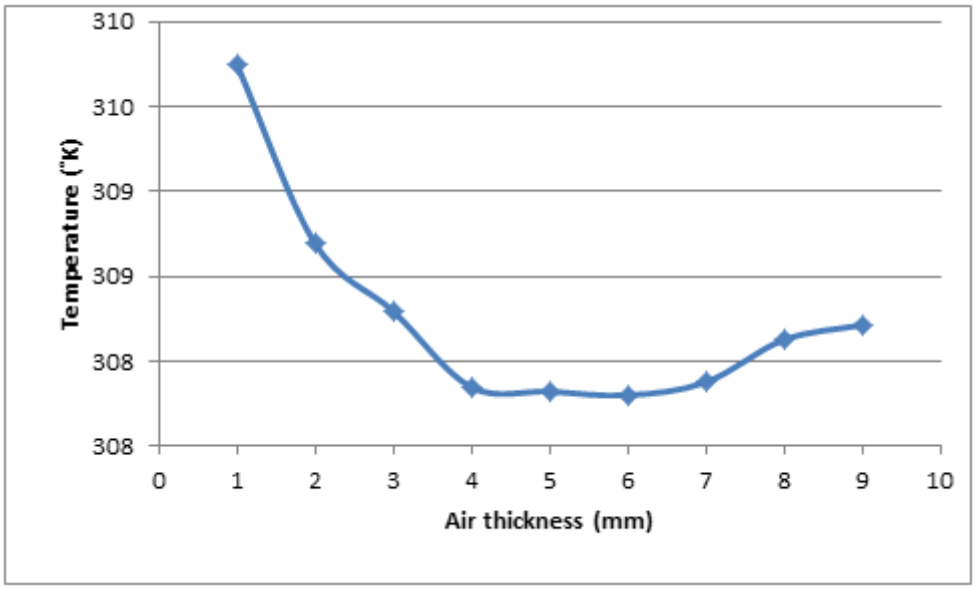


Figure 4.42 Effect of the air thickness between second and third glass.

As it is seen from figure 4.42 when the third glass gets closer to second glass outer average temperature of the fourth glass decreases until a point then it starts to increases again. Where the air thickness is between 4 mm and 7 mm, the temperature is lower than other thickness.

If we compare Figure 4.41 and 4.42 it can be seen that air thickness change between first and second glass greater effect than air thickness change between first and second glass. This result was same in the uncoated model. Temperature changes are quite small for this model but the characteristic of the air gaps are same.

4.4.15.3 Effect of the Gap between Glass Number 3 and 4

To investigate the effect of the air thickness between third and fourth glass, thickness was changed from 1 mm to 12 mm. While this thickness was changing other gaps were fixed. Figure 4.43 shows the effect of this gap on the outer average temperature of the fourth glass.

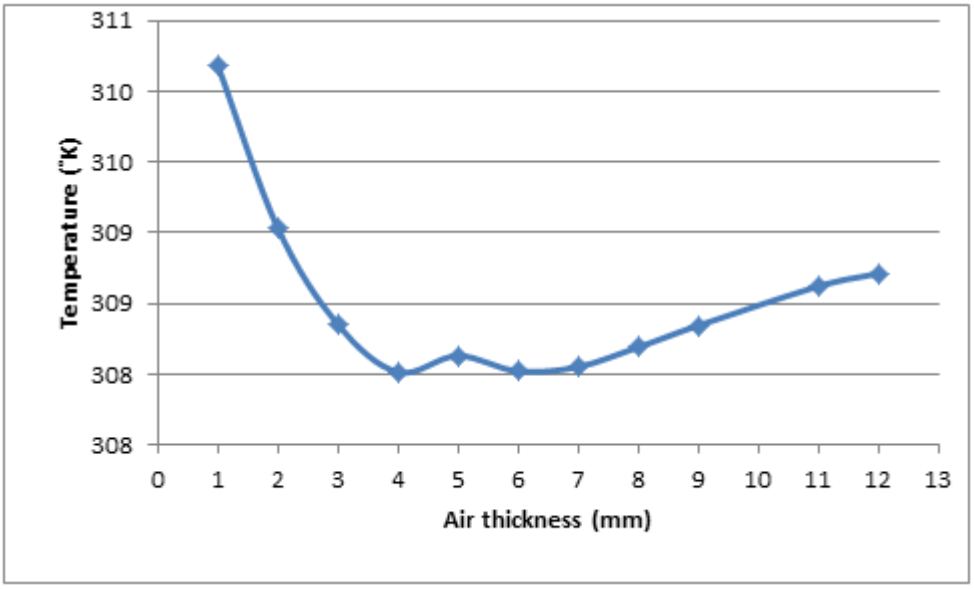


Figure 4.43 Effect of the air thickness between third and fourth glass.

As it is seen from Figure 4.43 while the air thickness is increasing, the outer average temperature of the fourth glass decreases until 4 mm then it is nearly steady until 7 mm, and then it starts to increase with a low slope.

Figure 4.41, 42 and 43 show that the air thicknesses change between first and second glass greater effect than other two gaps.

4.5 Effect of the Inlet Area at Inflow Channel

Active suction air provides the air circulation in the oven door cavity. Air goes in the door from ambient air and goes to the air suction channel by inflow channel. Some factors like not closing the door properly or some other reasons may reduce this area. Area changes by changing the height of the inlet height.

Figure 4.44 shows effect of the inlet area at inflow channel on the outer average temperature of fourth glass. Vertical axis shows the temperature in Kelvin and horizontal axis shows the height of the inflow channel inlet. Air velocity was fixed in all models.

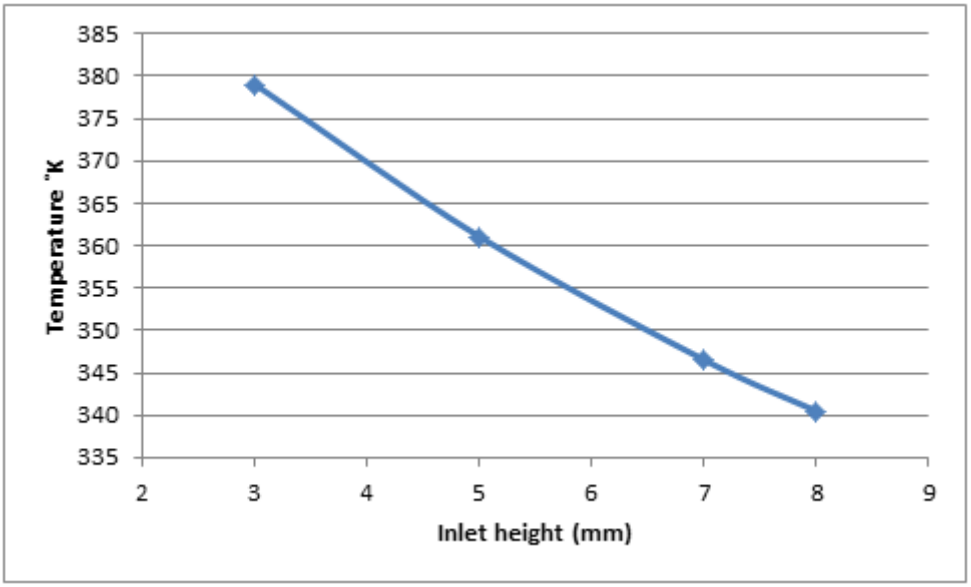


Figure 4.44 The effect of the inflow channel area on the outer average temperature of fourth glass.

As it is seen from Figure 4.44, if the inlet height of the inflow channel decreases, outer average temperature of fourth glass increases. By reducing the height, inlet area decreases and this causes the outer average temperature increase.

4.6 Effect of the Blocking Air Flow between the Glass Panes

It was seen from previous parameters that in some cases reducing the air thickness between the glass increases the speed in this gap and this reduces the outer average temperature of the fourth glass. Increasing the speed increases the convective heat transfer. Several models were prepared to see the effect of the blocking air flow between the glass panes on the outer average temperature of the fourth glass.

4.6.1 Blocking the Air Flow between Glass Number 2 and Number 4 from Bottom

For this study a model, which air flow was blocked between glass number two and number four from bottom was prepared. Prepared model can be seen from Figure 4.45a. Figure 4.45b shows the detailed view. Air blockage is provided by removing material between two panes from bottom so that it doesn't let the air flow. If we

define a material for the blockage, it would have little effect on heat transfer. Since it has very small height, its effect on heat transfer can be ignored.

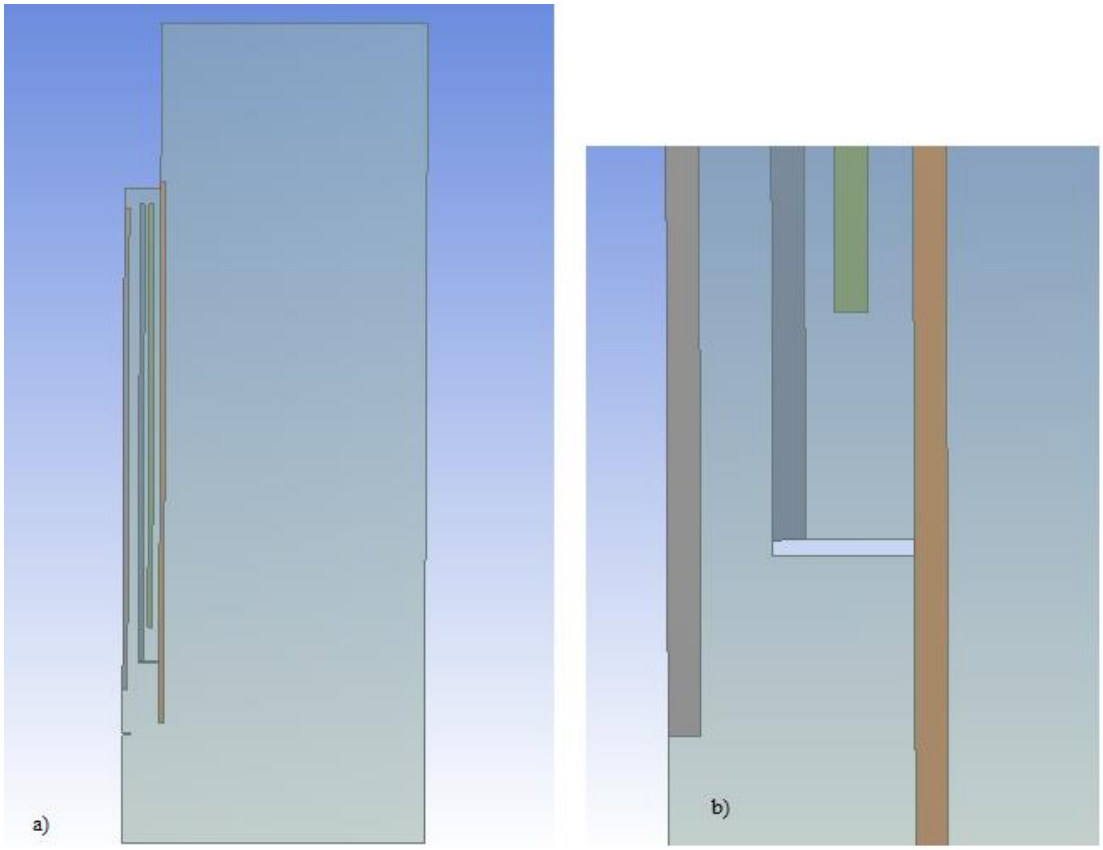


Figure 4.45 The prepared model (a) and detailed view (b) of the air blockage between second and fourth glass from top and bottom.

Figure 4.46 shows the velocity vectors of the model. As it is seen blocking the air gap between second and fourth glass air velocity increases in the gap which is between first and second glass.

Detailed view of the air velocity vectors are shown in the Figure 4.47a and 4.47b. Air is sucked from the gap which is between first and second glass. From Figure 4.47b we can see there is inflow from the upside of the gap which is between second and fourth glass. But the velocities in this blocked gap are too slow.

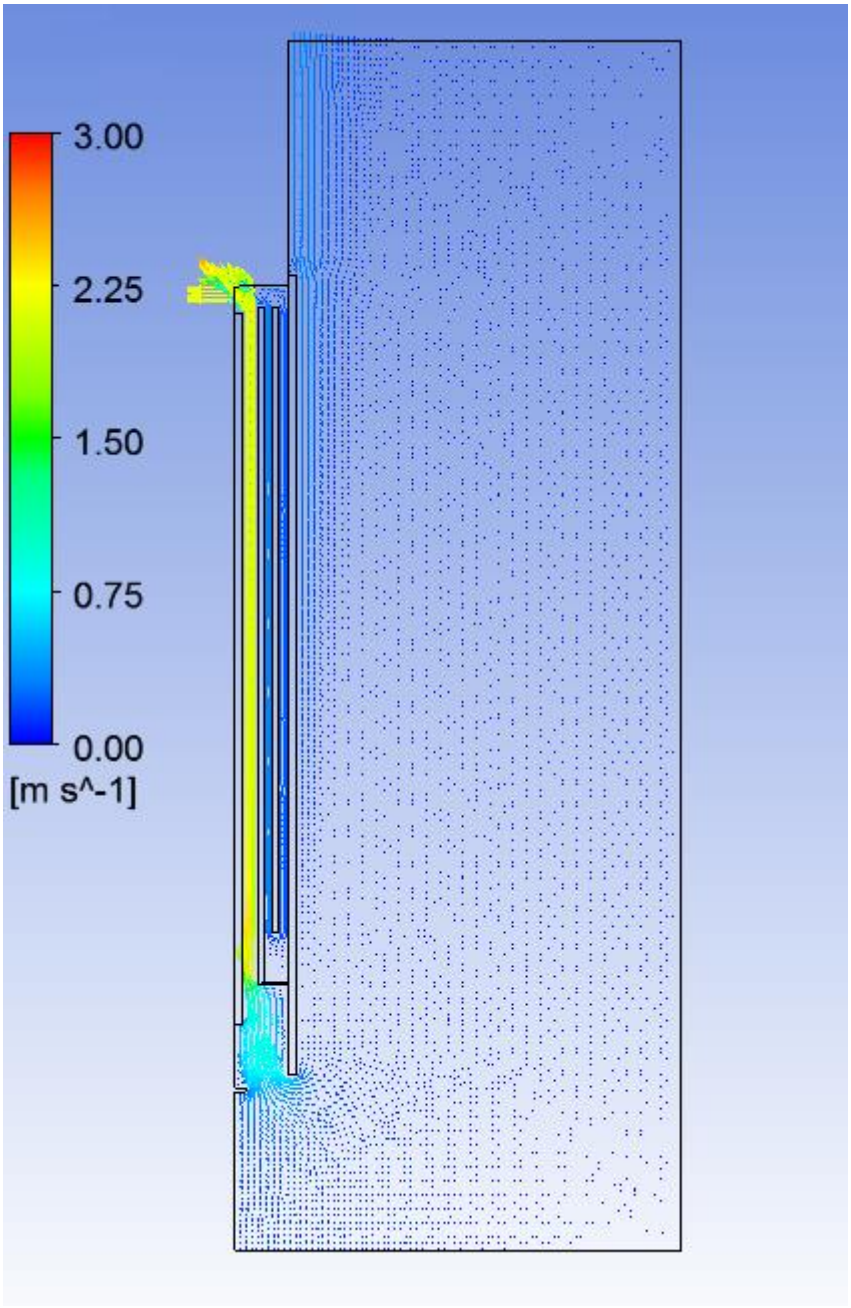


Figure 4.46 Velocity vectors of the model which airflow was blocked between glass number two and number four from bottom.

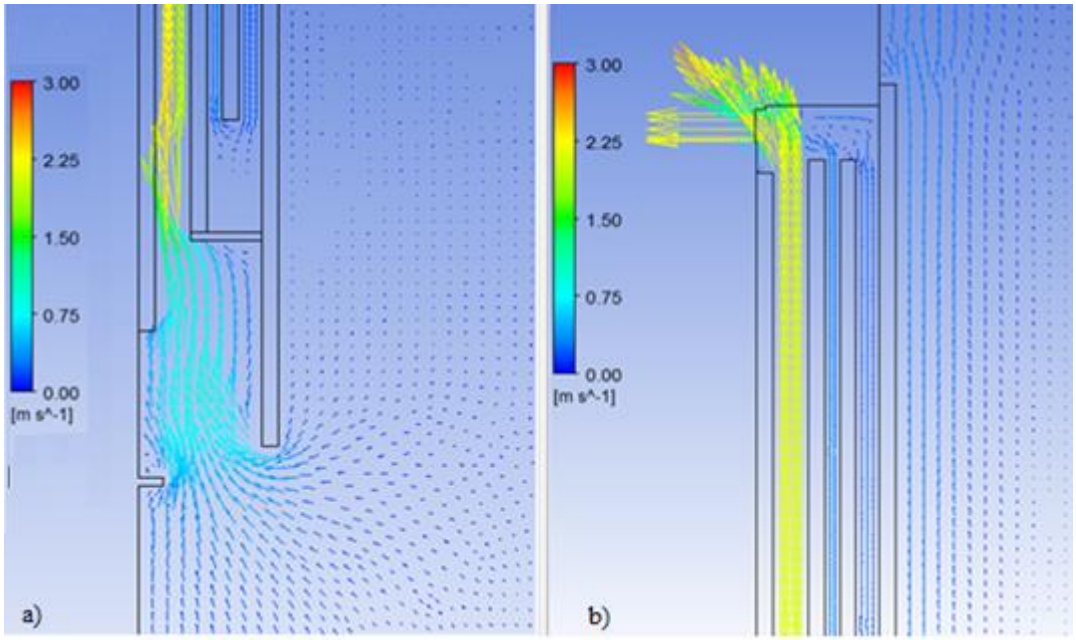


Figure 4.47 Upper side (a) and down blockage side (b) velocity vectors of the model which airflow was blocked between glass number two and number four from bottom.

Figure 4.48 shows the temperature contour of the model. The outer average temperature of the outer glass is 371.44 K. This temperature is higher than uncoated model. Figure 4.49a and 49b shows the detailed contour of the model.

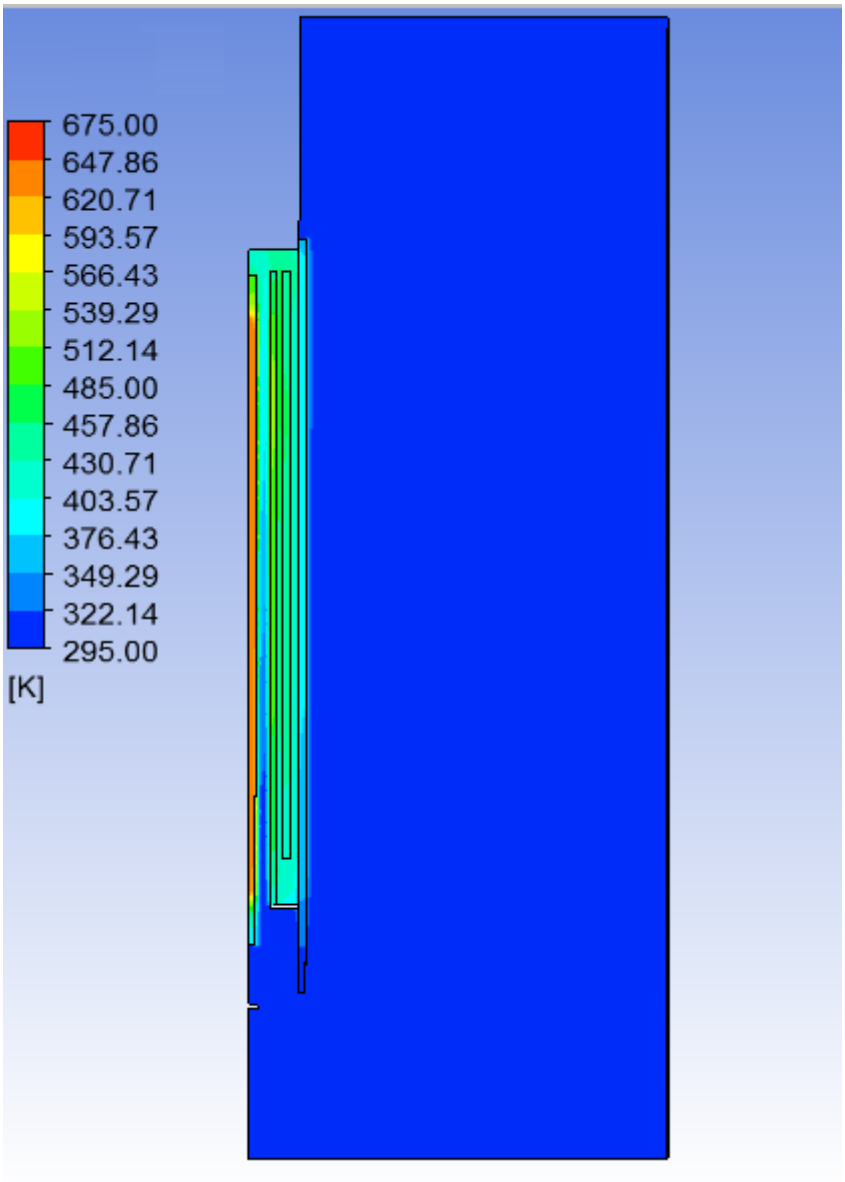


Figure 4.48 Temperature contour of the model which airflow was blocked between glass number two and number four from bottom.

As it is seen from Figure 4.49a and 49b, air flow between first and second glass is present but it is not enough to reduce the outer glass temperature of oven door.

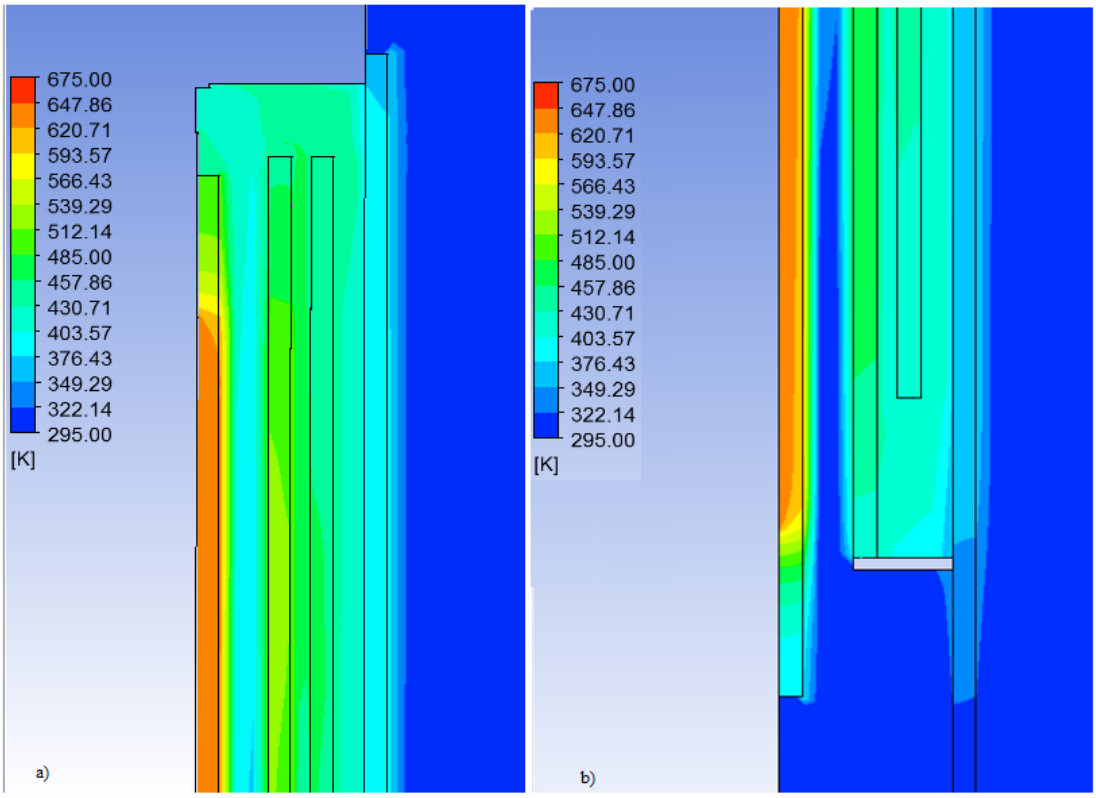


Figure 4.49 Upper side (a) and down blockage side (b) temperature contours of the model which airflow was blocked between glass number two and number four from bottom.

4.6.2 Blocking the Air Flow between Glass Number 2 and Number 4 from Bottom and Top

After blocking the air from bottom of air gap between second and fourth glass, air was blocked from top and bottom. So a cavity was created inside the oven door cavity. Prepared model can be seen in Figure 4.50.

Detailed view of the air blockage of the model can be seen from Figure 4.51. Figure 4.52 shows the velocity vectors of the model. As it is seen no air comes into the cavity that was created inside the oven door cavity. Naturel convection appears in inside cavity.

Figure 4.53 shows the detailed velocity vectors in the prepared model. The air velocities in the inside cavity that is created are very low.

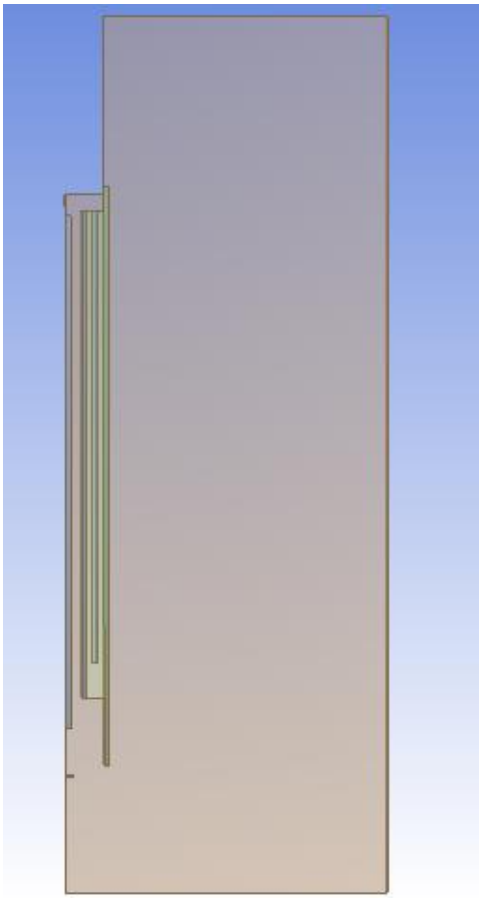


Figure 4.50 The prepared model which has air blockage between second and fourth glass from top and bottom.

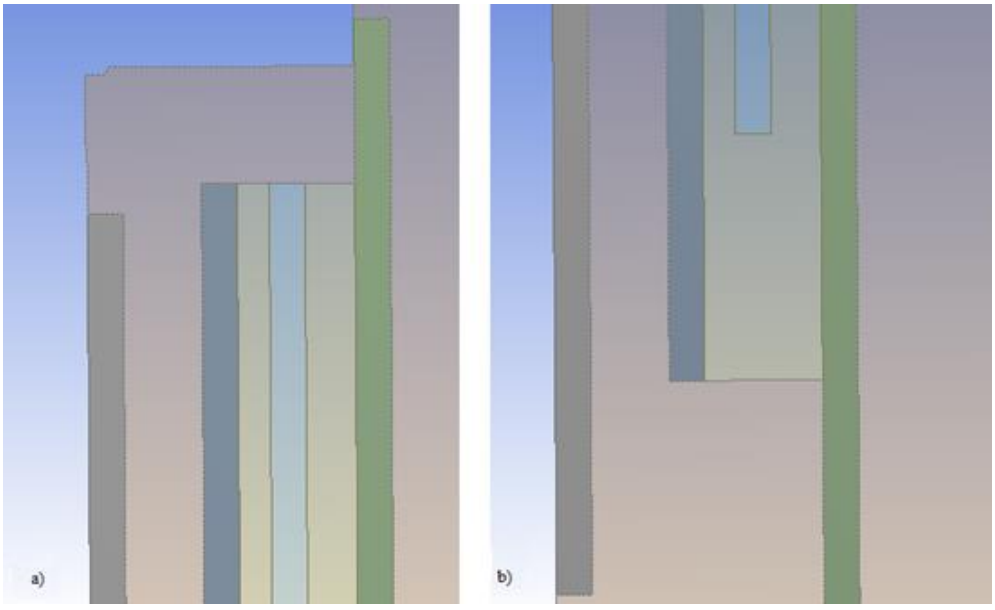


Figure 4.51 The top (a) and bottom (b) air blockage between second and fourth glass.

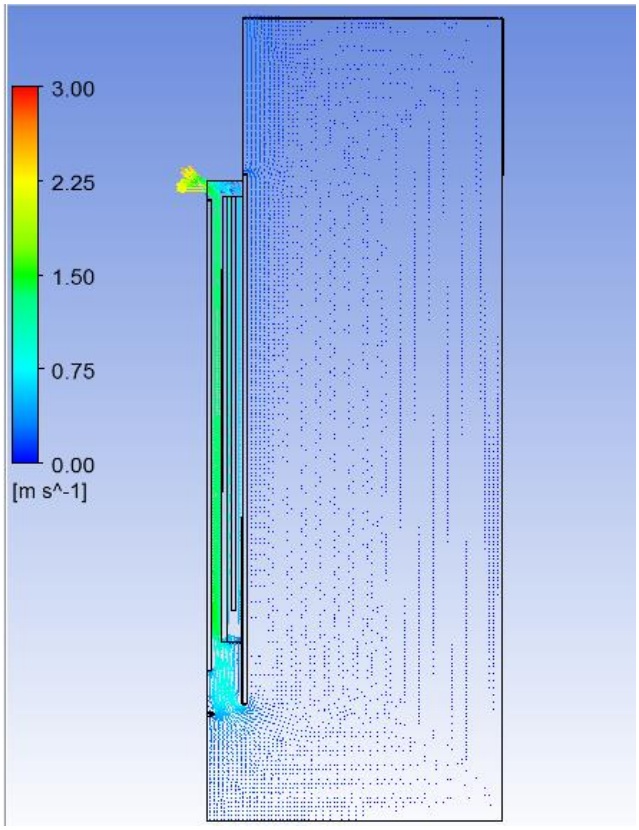


Figure 4.52 Velocity vectors of the model which airflow was blocked between glass number two and number four from top and bottom.

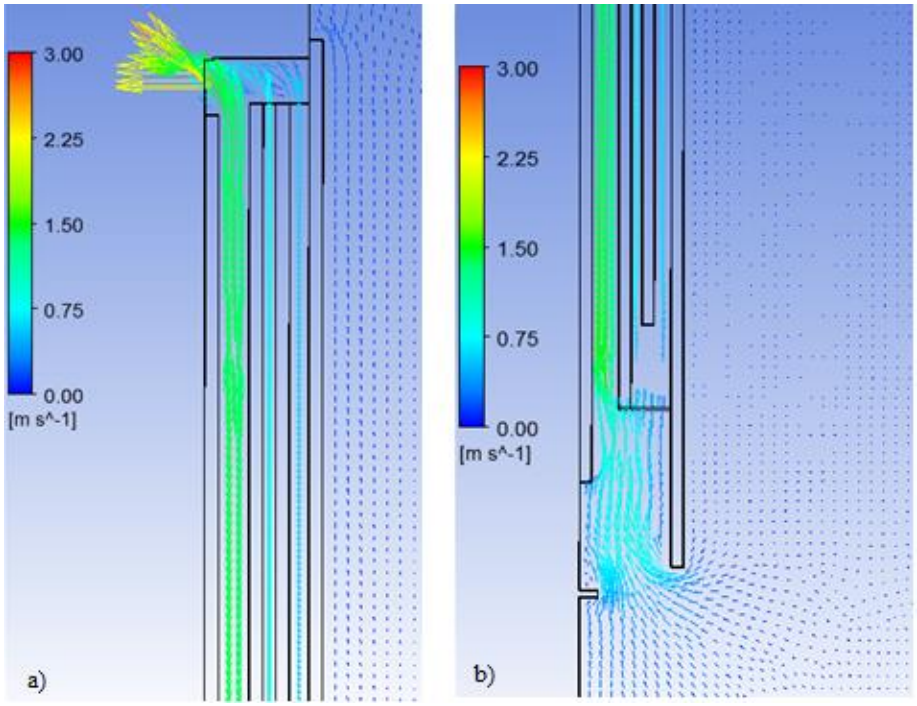


Figure 4.53 Upper (a) and down (b) blockage side velocity vectors of the model which airflow was blocked between glass number two and number four from top and bottom.

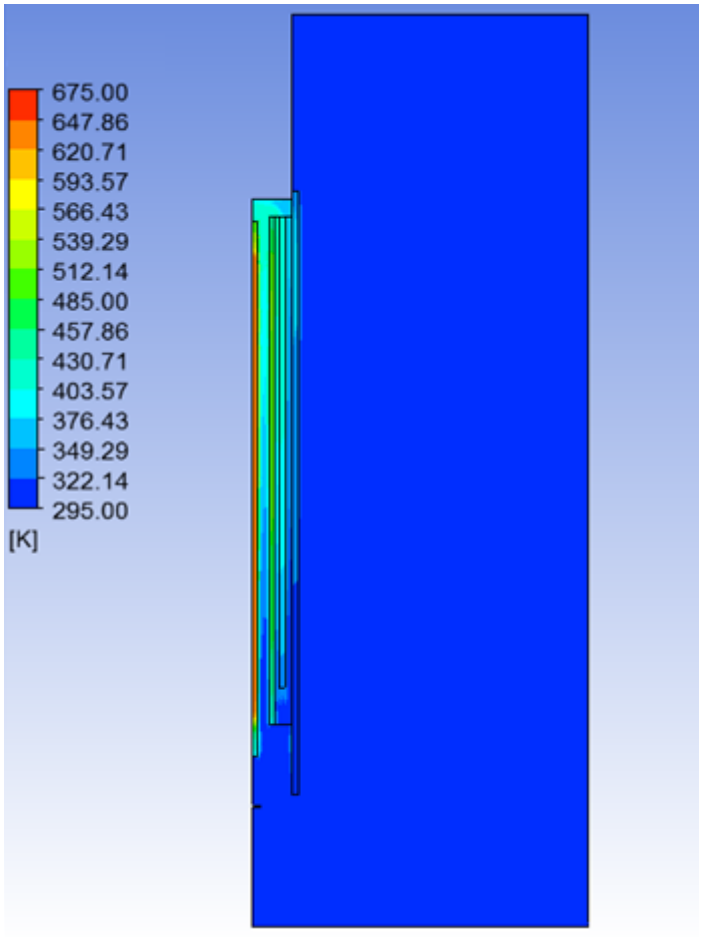


Figure 4.54 Temperature contour of the model which airflow was blocked between glass number two and number four from top and bottom.

Figure 4.54 shows the temperature contour of the model. As it is seen temperatures are lower than the model that has air blocking between glass number two and number four from bottom. For this model outer average temperature of the fourth glass is 330.867 K. this temperature is also lower than the model that was uncoated.

Figure 4.55a and 55b shows the detailed contour of the inside cavity. As it is seen temperature distributions are relatively lower than previous models and uncoated model.

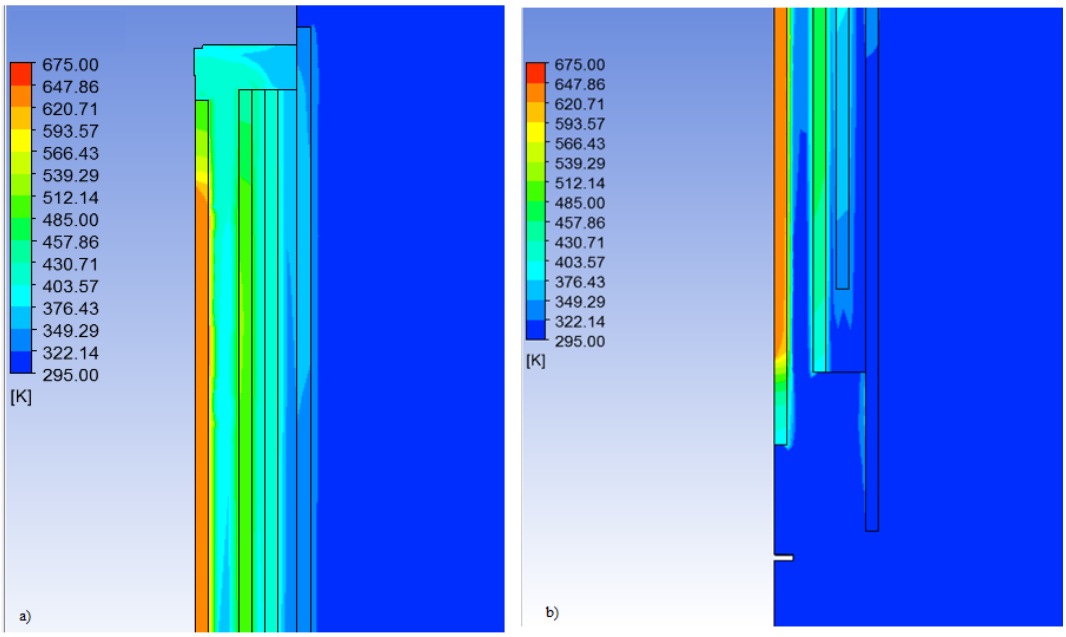


Figure 4.55 Upper blockage side (a) and down blockage side (b) temperature contours of the model which airflow was blocked between glass number two and number four from top and bottom.

4.6.3 Blocking the Air Flow between Glass Number 1 and Number 2 from Top

For this study a model which has air blockage on the top of the air gap that is between first and second glass prepared. Prepared model can be seen in Figure 4.56. This blockage was provided by removing material that has low height. So its effect to the heat transfer can be ignored. It doesn't allow the circulation air to get sucked from the gap that is between first and second glass.

Figure 4.57 shows the air velocity vectors of the model. As it is seen air isn't flowing between first and second glass. Air velocities are relatively higher in the other gaps which air can flow.

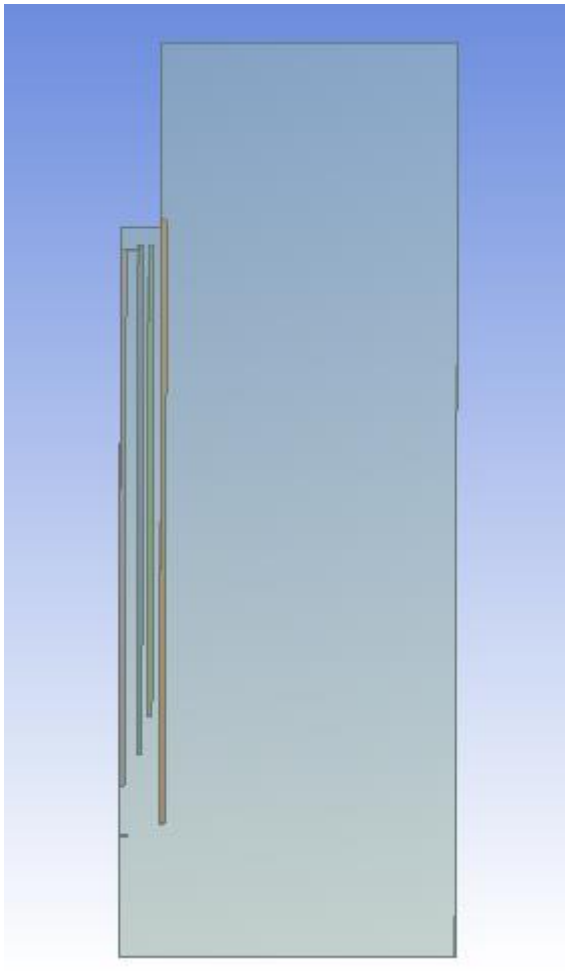


Figure 4.56 The prepared model which has air blockage between first and second glass from top.

Figure 4.59 shows the temperature contour of the model. As it is seen while temperatures between first and second glass are high, on the outer side of the second glass temperatures are relatively low. For this study outer average temperature of the fourth glass is 324.988 K. This temperature is lower than uncoated model. Figure 4.60a and 4.60b show the detailed temperature distribution of the model.

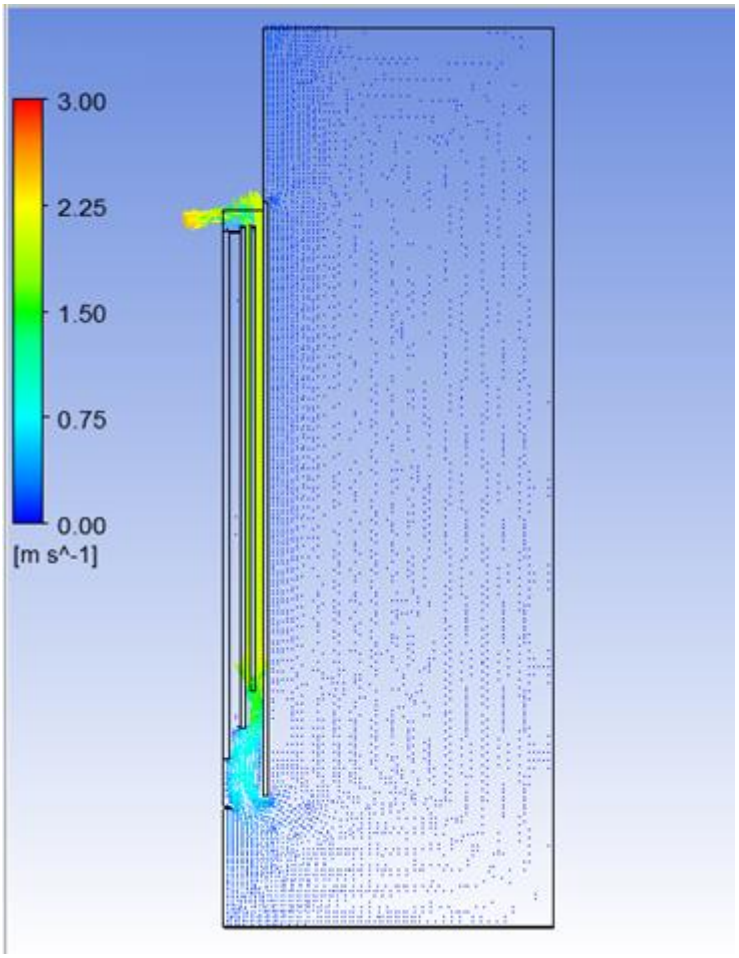


Figure 4.57 Velocity vectors of the model which airflow was blocked between glass number one and number two from top.

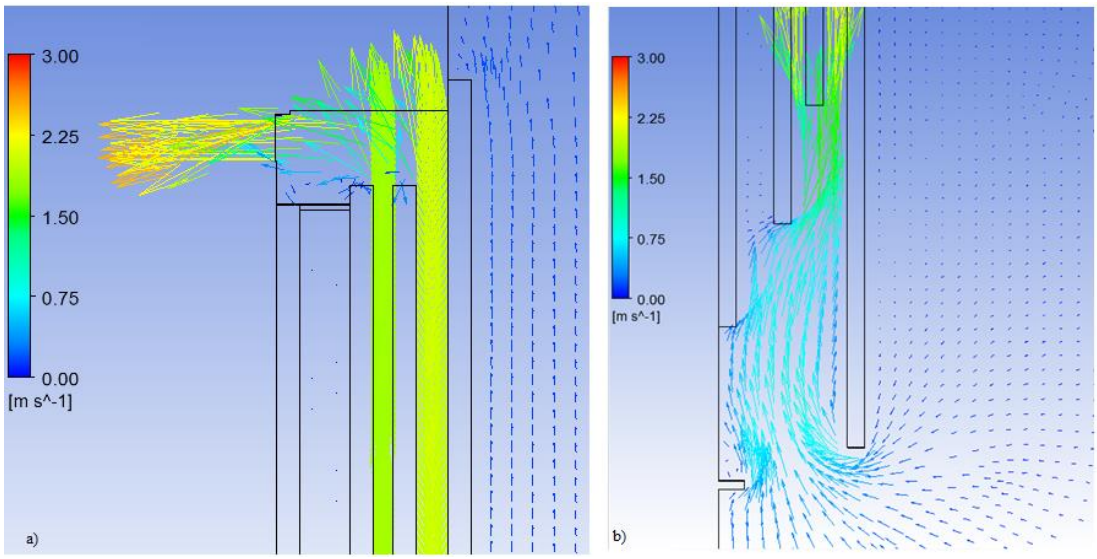


Figure 4.58 Upper blockage side (a) and down side (b) velocity vectors of the model which airflow was blocked between glass number one and number two from top.

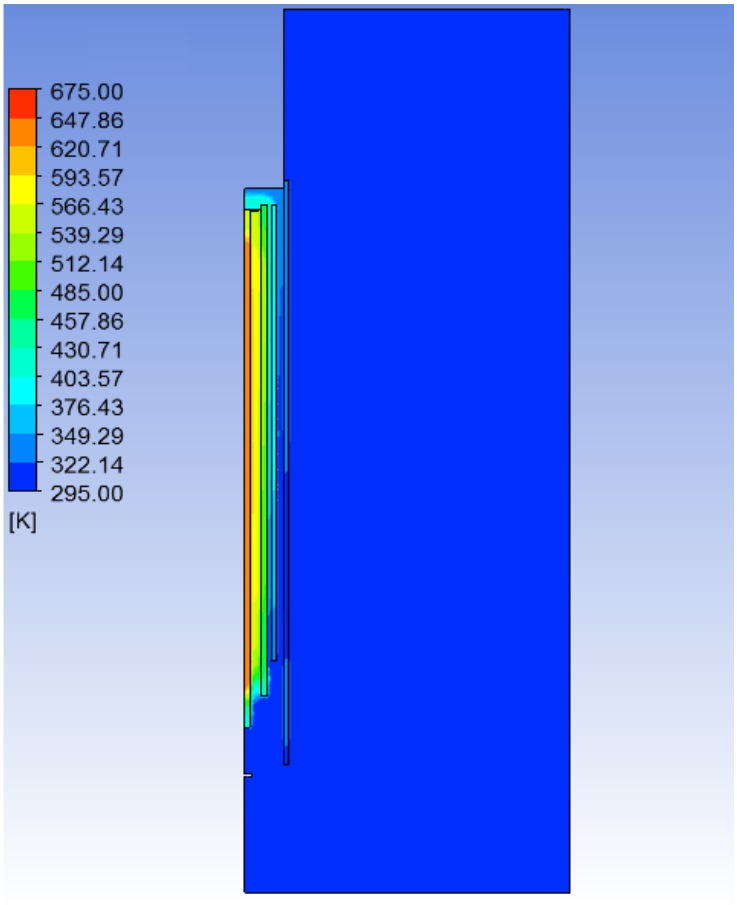


Figure 4.59 Temperature contour of the model which airflow was blocked between glass number one and number two from top.

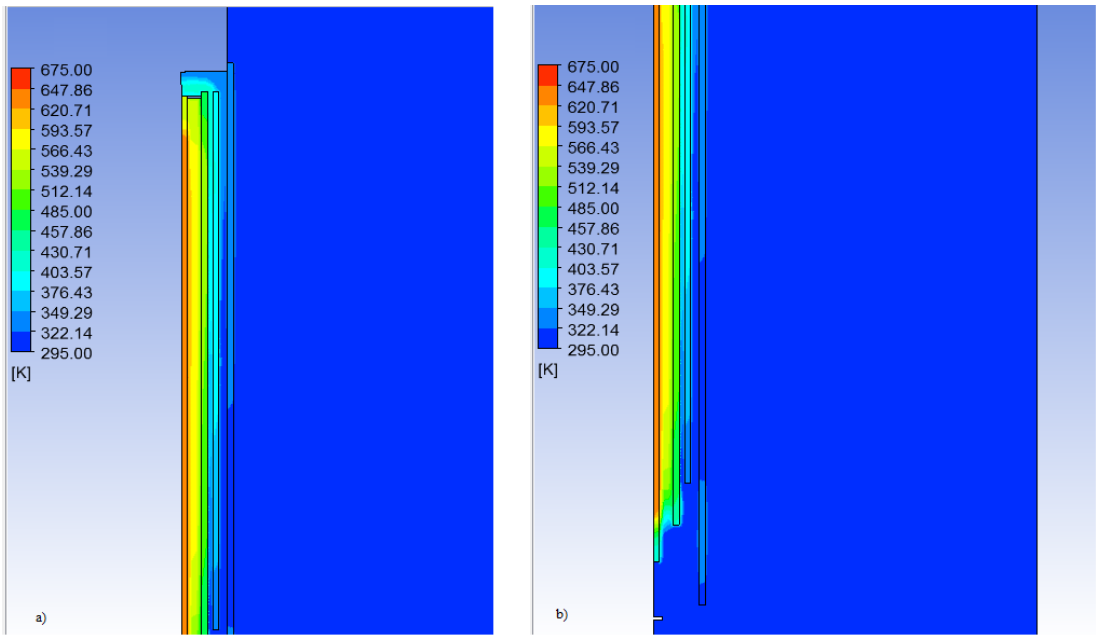


Figure 4.60 Upper blockage side (a) and down side (b) temperature contours of the model which airflow was blocked between glass number one and number two from top.

As it is seen from Figure 4.60a and 4.60b fourth glass has relatively lower temperatures from bottom towards the center.

4.7 Effect of Active Suction Air Velocity

At the oven door heat is transferred by conduction, convection and radiation. In the oven cavity the air is heated by heaters and it circulates in the oven. At pyrolytic type ovens radiation is the dominant heat transfer mechanism because of the high temperatures. Radiation that is emitted by the heaters causes the door cavity to heat up and active suction system causes to cool down the door cavity by convection.

To see the effect of active suction air velocity, average velocity of the inlet of inflow channel was changed from 1.4 m/s to 3 m/s. To see active suction air velocity effect two models were prepared. First model was uncoated which was the original model, second one is which has low emissivity coating on the outer side of first glass, inner side of second and third glass.

In Figure 4.61 and 4.62 The vertical axis shows the outer average temperature of fourth glass in Kelvin and horizontal axis shows the average velocity at the inflow channel inlet. Figure 4.61 shows the effect of active suction air velocity on the uncoated model and Figure 4.62 shows the effect of active suction air velocity on the model that has low emissivity coating on the outer side of first glass, inner side of second and third glass.

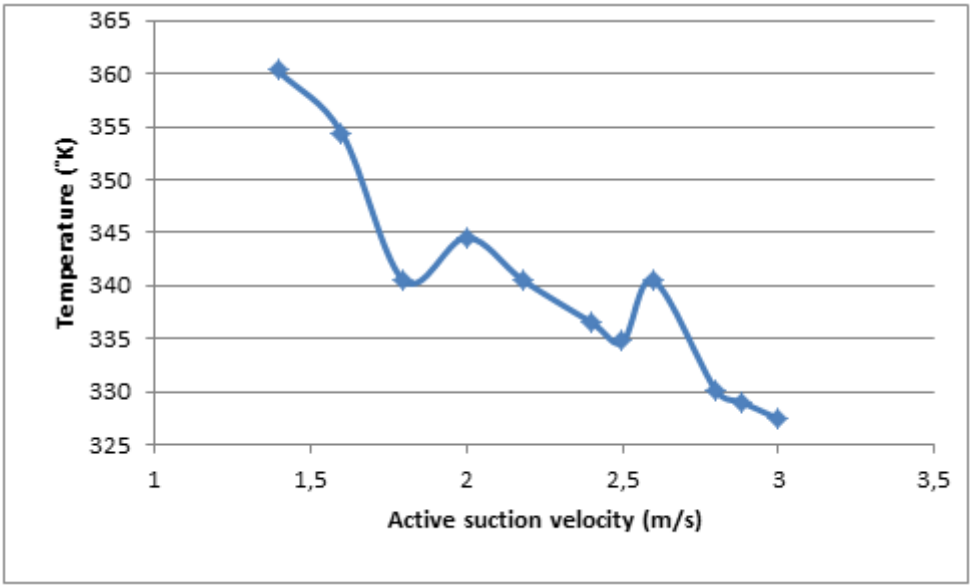


Figure 4.61 The effect of active suction air velocity on the uncoated model.

As it is seen from 4.61, as the average velocity of air increases outer average temperature of the fourth glass decreases.

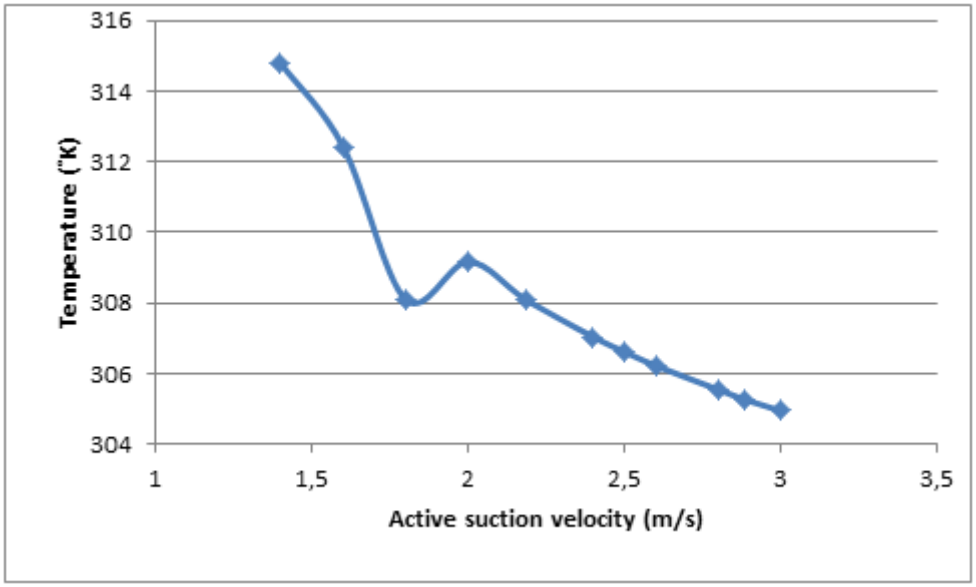


Figure 4.62 The effect of active suction air velocity on model which has low emissivity coating on the outer side of first glass, inner side of second and third glass.

As it is seen form 4.62, for the model which has low emissivity coating, as the average velocity of air increases outer average temperature of the fourth glass

decreases. The effect of the active suction air is changes for the model. For uncoated model, the effect is greater than the model which has coating.

After these results effect of the average air velocity on reducing the outer average temperature of fourth glass, study was done to increase the average velocity at the inlet of inflow channel.

CHAPTER FIVE
MODELING ACTIVE SUCTION SYSTEM

Active suction system provides the air circulation in the oven door cavity. Suction system is connected to chimney, inflow channel, outflow channel and back side of the oven. From previous chapter, effect of the average air velocity at the inlet of inflow channel on the outer average temperature is stressed. Increasing the inlet velocity reduces the outer temperature of oven door. A three dimensional half model was prepared for this study. Symmetric model halves the number of mesh. Changes in the upper fan cavity were done to increase the inlet velocity of the active suction system. Velocity experiment was done to validate the numerical model.

5.1 Preparing Cad Model for Numerical Study

The model which was taken from the white goods company was used in this study. After CAD model was taken modeling process began. Active suction is provided by upper fan of the oven.

For modeling the active suction system, inflow and outflow channels, chimney area, back side of the suction system and fan was modeled. Prepared model has two bodies which are fan and air cavity.

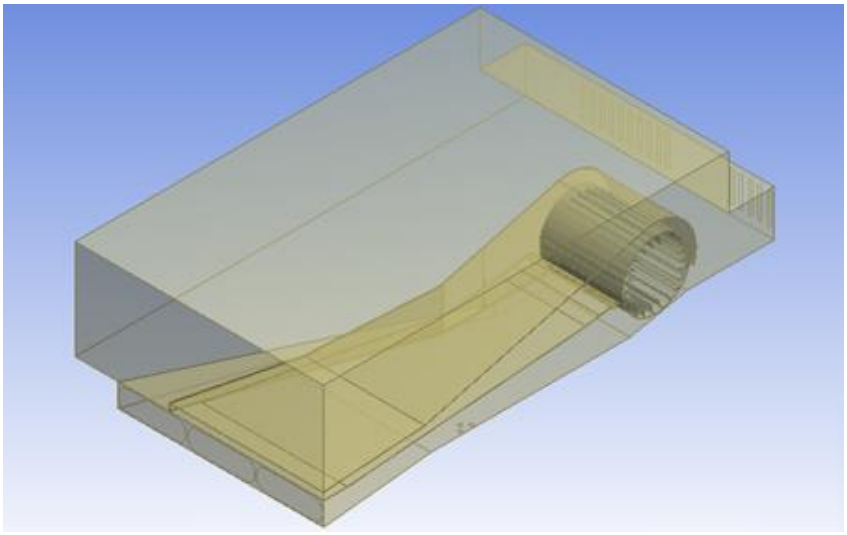


Figure 5.1 The prepared model geometry of the active suction system.

Prepared model can be seen from Figure 5.1. The prototype has small air holes that are behind the oven and opening to ambient atmosphere. Chimney surface is at the bottom surface of the air cavity.

5.2 Meshing of the Active Suction System

After preparing cad model is done meshing process begins. Meshing is very important as in the other CFD studies. After importing the cad model, meshing process started. Meshing process needs attention because very small and very entities are present in the model and they need to be meshed finely. Fins of the fan are very small comparing to air cavity. So different domains meshed by different elements sizes.

Figure 5.2 shows the mesh structure of the prepared model. As it is seen mesh elements are quite fine.

Fan domain, meshed by smaller element sizes than air domain mesh element sizes. Since fan domain rotating domain it has small element sizes. Air cavity was meshed with fine element sizes, some elements those are in the critical sides had smaller mesh sizes than the fan domain mesh sizes.

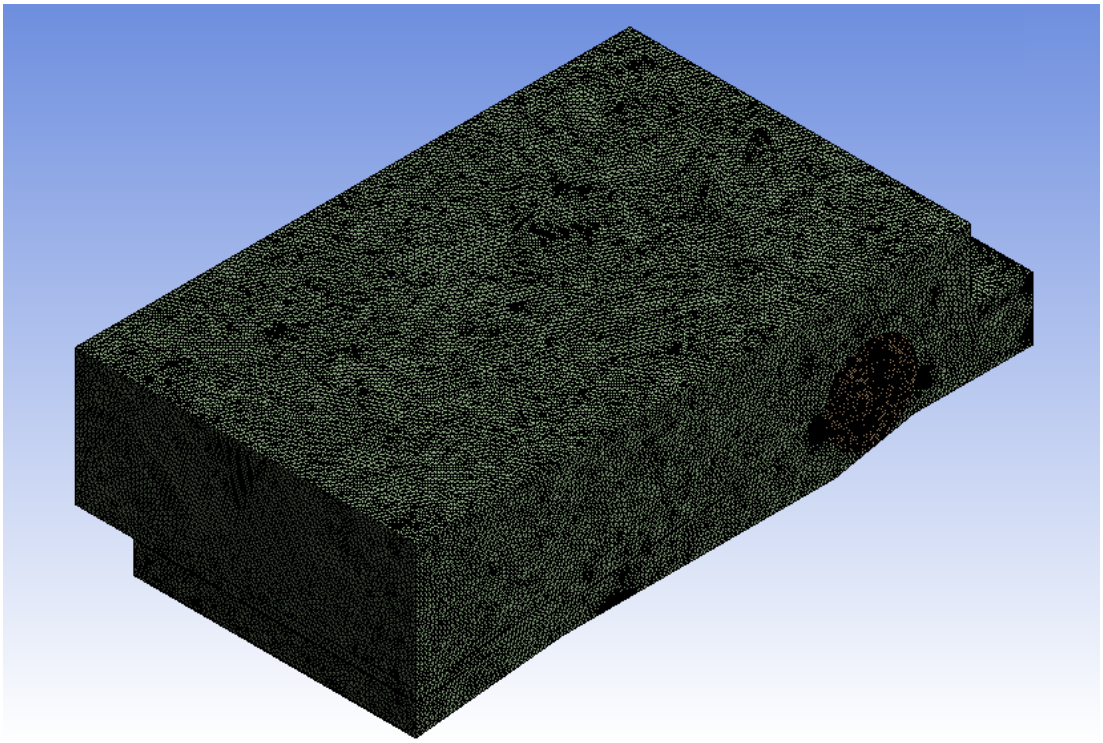


Figure 5.2 Mesh structure of the active suction system.

For defining the optimum number of mesh element models that have 7934184, 2574197 and 50158964 number elements have been created. After getting results from these models, the model which has 2574197 number elements chosen for final model.

After defining the mesh, the surfaces and bodies were named for getting advantage in next step, for defining boundary conditions easier.

5.3 Defining the Boundary Conditions

After preparing the mesh, model is transferred to pre-processing module. The model has one stationer and one rotating domain. Air is the stationary domain and fan is the rotating domain. Analysis type was isothermal and steady state.

For the defining rotating speed of fan, measurement was done by using stroboscope. Rotating speed of fan was 2400 rpm. This value was defined as boundary condition.

Inlet of the ınflow channel, outlet of the outflow channel and chimney surface defined as opening. Since the model was half, symmetry faces was defined to the symmetry plane. Since we had named the surfaces and bodies defining boundary conditions gets easier.

5.4 Solver

After defining the boundary conditions, initial conditions and material solver options must be done. Double precision is used in all studies. The momentum and mass residuals of the model is shown in Figure 5.4. Turbulence residuals are shown in Figure 5.5. The analysis has been completed in 4164 iterations.

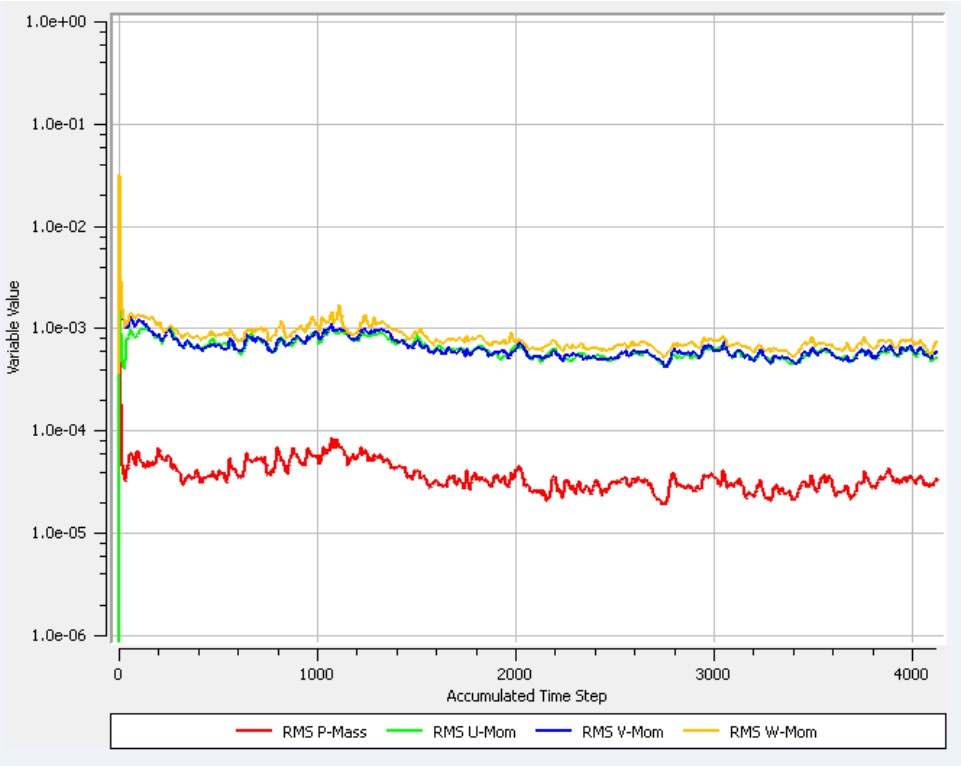


Figure 5.3 Momentum and mass residuals.

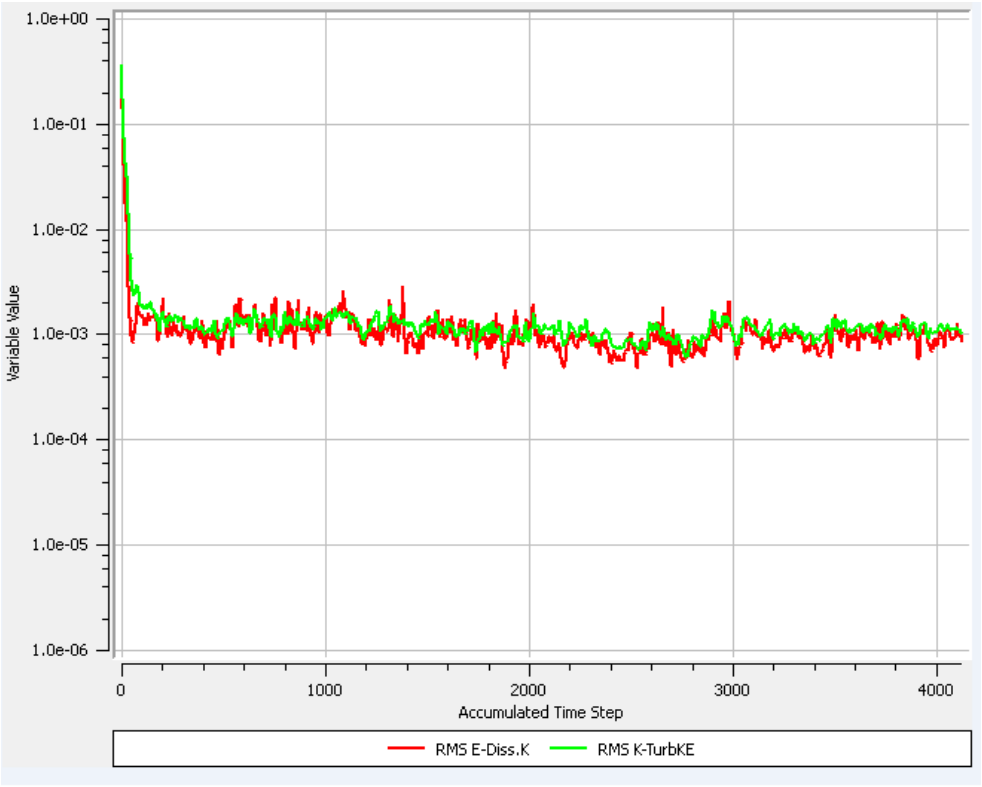


Figure 5.4 Turbulence residuals.

5.5 Validation of Numerical Study

To validate the results of numerical study, an experimental study has been done. For validation average air velocities at the inner and outer surface of the inflow and outflow channel. During this experiment probes which can measure both temperature and velocity values used. Six probes were placed on the inlet of inflow channel and four probes used at the outlet of the outflow channel.

Air flow data have been saved in every 0.3 second during the experiment. Experiment was carried on eight minutes. Data which is obtained from the experimental study validates the results of numerical study.

Table 5.1 Results of the numerical and experimental studies.

Average velocity (m/s)	Experimental study	Numerical study
Inlet	2.183	2.143
Outlet	5.906	6.611

The results of the numerical and experimental studies are shown in the Table 5.1. The average discrepancy of the average inlet velocity is 1.832 % and the average discrepancy of the average outlet velocity 10.664%. These discrepancies are in acceptable limits.

5.6 The Original and Modified Models of Active Suction Unit

After validating numerical results by experimental results, some modifications were made to increase inlet velocity of the inflow channel. Since the prototype is not final model, studies and modifications can be done. After examining the numerical results two models with modifications were created.

Original, unmodified model can be seen in Figure 5.1. Modifications are done to model. The aims of the models are increasing the average inlet velocity of inflow channel.

In first case, inclined surface which is at the bottom side of the fan was straightened. Then it was extended toward the back of the oven. This model can be seen in Figure 5.5.

In case two, inclines surface was created on the model of case two. This model can be seen in Figure 5.6.

After two modified models created, numerical study repeated for these models. After numerical study was done results were compared.

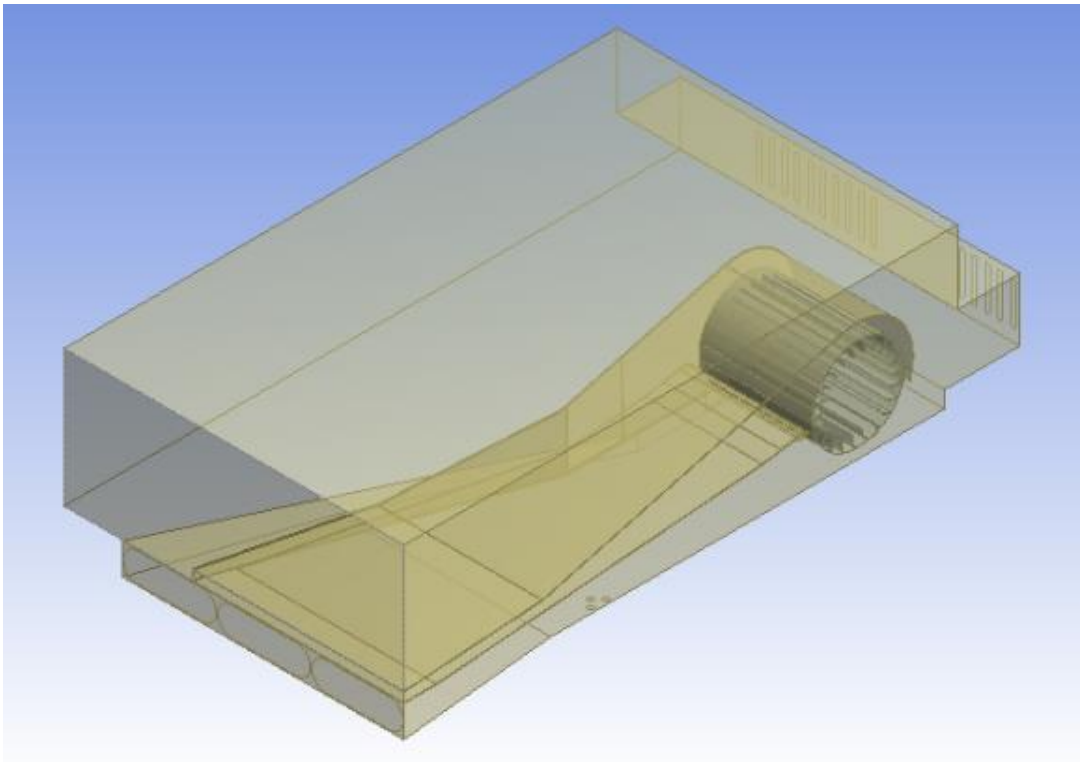


Figure 5.5 The modified geometry for the case one.

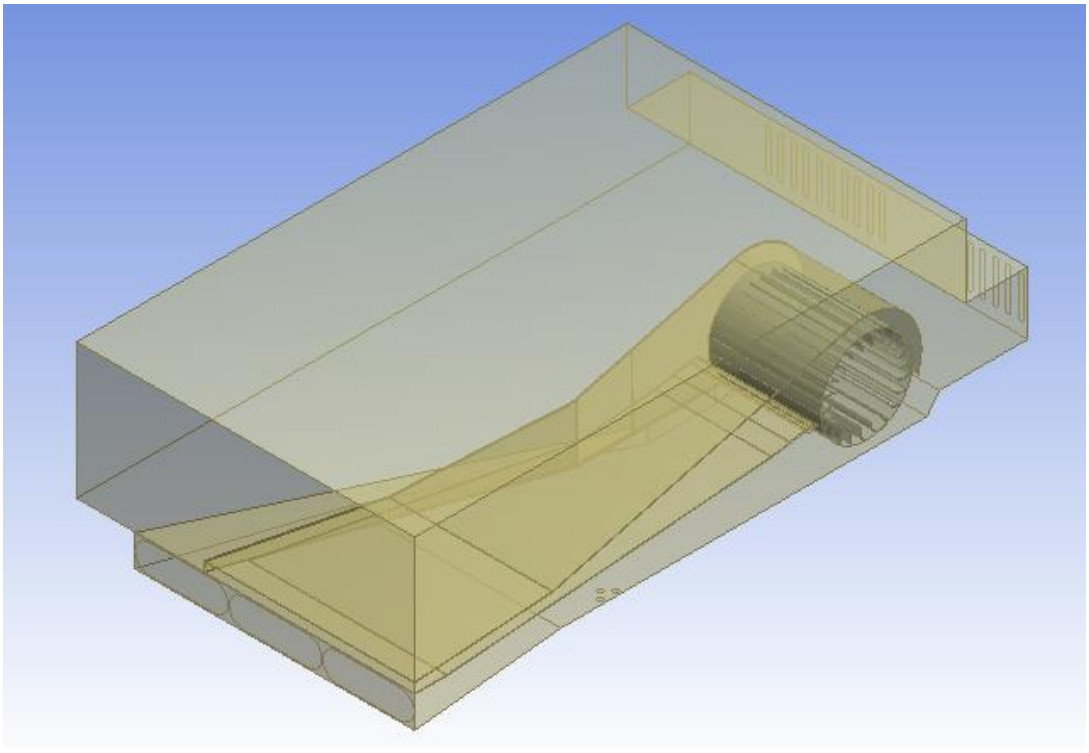


Figure 5.6 The modified geometry for the case two.

5.7 The Results of Original and Modified Models

The average inlet air velocity of the channel inflow area affects the average outer temperature of the fourth glass. Increasing the velocity of air at the inlet was the goal of these modified models. Results of the original model and modified models are shown in Table 5.2.

Table 5.2 The average inlet air velocity of inflow channel.

Model type	Average velocity at inlet (m/s)
Original	2.143
Case 1	2.559
Case 2	2.883

As it is seen from Table 5.2 original model had 2.143 m/s average inlet air velocity. The model in case one has higher air velocity. This decreases the average outer temperature of the fourth glass. But case two has the highest average velocity at inlet which is 2.883 m/s.

These results show that changing the geometry of active suction system changes the heat transfer rates of the oven door. Even a small change in the air cavity changes the thermal behavior of the oven.

CHAPTER SIX
CONCLUSIONS

The aim of this study is to investigate design parameters of oven door which are used commonly at households, by using numerical and experimental methods. Door of a domestic oven and its upper fan that provides active air suction from door unit were modeled using the Computational Fluid Dynamic and Heat Transfer (CFDHT) method. The numerical results were validated by comparing with the results obtained from experimental study. For optimization design parameters such as glass thickness, air thickness between the door glass, glass heights, active suction air velocity and the situation of using low-emissivity coating or not using were investigated.

As it is seen from literature, there are many studies on oven that investigates the heat transfer and fluid flow characteristics of oven inner cavity. In this study design parameters of oven was investigated in detail.

Oven door was modeled as two dimensional and steady state in the current study. Two dimensional model provided that more analyses were done in less time. Results of the numerical model were validated by experimental study. Then parametric studies were started. The average discrepancy of the oven door model was 5.8 %.

The active suction unit of the oven has been analyzed for increasing the average inlet air velocity of inflow channel. The results of this analysis had a maximum discrepancy of 10.664 % with the experimental results.

Effect of the glass thickness on the outer average temperature of the fourth glass was less than other design parameters. But results of the analysis showed that first glass thickness effect was more than second and third glass. Also second glass thickness effect was more than third, third glass has more than fourth glass. This showed that the glass thickness which is closer to the oven cavity has more effect on the outer average temperature of fourth glass.

Effects of the air thickness between the glass panes on the outer average temperature of the fourth glass were investigated. Optimum air thickness can be found while the other parameters are fixed. As in the effect of glass thickness, effect of air thickness between the glass listed in same way. The effect of the gap between glass first and second glass had more effect than other gaps. Results showed that first air thickness effect was more than second air thickness. Also second air thickness which is between second and third glass effect was more than third.

Effects of glass heights were investigated. The lengths of the glass were fixed. Only second and third glass heights were able to change because first glass was connecting to inside cavity of oven and fourth glass was covering the glass and door mechanism. While the glass was moving upwards they weren't blocking the air flow, they were resisting. Results showed that the effects of the glass heights were less than the effects of the air thickness but more than the glass thickness.

Radiation is the dominant heat transfer mechanism in the pyrolytic type domestic ovens. So a parameter that affects the radiation, affects the heat transfer mechanism. Effect of the low emissivity coatings were investigated in this study. The models with low emissivity coating on the first, second, third and fourth glass is modeled. It is seen from the results that coating on the first glass effect is more than coating on the second glass effect. The original uncoated model has higher outer average temperature than the models with low emissivity coatings except the model which has low emissivity coating on the outer side of fourth glass. It can be said from results, for this model using low emissivity coating on the outer side of fist glass has relatively closer outer average temperature to using low emissivity coating on the inner sides of second and third glass. So this can be alternative and economic design for the oven. After these studies an experiment was done which has low emissivity coating on the outer side of first glass, inner sides of second and third glass. Results of numerical and experimental study were very close. The discrepancy for this study was 3.04 %.

Inlet area of the inflow channel has great effect on the outer average temperature of the fourth glass. If this area reduces because of operating conditions active suction system cannot work properly. Effect of reducing this area was investigated.

Active suction system transfers the excess heat at the door cavity by convection. Increasıng the heat transfer rate in the door cavity reduces the average outer temperature of the fourth glass. Increase the heat transfer rate of convection and to see the effects of blocking air flow, models were prepared. From results it was seen that blocking air can both increase and decrease the convection rate. Blocking air flow has great effect on the outer average temperature of fourth glass.

To see the effect of average air velocity at the inlet of inflow channel velocity was changed from 1.4 m/s to 3 m/s. ın this range outer temperature of fourth glass was changed about 30 K. This shows the importance of convection rate. Increasing the average velocity causes the outer temperature of fourth glass.

After seeing the effect of average air velocity at the inlet of inflow channel velocity active suction system was modeled. The average air velocity at the inlet of inflow channel was increased to 2.883 m/s.

Design parameters of oven door were studied and for optimum values effects of the parameters were investigated. The design parameters of oven door that affect the outer surface temperature of oven door glass were investigated at the same time. Optimum values and alternative choices were defined for the model. Effects of the design parameters compared to each other. After seeing the effect of the active suction average air velocity at the inlet of inflow channel, active suction system was modeled. The active suction average air velocity at inlet of inflow channel was increased.

This thesis is taking placement under 3130615 encoded TÜBİTAK - TEYDEB project study and scope of this thesis is to provide and develop an optimization design parameters of oven door.

REFERENCES

Abraham, J. P., & Sparrow, E. P. (2004). A simple model and validating experiments for predicting the heat transfer to a load situated in an electrically heated oven, *Journal of Food Engineering, 62,* 409-415

Alvarez, G., Flores, J. J., Aguilar, J. O., Go´mez-Daza, O., Esrada, C. A., Nair, M. T. S, et al. (2005). Spectrally selective laminated glazing consisting of solar control and heat mirror coated glass: preparation, characterization and modeling of heat transfer, *Solar Energy, 78*, 113–124

Bergman, T. L., Lavine, A. S., Incropera, F. P., & DeWitt, D. P. (2011). *Fundamentals of heat and mass transfer* (7th ed.). USA: John Wiley & Sons.

Chhanwal, N., Anishaparvin, A., Indrani, D., Raghavarao, K. S. M. S. & Anandharamakrishnan, C. (2012a). Computational fluid dynamics (CFD) modeling of an electrical heating oven for bread-baking process, *Journal of Food Engineering, 100,* 452-460

Fahey, M., Wakes, S. J., & Shaw, C. T. (2008). Use of computational fluid dynamics in domestic oven design, *The International Journal of Multiphysics, 1,* 37-57

Fan, Y., Hyde, T., Hewitt, N., Eames , P.C., & Norton, B. (2009). Comparison of vacuum glazing thermal performance predicted using two-and three-dimensional models and their experimental validation, *Solar Energy Materials & Solar Cells 93,* 1492–1498

Mistry, H., Ganapathi-subbu, Dey, S., Bishnoi, P., & Castillo, J. L. (2006). Modeling of transient natural convection heat transfer in electric ovens, *Applied Thermal Engineering, 26,* 2448-2456

Rek, Z., Rudolf, M., & Zun, I. (2012b). Application of CFD simulation in the development of a new generation heating oven, *Journal of Mechanical Engineering, 58*, 134- 144

Shaughnessy, B. M., & Newborough, M. (2000). Energy performance of a low-emissivity electrically heated oven, *Applied Thermal Engineering, 20*,813-830

Xamán, J., Arce, J., Álvarez, G., & Chávez, Y. (2008). Laminar and turbulent natural convection combined with surface thermal radiation in a square cavity with a glass wall, *International Journal of Thermal Sciences, 47*, 1630–1638